Novel Roles for Cullin 3 in T Cell-Mediated Immunity

by

Emily Lynn Yarosz

A dissertation submitted in partial fulfillment
of the requirements for the degree of
Doctor of Philosophy
(Immunology)
in the University of Michigan
2022

Doctoral Committee:

       Professor Cheong-Hee Chang, Chair
       Professor Philip D. King
       Associate Professor Yasmina Laouar
       Associate Professor Costas A. Lyssiotis
       Professor Ling Qi

Emily L. Yarosz

eyarosz@umich.edu

ORCID iD: 0000-0003-3201-9534

Dedication

This dissertation is dedicated to Talia Heinly, a talented immunologist who undoubtedly would have changed the world with her passion and kindness.

Acknowledgements

If there is one thing I've learned over the course of my PhD training, it's that science doesn't happen in a vacuum. This dissertation is the result of many hours of feedback, collaboration, mentorship, and support. As such, I would like to begin by thanking my mentor, Dr. Cheong-Hee Chang, for molding me into a thoughtful, capable, and independent scientist. Her mentorship has taught me how to think about scientific questions, how to properly design experiments, and how to be a leader in a laboratory setting. I am grateful to have had the opportunity to grow as a person and a scientist under her mentorship. I would also like to thank my thesis committee: Drs. Philip King, Ling Qi, Yasmina Laouar, and Costas Lyssiotis. Each of you helped propel my projects forward by providing critical feedback and suggestions at our meetings. More importantly, each of you helped to build me back up when I was feeling low, and I am so grateful for your encouragement and words of support.

None of my success would have been possible without the members of the Chang Lab. Every person who has been in the lab during my graduate tenure has either contributed intellectually to my projects or has contributed to my personal growth, and I am very grateful for that. Specifically, I need to thank Dr. Yeung-Hyen Kim for being my first in-lab mentor and for teaching me everything I know about flow cytometry. I also need to thank Dr. Kalyani Pyaram for being my biggest role model. Kalyani, you are an incredibly gifted scientist who is an even better person, mother, and friend. Thank you for always being patient with me, for cheering me on, and for drying every tear. Most of all, thank you for showing me that there is life outside of the lab, and that I really can have it all. I could not have done this without your mentorship and friendship (or your palak paneer). I would also like to thank Dr. Ajay Kumar for his mentorship and friendship over the last 5 and a half years. Ajay is the most talented experimentalist I have ever met. He inspires me to try new things and to think deeper about questions. I am certain I wouldn't be half the scientist I am today without his guidance. Ajay, thank you for all of the life lessons, gossip, and laughs. To my fellow Chang Lab graduate student, Chenxian Ye, thank you for being my best friend in lab. The PhD journey was made so much easier by having you to

iii

laugh, cry, and eat sweets with. You are the most genuine person I have ever known. I can't wait to see all that you achieve in science and beyond. To our lab manager, Chauna Black, thank you for putting up with me. You always took my ~~uptight~~ superstitious scientific habits in stride, and I learned so much from you. Beyond that, you made Ann Arbor a super fun place to live. I am very grateful for your friendship both inside and outside of the lab. Lastly, to my undergraduate trainees Hana Kim, Lois Kim, and Janice Huang, thank you for giving me the opportunity to live my dream of mentoring students of my own. You are all wonderful, kind, and intelligent ladies. It was the greatest privilege of my graduate career to help guide you on your scientific journeys.

I would be remiss if I didn't thank my first scientific family, the Paulson Lab at the Pennsylvania State University. Dr. Robert Paulson was the first and only person to take a chance on me when I was searching for a research opportunity as an undergraduate student. My time in his lab taught me how to read a scientific paper, how to interpret my results, and how to be a careful scientist. Although I collected exclusively negative data, Dr. Paulson was always ecstatic to see my results. Beyond that, Dr. Paulson has supported me in every one of my endeavors, whether that was volunteering with THON, applying to graduate school, writing an F31 fellowship, and applying for jobs outside of academia. Dr. Paulson, thank you for teaching me that you can be both a gifted scientist and a good person. You have always been my biggest role model. I hope I made you proud. To my graduate student mentors Laura Bennett (LB), Laura Goodfield-Moreau (LG), Chang Liao, and Elly Song, thank you for taking on this stranded undergrad despite your busy schedules. You not only taught me how to properly use a pipette but also sacrificed your personal time to make my experiments work. I am so grateful to have had such wonderful, strong, and smart female role models during the most formative time in my scientific career. You all rock.

The Graduate Program in Immunology has been the best environment to learn to do science. I need to thank Dr. Beth Moore for recruiting me to the program and for supporting me every day since. Thank you, Beth, for all the laughs, wisdom, and tissues. I would also like to thank past Immunology Program administrator Zarinah Aquil, for her tireless dedication to the program since I joined. Zarinah, thank you for putting up with my 3AM emails and for being the encouraging voice I needed after every grant or fellowship rejection. I would also like to thank interim Immunology Program Directors Dr. Malini Raghavan and Dr. Durga Singer for their support over the past few years. Lastly, I'd like to thank Immunology Program Administrator

Molly Bannow for helping me through my last year of graduate school and for all the orange sodas.

Let's face it – grad school is tough. Long hours and failing experiments take their toll on you both physically and mentally. Luckily, I had two of the most compassionate and insightful people to help me through it. Dr. Kate Hagadone was my first ever therapist. She patiently listened to me sob about trivial things until I felt safe enough to get to the real issues, and she never thought any problem was too small. Kate, thank you for being my first good therapy experience. I was also extremely lucky to find and keep Christine Kelley, LMSW, as my long-term therapist through my final years of graduate school. Christine not only got me through a global pandemic but also gave me the tools to face demons that I have been running from for the past 28 years. Christine, thank you for your empathy, grace, patience, and wisdom. I truly could not have done this without you.

My time at the University of Michigan has blessed me with lifelong friends. I'm genuinely not sure how I got so lucky to have such great people in my life. To Holly Turula, thank you for seeing a struggling first year crying at the centrifuge and taking her under your wing. Your mentorship and friendship have meant more to me than you will ever know, and I'm pretty sure we're soul sisters. To Giovanny Martinez-Colon, thank you for being the best shoulder to cry on, fellow girlboss rap fan, and fellow foodie. You are the big brother I always wished I'd had, and I couldn't have done graduate school without you. To Haley Amemiya, thank you for always being my cheerleader, for making me an aunt to Ada, and for being the type of person I want to be when I grow up. You are a goddess among women. To Julie Ferrell-Olson, Vicki Heda, and Elanna Heda: thank you for being my people. I can be myself with you, and I'm so grateful to know such smart, talented, kind, and passionate ladies. Immunology Wives Club^{TM} for life. To Ashley Munie, thank you for never judging me, for always listening to me vent, and for being my favorite squad trip roommate. To Mikel Haggadone, thank you for being vulnerable and for teaching me that there is immense strength in persevering and in being kind. To Jazib Uddin, thank you for being my favorite person to have a nonscience chat with and for being an S tier friend. To Aric Brown, thank you for showing me that science and faith can coexist and for your constant support of my personal growth. I don't think I would be the person I am today if I hadn't met you. Thank you for being my COVID pod, for introducing me to mochas, and for ~~always screaming at me from across the produce aisle~~ all the laughs. I also need

to thank my day 1 friends, Drew Narwold and Eli Olson. Drew, thank you for all the Bachelor in Paradise watch parties and for sharing in the joy of the rainbow carwash with me. Most importantly, thank you for reminding me to slow down and enjoy the little things in life (i.e. lake time). Eli, you are the most patient and loyal person I've ever met. You have never let me down, and I am so grateful for your friendship. The world is a better place because people like you exist. And thanks for driving me 20 minutes back to the movie theater to get my phone that one time. That was clutch.

I also need to thank my PSU friends, Caitlin Gladwell and Ben Fowler. You both have been my most relentless cheerleaders since day 1. You have always believed in me, even when I didn't believe in myself. I am truly grateful for your support, hugs, and friendship. I'm blessed to have two friends who love Philly, mac and cheese pizza, the Gaff, PSU, and GoGo Gadjet as much as I do. Love you both times infinity.

I have always believed that soulmates exist in all aspects of our lives. I am lucky enough to have already found two of them in Adrienne Puglia and Korey Onulack. Adrienne, you have always accepted and loved me for who I was, even when I was a super nerdy social outcast. You bring out my confident side, and I know I can be myself when I'm with you. Thanks for being my unbiological sister, my cheerleader, and my favorite non-science person. You mean the world to me. Korey, I truly mean it when I say I don't know how to do life without you in it. You always give the best advice and are the best listening ear. I am a better person thanks to the things you've taught me about life and about the world. Thank you for always building me up, keeping my secrets, and being my go-to taco buddy. You are my person. Adrienne and Korey, I love you both more than you will ever know (and I still haven't given up on our future commune with the rainbow kitchen).

Lastly, I need to thank my family. My family means the world to me, and they have cheered me on through every low and celebrated with me in every high. I wouldn't be the person I am today without them. To my siblings – Aric, Hannah, Sam, Zoe, Olivia, Mia, Juliet, and Claire – thank you for being my built-in squad. You have all always been there for me, and you have believed in me when I didn't believe in myself. Thank you for never giving up on me. Thank you for teaching me to take myself less seriously; you've all filled my life with joy and laughter. Most of all, thank you for reminding me to love myself. To my Mom, thank you for always supporting me no matter which path I choose in life. To my bonus Mom, Traci, thank you

Table of Contents

List of Tables

List of Figures

Abstract

The proper development and function of T lymphocytes depend on a variety of processes. However, the roles of both intracellular iron metabolism and the E3 ubiquitin ligase Cullin 3 in controlling T cell-mediated immunity are vastly understudied. Here, we show that intracellular iron metabolism is crucial for proper CD4 T cell proliferation and mitochondrial function after activation. T cell receptor stimulation leads to coordinated changes in the expression of iron intake, storage, and export proteins as well as drastic loss of cytosolic labile iron levels. This change in cellular iron levels is important for T cell proliferation, as blocking labile iron flux during activation is associated with decreased proliferative capacity. We found that iron controls activated CD4 T cell proliferation by modulating IL-2 receptor signaling and supporting optimal mitochondrial function.

We also show that Cullin 3 modulates invariant natural killer T (iNKT) cell development by regulating cellular iron homeostasis. In the absence of Cullin 3, iNKT cells fail to develop and acquire their classical effector phenotype. This block in iNKT cell development also results in hyperproliferation and death of mature iNKT cells lacking Cullin 3. Additionally, Cullin 3 deficient iNKT cells display higher glycolytic activity compared to WT cells, which appears to be detrimental for mature thymic iNKT cells. We also show that mature iNKT cells lacking Cullin 3 harbor higher labile iron levels than wild type cells, potentially leading to increased cell death by ferroptosis during iNKT cell development. Feeding a low iron diet to mice with a T cell-specific deletion of Cullin 3 appears to rescue cellular iron accumulation in mature iNKT cells, revealing a role for Cullin 3 in controlling iNKT cell development by modulating intracellular iron metabolism.

Cullin 3 also appears to promote naive CD4 T cell peripheral maintenance by regulating iron homeostasis and tonic signaling. We found that Cullin 3 deficiency leads to a severe loss of naive CD4 T cells in the peripheral tissues. Residual naive CD4 T cells exhibit a pre-activated phenotype characterized by increased proliferation, cytokine production, and TCR signaling molecule expression. Additionally, naive CD4 T cells lacking Cullin 3 resemble effector cells in

terms of their expression of iron homeostatic molecules and labile iron levels. Cullin 3 also appears to restrain naive CD4 T cell responses after stimulation, as Cullin 3 deficient naive CD4 T cells proliferate better and secrete more inflammatory cytokines in comparison to wild type cells. This heightened proliferative capacity is also accompanied by an increase in glycolytic metabolism in Cullin 3 deficient naive CD4 T cells. Interestingly, these phenotypes appear to be dependent upon the presence of a polyclonal T cell pool, as expression of the OT-II transgenic T cell receptor by Cullin 3 deficient naive cells prevents naive T cell atrophy. We hypothesize that Cullin 3 may maintain naive CD4 T cell quiescence by modulating intracellular iron levels and inhibiting aberrant T cell receptor signaling in response to either self or gut microbial peptides. In all, my thesis work furthers our understanding of the role of Cullin 3 in controlling T cell-mediated immune responses.

Chapter 1 – Introduction

I began the work described in this dissertation with the goal of understanding how the ubiquitin ligase Cullin 3 controls invariant natural killer T cell development. As with most scientific endeavors, the path to answer this question was not linear. My scientific journey took me to areas of research I never expected to investigate, allowing to me acquire a working understanding of a variety of topics. In this Introduction, I will describe Cullin 3, its regulation, and some of its roles in mammalian cells. I will also provide background into invariant natural killer T cells and their development in the thymus. Additionally, I will outline the cellular iron homeostasis pathway and roles for iron in T cell-mediated immunity. Finally, I will end by providing background and context for each of the chapters of this dissertation.

What is Cullin 3?

Cullin-RING ligases (CRLs) control cellular ubiquitination pathways by binding adaptor proteins that confer substrate specificity. Having 7 identified members, CRLs comprise the largest family of ubiquitin ligases in mammalian cells (1, 2). CRLs are named for the specific cullin protein that forms the backbone of the CRL complex. This cullin protein acts as a scaffold onto which other components of the ligase bind (2). All CRLs possess a RING-domain-containing protein on the C-terminus of the complex (3). Together, the cullin scaffold and RING protein are referred to as the catalytic core of the CRL, as the RING protein acts as a docking site for the E2 ligase (1, 3). On the other hand, the N termini of the different CRLs are variable (1), which allows each CRL to bind a unique adaptor protein (3). Therefore, the adaptor protein confers substrate specificity to the CRL (Table 1.1).

Activation of CRLs is dependent upon neddylation of the cullin scaffold. Neddylation is a process by which the ubiquitin-like molecule neural precursor cell expressed developmentally downregulated-8 (NEDD8) is deposited onto proteins, modifying their function. The cullin proteins are major targets of the neddylation pathway (4), and neddylation of the cullin scaffold is known to recruit E2 ligases to the CRL complex (5-7). Additionally, neddylation allows the

CRL to shift from a closed conformation to an open conformation that facilitates ubiquitin deposition onto target proteins (8). CRLs can then be deactivated by the removal of NEDD8 by the COP9 signalosome (6). In all, neddylation and deneddylation control the activity of CRLs *in vivo* and prevent aberrant degradation of cellular proteins.

Many of the CRLs, including Cullin 1 and Cullin 4, associate with a fixed adaptor protein (Table 1.1) (2). In contrast, Cullin 3 (Cul3) can bind a variety of BTB-domain-containing adaptor proteins (Table 1.1) (2). These adaptors link Cul3 to its substrates, allowing for polyubiquitination and degradation of these substrates. The human genome encodes approximately 200 different BTB-domain containing proteins (9); however, only those containing a 3-box motif in addition to the BTB-domain have been shown to be viable adaptors for Cul3 (10). Despite this, Cul3 is known to target upwards of 188 proteins for degradation (11). These targets span several biological systems, giving Cul3 tissue- and system-specific functions.

Table 1.1 – Summary of the Cullin-RING ligases and their substrate specificities.
Recreated from Sarikas, Hartmann, and Pan 2011 (2).

CRL Name	Cullin Scaffold	Adaptor Protein	Substrate Specificity
CRL1	Cul1	Skp1	F-box proteins
CRL2	Cul2	Elongin B/C	VHL-box proteins
CRL3	Cul3	BTB-domain proteins	variable
CRL4A	Cul4A	DDB1	DCAF
CRL4B	Cul4B	DDB1	DCAF
CRL5	Cul5	Elongin B/C	SOCS-box proteins
CRL7	Cul7	Skp1	Fbw8

Biological Roles of Cullin 3

Because it can bind so many different adaptor proteins, Cul3 is known to modulate a variety of cellular functions. Here, I will outline the role of Cul3 in controlling both cellular redox states and cell cycle progression in greater detail.

Antioxidation

Cul3 is a key member of the Cul3-Keap1-Nrf2 trimeric complex, which is a major contributor to the maintenance of cellular redox states in mammalian cells. The transcription factor nuclear factor erythroid 2-related factor 2 (Nrf2) lends this complex its antioxidant

function, as Nrf2 has been shown to be a major activator of antioxidant response element (ARE)-containing genes both *in vitro* and *in vivo* (12-14). Following oxidative stress, Nrf2 translocates from the cytoplasm into the nucleus, where it forms a heterodimer with nuclear Maf proteins (15). The Nrf2 heterodimers then bind to the ARE, leading to the recruitment of other factors responsible for the activation of antioxidant response genes (16).

Because some level of reactive oxygen species (ROS) is necessary for cellular activation and function, the Nrf2-regulated antioxidant genes cannot be constitutively active. Therefore, nuclear translocation of Nrf2 is tightly regulated by Keap1, which has been shown to bind to the amino terminus of Nrf2 (17). Keap1 is also structurally homologous to the *Drosophila* protein Kelch, which functions as an actin-binding protein in *Drosophila* cells (17). As such, the longstanding belief was that Keap1 prevented Nrf2 translocation to the nucleus by sequestering it in the cytoplasm, thereby preventing the antioxidant genes from being expressed.

Continued research has since disproven this theory by revealing that Keap1 instead acts as an adaptor protein for the binding of the Cul3 to cytosolic Nrf2 (15). Cul3 has also been shown to catalyze the ubiquitination of Nrf2, subsequently targeting Nrf2 for degradation by the proteasome (18, 19). In this way, Keap1 and Cul3 act in concert to mediate the degradation of Nrf2 in the cytoplasm when homeostatic levels of ROS are present. During times of oxidative stress, the structure of Keap1 is modified in such a way that it can no longer bind Nrf2, allowing Nrf2 to enter the nucleus and activate the antioxidant response (Fig. 1.1) (16).

Although this pathway has been well characterized in various cell types, regulation of antioxidant genes by the Cul3-Keap1-Nrf2 trimeric complex has only recently begun to be explored in T cells. Several studies have revealed a role for Nrf2 in maintaining various aspects of T cell-mediated immunity. For one, Nrf2 has been shown to be important in T cell activation. Research has shown that induction of Nrf2 in both Jurkat cells and human primary CD4 T cells leads to decreased expression of the early activation markers CD25 and CD69 as well as decreased production of IL-2 (20, 21). Increased expression of Nrf2 also decreases the DNA binding-capability of NFκB, a transcription factor important in T cell activation (20, 21). Additionally, Keap1 deficiency and subsequent systemic activation of Nrf2 in scurfy mice leads to decreased effector T cell activation as measured by CD25, CD44, and CD69 expression (22). Both systemic and T cell-specific Nrf2 activation also leads to decreased IFN-γ production by

effector Th1 and CD8 T cells in the scurfy model (22). In all, these data show that increased Nrf2 expression limits T cell activation.

Beyond its ability to impact T cell activation, studies have also revealed that Nrf2 mediates T helper cell differentiation. Induction of Nrf2 by *in vitro* treatment with Nrf2 activators has been shown to lead to decreased IFN-γ production and increased IL-4, IL-5, and IL-13 production (20, 23). Additionally, Nrf2 activation promotes the ability of GATA-3 to bind DNA while simultaneously suppressing T-bet from binding DNA (23). Nrf2 has also been shown to play some role in the development of Th17 cells. A recent study revealed that deficiency in Nrf2 increased Th17 differentiation both *in vitro* and in a murine model of lupus nephritis, promoting the early onset of disease (24). Contrastingly, T cell-specific overexpression of Nrf2 has been shown to lead to increased T regulatory cell development (25). Taken together, these findings indicate that Nrf2 prevents the differentiation of inflammatory T helper cell subsets and skews the immune response towards more anti-inflammatory phenotypes.
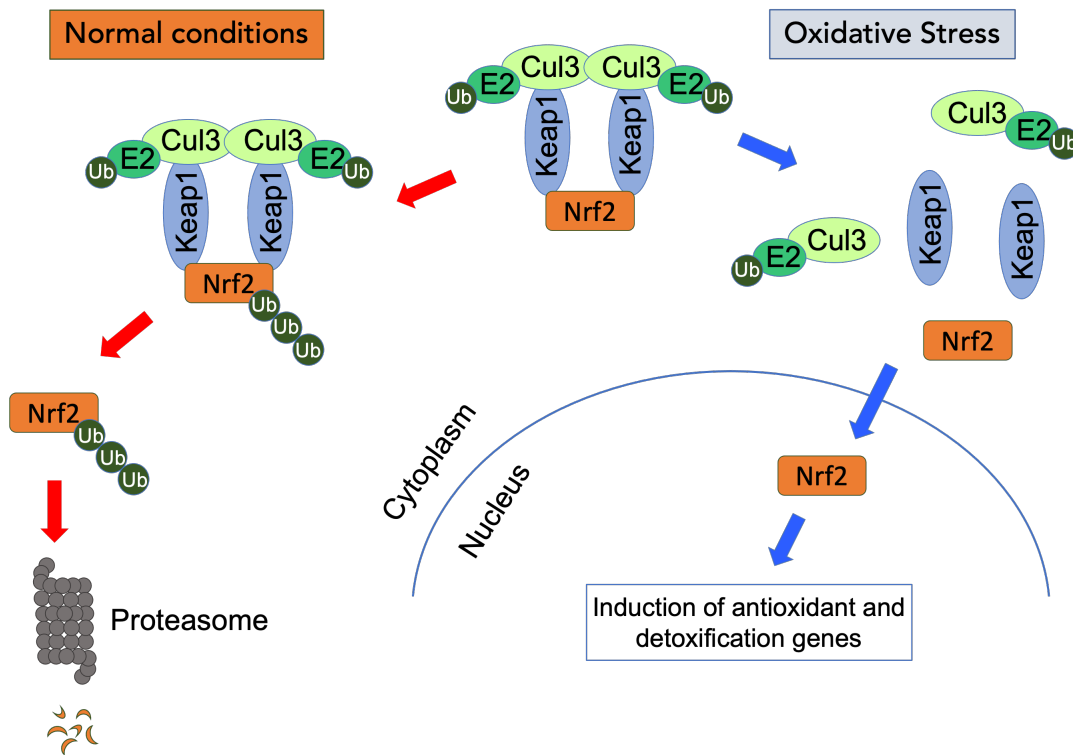
Figure 1.1 – The Cul3-Keap1-Nrf2 trimeric complex controls cellular redox states.
Under normal conditions, the trimeric complex remains intact, allowing Cul3 to use Keap1 as an adaptor protein to bind and ubiquitinate Nrf2. Polyubiquitination of Nrf2 by Cul3 leads to proteasomal degradation of Nrf2. During oxidative stress, the trimeric complex dissociates, allowing Nrf2 to enter the nucleus and activate transcription of various antioxidation and detoxification factors.

Although progress has been made in elucidating the role of Nrf2 in T cells, further work is necessary to determine the effects of Nrf2 activation on other aspects of T cell biology such as proliferation and maintenance. Additionally, little is known about the functions of Keap1 and Cul3 in controlling T cell biology. Therefore, continued research into the effects of the dysregulation of this complex in T cells is highly warranted.

Cell Cycle Regulation

Cell division involves a series of phases that are tightly regulated by checkpoints and protein mediators to prevent uncontrolled cell growth. The cell division cycle begins when a cell leaves the quiescent G_0 stage and enters the G_1 phase, in which the cell grows in size and copies all of its organelles. This process is mediated by an increase in both cyclin D and cyclin-dependent kinase (Cdk) 4/6 levels (26). Together, these proteins form an active kinase that phosphorylates retinoblastoma, a protein that inhibits G_1 progression by binding to E2 transcription factors (E2F) (26, 27). As phosphorylation of retinoblastoma increases, its ability to bind E2F decreases (27). Free E2F then enters the nucleus and mediates transcription of cyclin E, which enters the cytoplasm and binds Cdk2. Cdk2-cyclin E complexes not only further phosphorylate retinoblastoma but also mediate the deposition of DNA replication machinery onto replication forks (26, 27), allowing entry into S phase. During S phase, cells rapidly copy their DNA. Once DNA replication is complete, cells move into G_2 phase with the help of cyclin A and Cdk1 (26). Cells in G_2 finish duplicating their intracellular contents to prepare for cell division, which occurs during the mitosis (M) phase of the cell cycle. The transition from G_2 to M phase is governed by the replacement of cyclin A for cyclin B in the Cdk1-cyclin complex (26). During M phase, 50% of a growing cell's DNA, organelles, and proteins are partitioned into a second daughter cell. Daughter cells can then either continue dividing or re-enter quiescence (G_0).

Healthy progression through the cell cycle depends on the degradation of cyclins and other DNA replication components by Cul3. After DNA has been successfully duplicated during S phase, cyclin E-Cdk2 levels need to be decreased to prevent uncontrolled cell growth and chromosomal abnormalities (26). One way cyclin E is destroyed is through ubiquitination and proteasomal degradation mediated by Cul3. Cul3 has been shown to work in concert with Cul1 to ubiquitinate and degrade cyclin E in mouse embryonic fibroblasts, promoting cell survival and

embryonic development (28, 29). Additionally, Cul3 has been shown to use Keap1 as an adaptor protein to ubiquitinate the DNA helicase minichromosome maintenance 3 (MCM3) (30), which is one of the components of the DNA replication complex used during S phase. However, it is unclear whether ubiquitination of MCM3 by Cul3 leads to the degradation of MCM3 or instead leads the helicase complex to disassociate from the DNA (30). In addition to its roles in S phase progression, Cul3 modulates chromosomal segregation during mitosis. As cells divide, two copies of each chromosome are pulled into each daughter cell by the chromosomal passenger complex, which includes the protein Aurora B. Ubiquitination of Aurora B by Cul3 is required for Aurora B to attach newly synthesized chromosomes to the microtubules of the mitotic spindle, allowing cells to successfully enter M phase (31, 32). However, the role of Cul3 in controlling the cell cycle in T cells has yet to be investigated.

Cullin 3 in Immunity

Despite having these well-characterized roles, the importance of Cul3 in the immune system is just beginning to be understood. Cul3 has been shown to promote STAT3 phosphorylation in macrophages by regulating the expression of OGT, an enzyme responsible for protein O-GlcNAcylation (33). O-GlcNAcylation prevents STAT3 from becoming phosphorylated, inhibiting STAT3 nuclear translocation and subsequent IL-10 production by macrophages (33). OGT is a target of Nrf2; therefore, Cul3 modulates OGT expression and hexosamine biosynthesis pathway activity in macrophages by ubiquitinating and degrading Nrf2 (33). Cul3 in macrophages has also been shown to dampen gut inflammation and disease severity in murine models of colitis (33). Based on this data, it is tempting to speculate that Cul3-driven cytokine production in the myeloid compartment could influence T cell function in the context of disease. However, this possibility has not yet been explored.

Cul3 has also emerged as a key regulator of B and T cell responses. Recent work has revealed that Cul3 regulates B cell development and peripheral maintenance (34). Cul3 deficiency causes B cells to adopt a pre-activated phenotype, expressing higher levels of MHC class II, CD86, and B cell receptor signaling proteins (34). Additionally, Cul3 promotes B cell survival by inhibiting apoptotic cell death through active caspase 3 activity (34). In addition to its effects on the B cell compartment, Cul3 has been found to influence T cell development and differentiation. Published work has shown that T cell-specific deletion of Cul3 leads to enhanced

T regulatory cell and T follicular helper cell differentiation (35, 36). Increased differentiation of T follicular helper cells in the absence of Cul3 also leads to the expansion of B cells and germinal centers in the secondary lymphoid tissues (36). Interestingly, T cell-specific deletion of Cul3 results in a severe block in the development of invariant natural killer T (iNKT) cells (36). What are iNKT cells? How do they develop, and what roles do they play in modulating immunity and tissue homeostasis? These questions will be answered in detail in the next section.

Introduction to Invariant Natural Killer T Cells

Natural killer T cells are innate-like T cells that recognize glycolipid antigens in the context of the MHC class I-like molecule CD1d (37). There are two major categories of natural killer T cells: invariant natural killer T (iNKT) cells and type II natural killer T cells. The development of both types of natural killer T cells depends on the expression of the lineage defining transcription factor promyelocytic leukemia zinc finger (PLZF) (38, 39). However, the two types of cells differ in the makeup of their T cell receptors (TCR). iNKT cells express a semi-invariant $\alpha\beta$ TCR, while type II natural killer T cells express diverse $\alpha\beta$ TCRs (40-43).

As part of the T cell lineage, iNKT cells undergo stage-wise development in the thymus. iNKT cells are positively selected on cortical thymocytes expressing CD1d during the DP stage of development (44). Following positive selection, iNKT cells mature through a series of stages that are classified by CD24, CD44, and NK1.1 expression: $CD24^+ CD44^- NK1.1^-$ stage 0 cells, $CD24^- CD44^- NK1.1^-$ stage 1 cells, $CD24^- CD44^+ NK1.1^-$ stage 2 cells, and $CD24^- CD44^+ NK1.1^+$ stage 3 cells (45-47). Of these stages, stage 0 and stage 1 cells are the most immature and have a highly proliferative phenotype, whereas stage 3 iNKT cells are the most mature and have a quiescent phenotype (45). PLZF expression is also tightly regulated during stagewise development, with stage 0 and stage 1 iNKT cells having the highest levels of PLZF and stage 3 cells having the lowest levels of PLZF (38, 39). Additionally, iNKT cell subsets have been reported in the thymus. These subsets are termed iNKT1, iNKT2, and iNKT17 cells and are classified by the expression of the transcription factors T-bet, GATA-3, and RORγt, respectively (44). Like the conventional T helper cell subsets, thymic iNKT cell subsets display distinct cytokine profiles, with iNKT1 cells producing high levels of IFNγ, iNKT2 cells producing high levels of IL-4, and iNKT17 cells producing high levels of IL-17 (44).

Each of the stages of iNKT development have unique metabolic requirements. Immature iNKT cells have higher glucose uptake and higher expression of the glucose transporter Glut1 compared to mature iNKT cells in the thymus (48, 49). This heightened reliance on glucose is thought to fuel the rapid proliferation of stage 0 and stage 1 iNKT cells (48). iNKT cells also rely on autophagy to control ROS levels and prevent cellular damage during development. Loss of the autophagy-related genes Atg5 and Atg7 leads to iNKT cell developmental arrest during the early stages of development (48, 50). Autophagy has also been shown to be a key regulator of cell cycle progression in thymic iNKT cells (50). Mitophagy, a specialized form of autophagy dedicated to the breakdown of mitochondria, regulates iNKT cell mitochondrial mass and mitochondrial reactive oxygen species (mtROS) production as the cells progress through development (48). In fact, iNKT cells lacking Atg7 show increased mitochondrial content and mtROS production compared to wild type cells (48), leading to increased rates of apoptosis in autophagy deficient iNKT cells (48, 50). Therefore, tight regulation of cellular metabolism is crucial to maintain proper iNKT cell development (49).
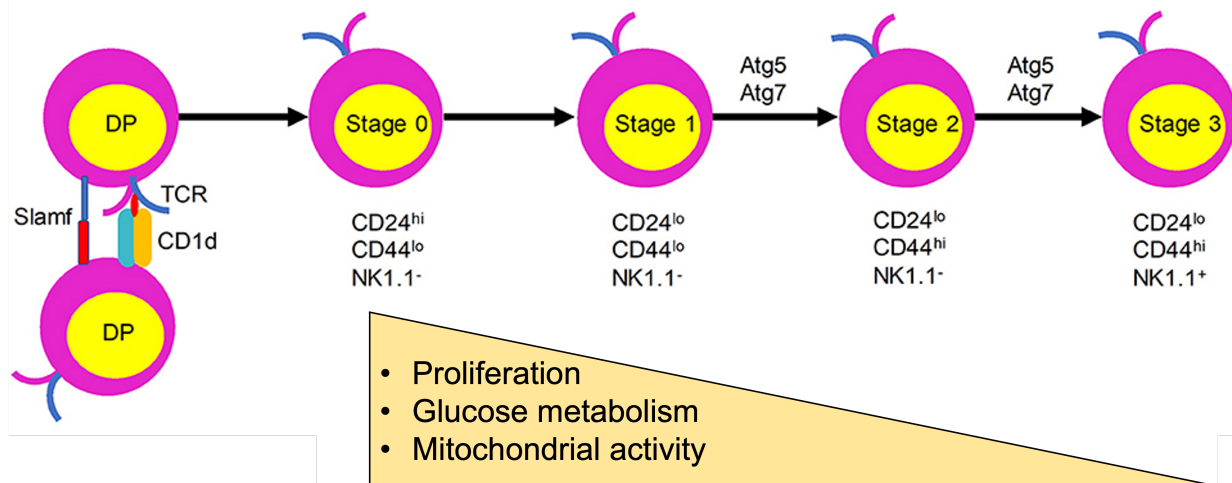
Figure 1.2 – Overview of iNKT cell thymic development.
iNKT cells are positively selected in the thymus by cortical thymocytes expressing CD1d. After positive selection, iNKT cells exit the DP stage as highly proliferative, immature stage 0 cells that express CD24. iNKT cells then undergo stagewise development characterized by the loss of CD24 expression but the gradual gain of CD44 and NK1.1 expression. Developing iNKT cells also become less proliferative and decrease their dependency on metabolic programs requiring high levels of glucose and mitochondrial activity as they mature. This shift towards metabolic quiescence is due to Atg5- and Atg7-mediated autophagic pathways. Finally, iNKT cells reach terminal maturation at stage 3. Adapted from Yang, Driver, and Van Kaer 2018 (49).

8

Mature iNKT cells exit the thymus and populate the peripheral tissues as effector cells capable of rapidly responding to antigen. The liver is home to a large depot of iNKT cells, with IFNγ-producing iNKT1 cells making up 40% of all T cells in this organ (51). iNKT1 cells are also enriched in the spleen, but these cells are balanced by the presence of iNKT2 and iNKT17 cells (51). The lungs, intestines, and lymph nodes exhibit a similar iNKT cell composition to the spleen (51). Some iNKT cells produce high levels of IL-10 (52), imparting a regulatory phenotype upon this group of cells. Regulatory iNKT cells are often termed iNKT10 cells, and these cells typically seed the adipose tissue. iNKT10 cells maintain adipose tissue homeostasis by clearing apoptotic adipocytes from fat depots, controlling adipose tissue-resident T cell and macrophage populations, and promoting an anti-inflammatory tissue microenvironment (51, 53-55). However, iNKT10 cells can also mediate harmful effects in the context of obesity and other metabolic syndromes (53). In all, iNKT cells maintain tissue homeostasis by acting as a lymphoid bridge between the innate and adaptive immune systems.

Scope of the Dissertation

Although Cul3 is required for iNKT cell development, the mechanisms by which Cul3 ensures proper iNKT cell development are unknown. Additionally, whether Cul3 plays a role in conventional T cell subsets beyond T regulatory cells and T follicular helper cells remains an open question. As such, I sought to address these gaps in knowledge during my thesis work. While expanding the mouse strains necessary to answer these questions, I pioneered a project focused on uncovering the role of iron in T cell-mediated immune responses. The background and context necessary to understand each of these projects can be found below.

Context for Chapter 2 – Characterization of Iron Homeostasis in CD4 T Cells

Regulation of iron metabolism is crucial for cell function. A cell can take up two different types of iron: transferrin-bound iron and non-transferrin-bound iron (NTBI). Transferrin-bound iron is taken up by the transferrin receptor (TfR1) via receptor-mediated endocytosis (56). Once inside intracellular vesicles, iron is freed from transferrin through the action of STEAP3, which reduces iron from its ferric (Fe^{3+}) to its ferrous (Fe^{2+}) form (57, 58). Ferrous iron then leaves intracellular vesicles through divalent metal transporter 1 (DMT1) and enters the cytosol (59). Ferric iron also exists in the extracellular environment as NTBI (60, 61). NTBI can be reduced to

ferrous iron by metalloreductases in the plasma membrane (62), allowing it to be taken up directly by DMT1 or the metal ion transport proteins ZIP8 and ZIP14 (59, 63, 64). Free iron in the cytoplasm is referred to as the labile iron pool (LIP). LIP can either be used directly by the cell, stored for future use, or exported from the cell. LIP serves as a cofactor for a variety of cellular enzymes, and LIP is crucial for maintaining proper function of the electron transport chain in the mitochondria (65). If a cell does not have an immediate need for iron, LIP is stored in ferritin molecules (66). Lastly, LIP is exported from the cell via ferroportin (Fpn), which is the only known iron export protein in mammalian cells (67, 68). An overview of cellular iron homeostasis is shown in Figure 1.3.

The role of iron in regulating CD4 and CD8 T cell activation and function has been historically understudied. Iron is critical for T cell development but not B cell development (69-71), indicating a unique role for iron in T cells. Previous work has also shown that iron is required for optimal T cell activation and proliferation (72-75). However, the mechanisms by
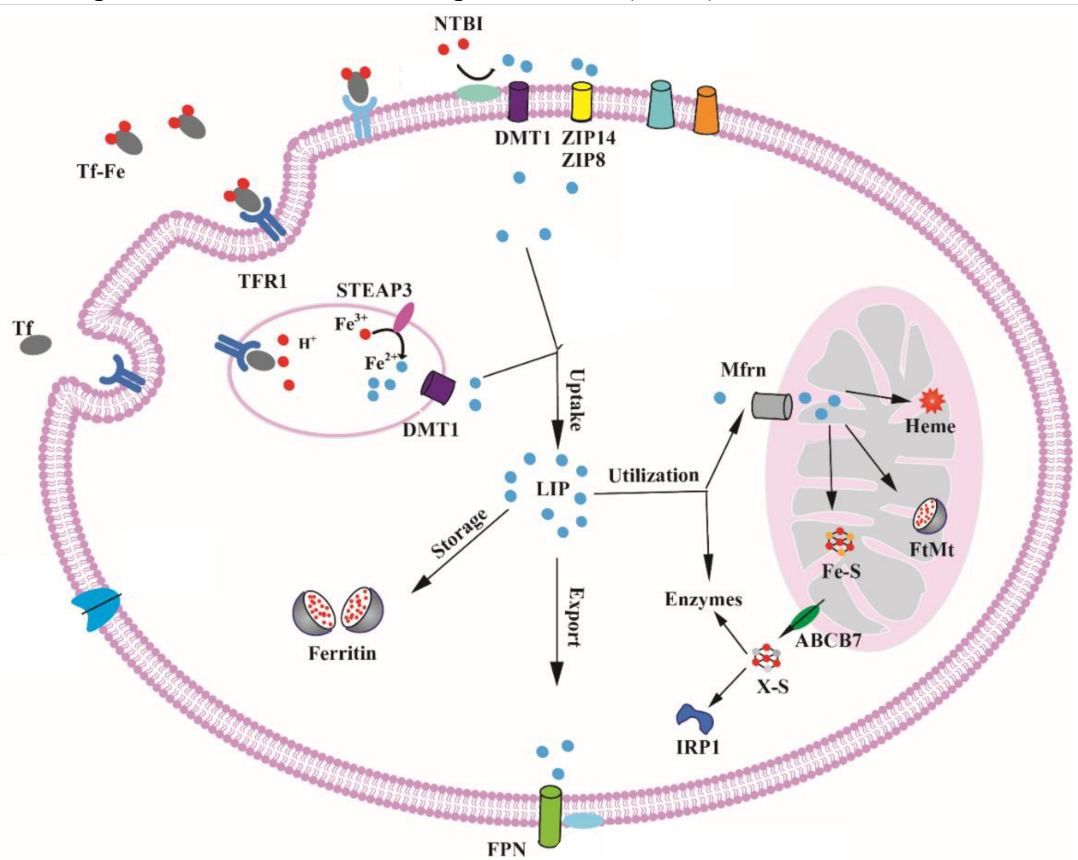

Figure 1.3 – Cellular regulation of iron.
Tf-Fe = transferrin-bound iron; NTBI = non-transferrin bound iron; TFR1 = transferrin receptor 1; DMT1 = divalent metal transporter 1; ZIP8/14 = ZRT/IRT-like proteins 8/14; LIP = labile iron pool; FPN = ferroportin. Adapted from Zhou et al. 2018 (65).

which iron regulates activation and proliferation in CD4 and CD8 T cells are unknown. We found that iron is dynamically regulated during CD4 T cell activation. We also showed that intracellular iron flux is crucial for maintaining mitochondrial function and IL-2 receptor signaling, which are essential for CD4 T cell proliferation after stimulation. Our approach and data supporting these conclusions are outlined in Chapter 2.

Context for Chapter 3 – Determining the Role of Cullin 3 in Regulating iNKT Cell Development

In recent years, Cul3 has emerged as a key regulator of iNKT cell development. T cell-specific deletion of Cul3 leads to iNKT cell developmental arrest (36). In the absence of Cul3, iNKT cell frequencies and numbers are extremely low in both the thymus and the periphery, with residual iNKT cells failing to acquire their classical effector phenotype (36). Cul3 is known to interact in complex with PLZF (36), the lineage defining transcription factor for iNKT cells. This interaction between Cul3 and PLZF is thought to facilitate the movement of Cul3 from the cytoplasm into the nucleus, where it can interact with and ubiquitinate various epigenetic modifiers (36). However, the mechanism(s) by which Cul3 controls iNKT cell development remain unknown. Additionally, whether the interaction between Cul3 and PLZF is necessary for iNKT cell development is unclear.

We sought to uncover mechanistic roles for Cul3 in iNKT cell development using a T cell-specific Cul3 deficient mouse model. We found that thymic Cul3 knockout (KO) NK1.1^{hi} iNKT cells, which represent stage 3 iNKT cells, proliferate and die more than wild type cells. We also found that Cul3 KO NK1.1^{hi} iNKT cells retain high levels of intracellular iron, potentially leading to their death by ferroptosis. In line with this, feeding a low iron diet to Cul3$^{fl/fl}$ CD4-Cre mice partially rescued both iNKT cell development and LIP levels in mature Cul3 KO iNKT cells. Additionally, preliminary data indicates that the interaction between Cul3 and PLZF is not directly related to iNKT cell development. These findings are outlined in more detail in Chapter 3.

Context for Chapter 4 – A Novel Role for Cullin 3 in Naive CD4 T Cell Maintenance

Cul3 has also been shown to modulate CD4 T cell differentiation. Unlike iNKT cells, conventional CD4 and CD8 T cells exit the thymus as naive cells. These cells remain quiescent until they encounter their cognate antigens in the periphery. Upon antigenic stimulation, CD4 T

cells proliferate and differentiate into various effector cell subsets to fight pathogens. Published work has shown that Cul3 represses both T regulatory cell development and T follicular helper cell responses (35, 36). However, the role of Cul3 in maintaining naive CD4 T cell homeostasis has yet to be explored. In Chapter 4, we show that Cul3 deficient naive CD4 T cells exhibit a pre-activated phenotype in the periphery, indicating a break in peripheral tolerance in the absence of Cul3. Although preliminary, our results indicate that Cul3 maintains naive CD4 T cell quiescence in the peripheral tissues.

Chapter 2 – Activation-Induced Iron Flux Controls CD4 T Cell Proliferation by Promoting Proper IL-2R Signaling and Mitochondrial Function

Abstract

Iron has long been established as a critical mediator of T cell development and proliferation. However, the mechanisms by which iron controls CD4 T cell activation and expansion remain poorly understood. Here, we show that stimulation of CD4 T cells from C57BL/6 mice not only decreases total and labile iron levels but also leads to changes in the expression of iron homeostatic machinery. Additionally, restraining iron availability *in vitro* severely inhibited CD4 T cell proliferation and cell cycle progression. Although modulating cellular iron levels increased IL-2 production by activated T lymphocytes, CD25 expression and pSTAT5 levels were decreased, indicating that iron is necessary for IL-2 receptor-mediated signaling. We also found that iron deprivation during T cell stimulation negatively impacts mitochondrial function, which can be reversed by iron supplementation. In all, we show that iron contributes to activation-induced T cell expansion by positively regulating IL-2 receptor signaling and mitochondrial function.

Introduction

As an essential microelement, iron takes part in a wide variety of physiological processes including erythropoiesis, DNA synthesis and repair, and immunity. Human disease states leading to either iron deficiency or iron overload have been shown to adversely affect the adaptive immune response (76, 77). As such, iron homeostasis is vital to the development of effective T cell-mediated immunity. In healthy individuals, most of the bioavailable iron in circulation is bound to

13

transferrin (Tf). These Tf-iron complexes are taken up by cells via transferrin receptor 1 (TfR1)-mediated endocytosis (56), and T cell surface expression of TfR1 increases after activation (78). In addition to TfR1-mediated iron import, T cells have also been shown to take up non-transferrin-bound iron (NTBI) (60, 61), which is known to occur through the action of several nonspecific metal ion transporters such as divalent metal transporter 1 (DMT1) and the ZRT/IRT-like proteins 8/14 (ZIP8/14) (59, 63, 64). Once in the cytosol, iron is freed from its binding partners and enters a redox active pool known as the labile iron pool (LIP), which can then be transported to ferritin for storage (66) or used as a cofactor for other cellular proteins and enzymes. Alternatively, LIP can be directly released by the cell through ferroportin (Fpn), the only known iron exporter in mammalian cells (67).

Dysregulation of the iron homeostatic pathway can be detrimental to T cells. Early thymocyte differentiation and maturation are dependent on iron acquisition via TfR1, and the absence of TfR1 has been shown to lead to T cell developmental arrest (69, 70). Additionally, iron deficiency impairs both the activation status and proliferative capacity of peripheral T lymphocytes (73, 74). Nevertheless, the exact mechanism by which iron regulates T cell proliferation remains unclear. Here, we show that T cell activation mobilizes intracellular iron stores, which promotes proper CD4 T cell expansion by fueling IL-2 receptor (IL-2R) signaling and mitochondrial function after stimulation.

Materials and Methods

Mice

Male and female C57BL/6 mice ranging from 8-12 weeks of age were either bred in-house or purchased from Jackson Laboratories. Mice were housed in specific pathogen free conditions. All animal experiments were performed in accordance with the Institutional Animal Care and Use Committee of the University of Michigan.

Cell Isolation, Purification, and Culture

CD4 T cells were enriched from murine splenocytes and human PBMC using a positive selection kit according to the manufacturer's instructions (Miltenyi Biotec). T cells were activated with plate-bound αCD3 (5 μg/mL) and soluble αCD28 (1 μg/mL for murine studies; 2 μg/mL for human studies) antibodies (eBioscience) for an indicated time in RPMI 1640 medium

supplemented with 10% FBS, 2 mM glutamine, and penicillin/streptomycin at 37°C. Cells were treated with the indicated amounts of deferoxamine mesylate (DFO) (Sigma Aldrich) or ferric ammonium citrate (FAC) (Sigma Aldrich) during certain experiments. 50 units of recombinant IL-2 (PeproTech) was used for all IL-2 supplementation experiments. For cell proliferation, CD4 T cells were labeled with CellTrace^{TM} Violet (CTV) (5 µM) (Invitrogen) in 1X PBS containing 0.1% BSA for 30 min at 37°C.

Flow Cytometry Assays

The fluorescently-conjugated antibodies used for surface and intracellular staining in the presence of anti-FcγR mAb (2.4G2) were: anti-mouse TCR-β (H57-597) Pacific Blue/APC, anti-mouse CD4 (GK1.5) APC-Cy7, anti-mouse CD8 (53-6.7) PE-Cy7, anti-mouse CD71 (R17217) FITC/PerCP-Cy5.5, anti-mouse CD25 (PC61.5) PerCP-Cy5.5/PE-Cy7, anti-mouse CD69 (H1.2F3) PE-Cy7, and IL-2 (JES6-5H4) PE (all from eBioscience).

For Fpn, fixed cells were incubated with metal transporter protein antibody (rabbit anti-mouse MTP1/IREG1/Ferroprotein, Fpn) (Alpha Diagnostic) in flow cytometry buffer. Ferritin expression was measured by anti-mouse ferritin (EPR3004Y) (Abcam) staining in permeabilization buffer after fixation. To analyze STAT5 phosphorylation, cells were fixed in 80% methanol and stained with rabbit anti-mouse pSTAT5 (Tyr694) (Cell Signaling) antibody. In all stainings, AF488-conjugated anti-rabbit secondary antibody (Invitrogen) was used. For intracellular cytokine expression, stimulated CD4 T cells were re-stimulated with 50 ng/mL of PMA (Sigma Aldrich) and 1.5 µM Ionomycin (Sigma Aldrich) in the presence of 3 µM Monensin for 4 h, followed by intracellular cytokine staining (BD Biosciences). Dead cells were excluded from the analysis based on propidium iodide (PI) (1 µg/mL) or LIVE/DEAD ^{TM} Fixable Aqua Dead Cell Stain (Invitrogen) signal. To measure cell cycle progression, cells were fixed with 70% ethanol then stained with 50 ng/mL PI for 15 min. Cells were acquired on a FACS Canto II (BD Bioscience) and data was analyzed using FlowJo (TreeStar software ver. 10.5).

Trace Element Analysis

Enriched CD4 T cells were split into replicates containing 1 x 10^6 live cells each and spun down. After removing the supernatant, the cells were analyzed for metals by inductively coupled plasma mass spectrometry (ICP-MS) as described previously (79).

Labile Iron Pool (LIP)

To measure LIP, cells were stained with calcein-acetomethoxy (Calcein-AM) dye (0.02 µM) (Thermofisher) for 10 min at 37°C and analyzed by flow cytometry. LIP was calculated based on the ratio of Calcein mean fluorescent intensity (MFI) of control vs. test samples.

qPCR Assay

Total RNA was isolated from both unstimulated and stimulated CD4 T cells using the RNeasy Plus mini kit (Qiagen) according to the manufacturer's instructions. cDNA was synthesized and qPCR was performed using SYBR Green with Applied Biosystem's 7500HT Sequence Detection System. Fold changes were calculated from ΔCt values using the ΔΔCt method. Expression of target genes was normalized to β-actin.

ELISA

Supernatants were collected from CD4 T cells stimulated with or without DFO for 3 days. ELISA assays were done in conjunction with the University of Michigan ELISA core.

Mitochondrial Function

Mitochondrial potential, mitochondrial mass, and mitochondrial ROS (mtROS) were measured using tetramethylrhodamine methyl ester perchlorate (TMRM) (60 nM) (Invitrogen), MitoTracker[TM] Green (30 nM) (Invitrogen), and MitoSOX (2.5 µM) (Invitrogen), respectively. Cells were then analyzed by flow cytometry.

Statistical Analysis

All graphs were prepared using Prism software (Prism version 7; Graphpad Software, San Diego, CA). For comparison among multiple groups, data was analyzed using one-way ANOVA with multi-comparison post-hoc test. For comparison between two groups, unpaired Student t-tests were used. $P < 0.05$ was considered statistically significant.

Results

T cell activation changes intracellular iron homeostasis

The degree to which CD4 T cells require biometals for their maintenance and function is poorly understood. We used inductively coupled plasma mass spectrometry (ICP-MS) to measure the levels of several metals in unstimulated CD4 T cells. Interestingly, resting CD4 T cells contain significantly higher amounts of intracellular iron than any other tested metal (Table 2.1). Furthermore, ICP-MS analysis revealed that CD4 T cells drastically downregulate total intracellular iron levels after activation (Fig. 2.1A), which corresponds with accumulation of iron in the media over time (Fig. 2.1B). Because ICP-MS detects both protein-bound iron and LIP, we examined whether conventional αβ T cell subsets maintain distinct levels of LIP at steady state using Calcein-AM dye, a cell-permeable fluorescent probe that binds to free iron in the cytoplasm (Fig. 2.2A). We found that CD4 T cells contain lower levels of LIP than CD8 T cells (Fig. 2.1C), prompting us to investigate what happens to LIP following T cell activation. The data showed that CD4 T cells steadily downregulate LIP over time after stimulation (Fig. 2.1D, top panel; Fig. 2.2A), and this reduction of LIP can be observed as early as 2 h after receiving a TCR stimulus (Fig 2.2B). Activation-induced downregulation of LIP appears to be conserved across the T cell lineage, as CD8 T cells also reduce LIP after stimulation (Fig. 2.1D, bottom panel). This phenomenon was found to occur in human CD4 T cells as well (Fig. 2.1E).

We next investigated whether other iron homeostatic processes are influenced by TCR stimulation. We began by examining changes in TfR1 and found that both mRNA and protein levels are dramatically upregulated after activation, with peak expression occurring at 2 days

Table 2.1 – T cells contain high basal levels of Fe.

	Fe	Zn	Cu	Mn	Se	Pb	Cd	Co
Average	193.88	N.D.	0.06	1.54	0.01	N.D.	0.01	N.D.
STDEV	348.78	N.D.	0.61	3.42	0.17	N.D.	0.07	N.D.

Splenic CD4 T cells were enriched and analyzed for biometals by inductively coupled plasma mass spectrometry (ICP-MS). The average detected amount of the indicated metals is reported above in parts per billion (ppb) per 1×10^6 cells. Data is cumulative of 5 independent experiments. N.D. = not detected.
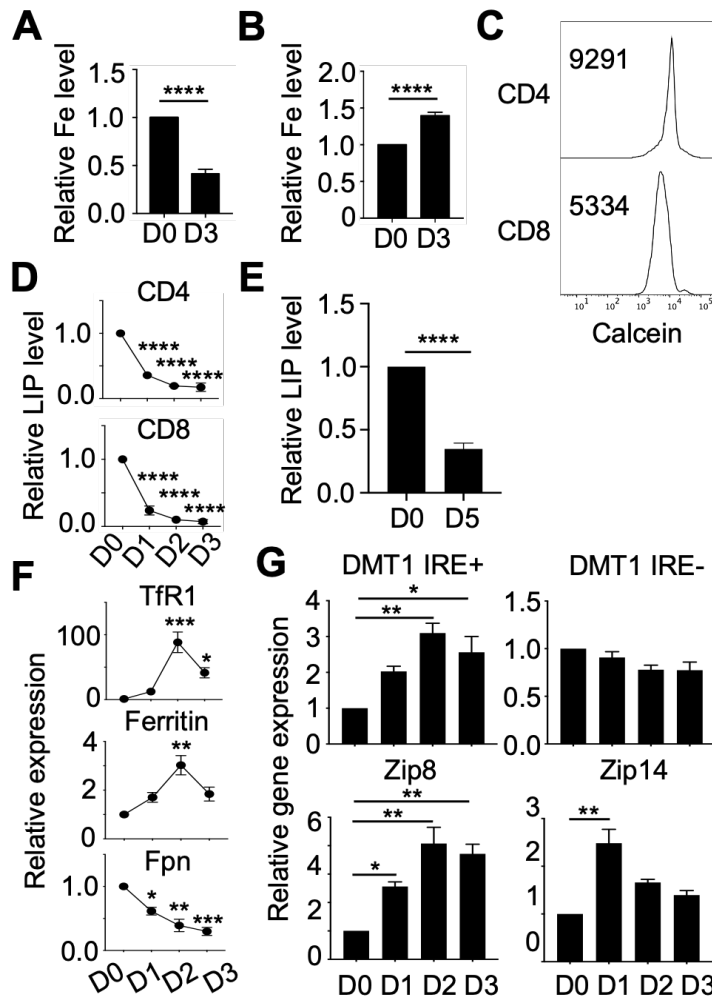
Figure 2.1 – Iron homeostasis is dynamically regulated during T cell activation.
(A) Both unstimulated (D0) and stimulated (D3) CD4 T cells were subjected to ICP-MS analysis. The graph shows the fold change in total iron level [reported in parts per billion (ppb) per 1 x 10^6 cells] relative to D0. (n=6) (B) Enriched CD4 T cells were stimulated for 3 days, and total iron levels were measured in both fresh media (D0) and media collected from cell cultures (D3). (n=3) (C) Splenocytes were stained with 0.02 μM Calcein-AM dye and analyzed via flow cytometry. Representative histograms show the LIP levels in CD4 and CD8 T cells as a function of mean fluorescent intensity (MFI) of Calcein. (n=3) (D) Splenocytes were stimulated with αCD3/αCD28 antibodies after B cell depletion with αCD19 magnetic beads. Representative graphs show the LIP levels in CD4 and CD8 T cells over time post-activation relative to D0. (E) Bar graph illustrates the LIP level in human CD4 T cells at day 5 (D5) relative to that at D0. (n=4) (F) Enriched CD4 T cells were stimulated for up to 3 days and stained for TfR1, ferritin, and Fpn as described in the Materials and Methods. Graphs show the change in expression of each of the aforementioned proteins relative to D0. (n=3) (G) Bar graphs represent the relative gene expression from both unstimulated and stimulated CD4 T cells over time, which was calculated as described in the Materials and Methods. (n=3). Error bars represent mean ± SEM. All statistics were performed by comparing each time point to D0. *p<0.05, **p<0.005, ***p<0.0005, ****p<0.0001.

post-stimulation (Fig. 2.1F, top panel; Fig. 2.2C and 2.2D, left panels). Additionally, mRNA expression of the NTBI transporters Zip8 and Zip14 as well as the iron-response element (IRE)-containing isoform of DMT1 was increased over time after T cell activation, whereas expression of the IRE-null isoform of DMT1 was unchanged (Fig. 2.1G). We next asked whether activated T cells have increased capacity to store iron by measuring ferritin expression. Although ferritin mRNA levels decreased over time after T cell stimulation (Fig. 2.2D, middle panels), ferritin protein expression increased (Fig. 2.1F and Fig. 2.2C, middle panels). To understand whether the decrease in both total iron and LIP levels following activation is due to iron export, we measured Fpn expression. Unexpectedly, both Fpn mRNA (Fig. 2.2D, right panel) and protein (Fig. 2.1F, bottom panel; Fig. 2.2C, right panel) expression were drastically decreased following stimulation, indicating that Fpn-mediated export is not the main mechanism of iron export in activated T cells. Taken together, our results show that T cells actively take up, store, and export iron during the response to TCR stimulation.

Iron chelation sustains high LIP levels and prevents T cell proliferation

Our data showing the downregulation of iron after activation prompted us to further investigate the role of TCR signaling strength on total iron levels. We observed that strong TCR stimuli decreased cellular iron levels dramatically whereas weak TCR stimuli had only a negligible effect on total iron amount (Fig. 2.3A). LIP levels were also impacted by TCR signaling strength, with only strong TCR stimuli prompting both a dramatic decrease in LIP and efficient T cell proliferation (Fig. 2.3B). This data revealed that LIP levels are inversely correlated with activation-induced proliferation, and this phenomenon is dependent on the strength of the TCR stimulus (Fig. 2.3B). Next, we sought to examine whether CD28 signaling also contributes to the regulation of iron homeostasis. We found that CD28 signaling had only a marginal effect on the downregulation of LIP, and that TCR signaling alone was sufficient in reducing LIP levels after T cell activation (Fig. 2.3C).

The relationship between intracellular iron levels and T cell proliferation prompted us to examine whether modulating iron levels in culture affects CD4 T cell expansion. We found that treatment with the iron chelator deferoxamine mesylate (DFO) significantly inhibited activation-induced downregulation of both total iron levels and LIP levels (Fig. 2.3D and 2.3E). Additionally, DFO treatment inhibited proliferation in a dose-dependent manner, leading to an

inverse correlation between T cell proliferation and LIP levels at either high or low concentrations of DFO (Fig. 2.3E). DFO treatment also reduced CD4 T cell numbers (Fig. 2.4A), consistent with the observed block in T cell proliferation. Similarly, DFO treatment severely inhibited human CD4 T cell proliferation (Fig. 2.3F) while simultaneously stabilizing LIP levels (Fig. 2G). In addition to its effects on LIP, exposure to DFO led to a reduction in the surface expression of TfR1, ferritin, and Fpn in activated T lymphocytes (Fig. 2.4B). In all, strong TCR stimuli induce rapid mobilization of iron within the cell that correlates with downstream proliferation.
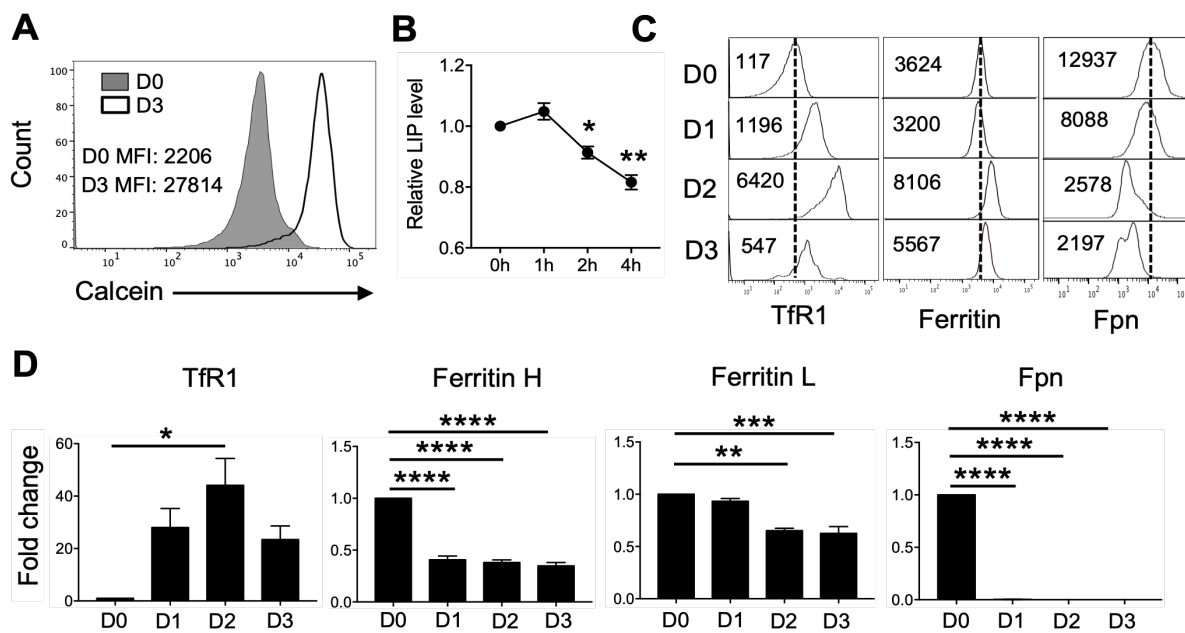

Figure 2.2 – T cell activation leads to dynamic changes in iron homeostatic machinery.
(A) CD4 T cells were enriched and stimulated for 3 days with αCD3/αCD28 antibodies. Both unstimulated (D0) and stimulated (D3) CD4 T cells were stained with 0.02 µM Calcein-AM dye to examine labile iron pool (LIP) levels. As Calcein binds iron, the fluorescent signal is quenched, leading to a concomitant decrease in mean fluorescent intensity (MFI). As such, high levels of Calcein correlate with low LIP levels. Histograms are representative of at least 3 independent experiments. (B) Enriched CD4 T cells were stimulated for up to 4 h with αCD3/αCD28 and stained with 0.02 µM Calcein-AM dye. The graph is cumulative of 3 independent experiments. (C) Enriched CD4 T cells were stimulated for up to 3 days and stained for TfR1, ferritin, and Fpn as described in the Materials and Methods. Representative histograms show the change in expression of each of the aforementioned proteins. The numbers in each frame represent the MFI at the designated time point. (n=3) (D) mRNA from both unstimulated (D0) and stimulated (D1, D2, D3) CD4 T cells was prepared and probed for TfR1, ferritin heavy chain (Ferritin H), ferritin light chain (Ferritin L), and Fpn expression. The bar graphs show the fold change in expression of each of these genes relative to β-actin. (n=3). Error bars represent mean ± SEM. All statistics were performed by comparing each time point to time 0 (0h or D0). *p<0.05, **p<0.005, ***p<0.0005, ****p<0.0001.
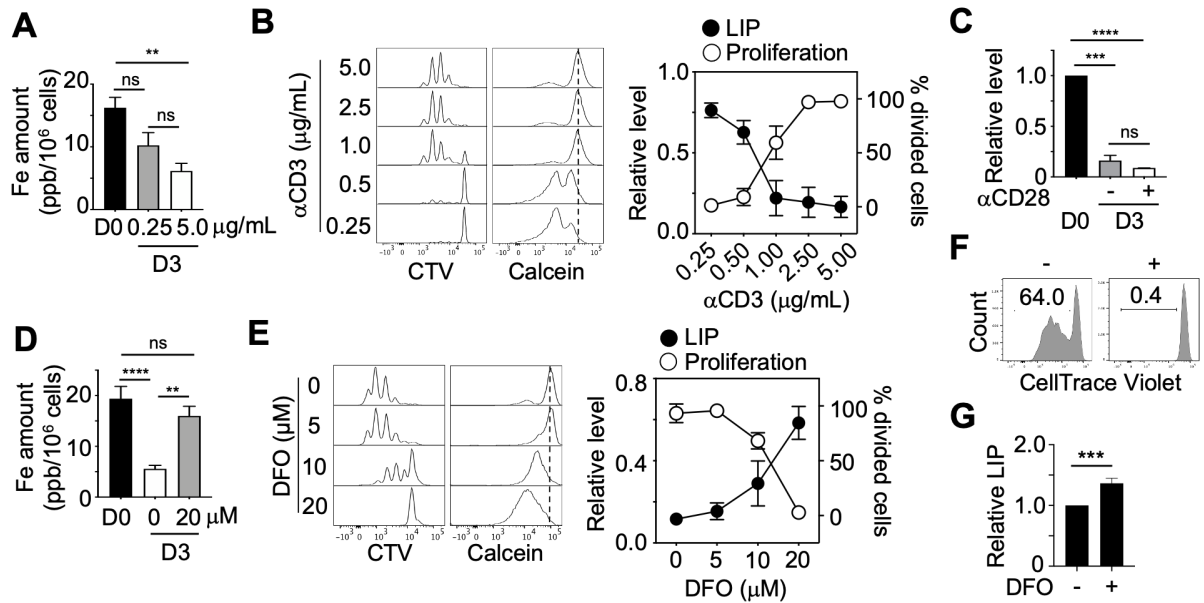
Figure 2.3 – T cell proliferation correlates with downregulation of intracellular iron levels.
(A) The bar graph represents total iron levels in CD4 T cells that were freshly isolated or stimulated for 3 days with either 0.25 µg/mL or 5 µg/mL αCD3. (n=3) (B) CD4 T cells were stained with CellTrace Violet (CTV) and stimulated for 3 days with the indicated concentrations of αCD3. Representative histograms show both the change in Calcein signal and cell proliferation as measured by CTV dilutions under each of the indicated stimulation conditions. (n=3) (C) CD4 T cells were stimulated for 3 days with either αCD3 only or both αCD3/αCD28. The bar graph shows relative LIP levels. (n=3) (D) CD4 T cells were stimulated for 3 days in the presence (20 µM) or absence (0 µM) of DFO. The bar graph shows the total iron levels of cells from each of the aforementioned culture conditions. (n=3) (E) CD4 T cells were stained with CTV and stimulated for 3 days in the presence of the indicated concentrations of DFO. Representative histograms show both the change in Calcein signal and cell proliferation as measured by CTV dilutions at each of the indicated DFO concentrations. (n=3) (F) Representative histograms show human CD4 T cell proliferation using CTV dilutions with (+) or without (-) 10 µM of DFO after 4 days of activation. (n=4) (G) The bar graph shows the LIP level in human CD4 T cells at day 4 post-activation with and without DFO. All graphs are cumulative of at least 3 independent experiments. Error bars represent mean ± SEM. **p<0.005, ***p<0.0005, ****p<0.0001, ns: not significant.

Iron controls T cell proliferation by favoring optimal IL-2 receptor signaling

The profound effect of iron availability on proliferation prompted us to investigate possible mechanisms by which iron may be controlling T cell expansion. We began by asking whether CD4 T cells are properly activated when iron availability is limited. To test this, we measured the expression of the activation markers CD25 and CD69 on DFO-treated CD4 T cells. The results showed that iron chelation reduced CD25 but not CD69 expression (Fig. 2.5A and
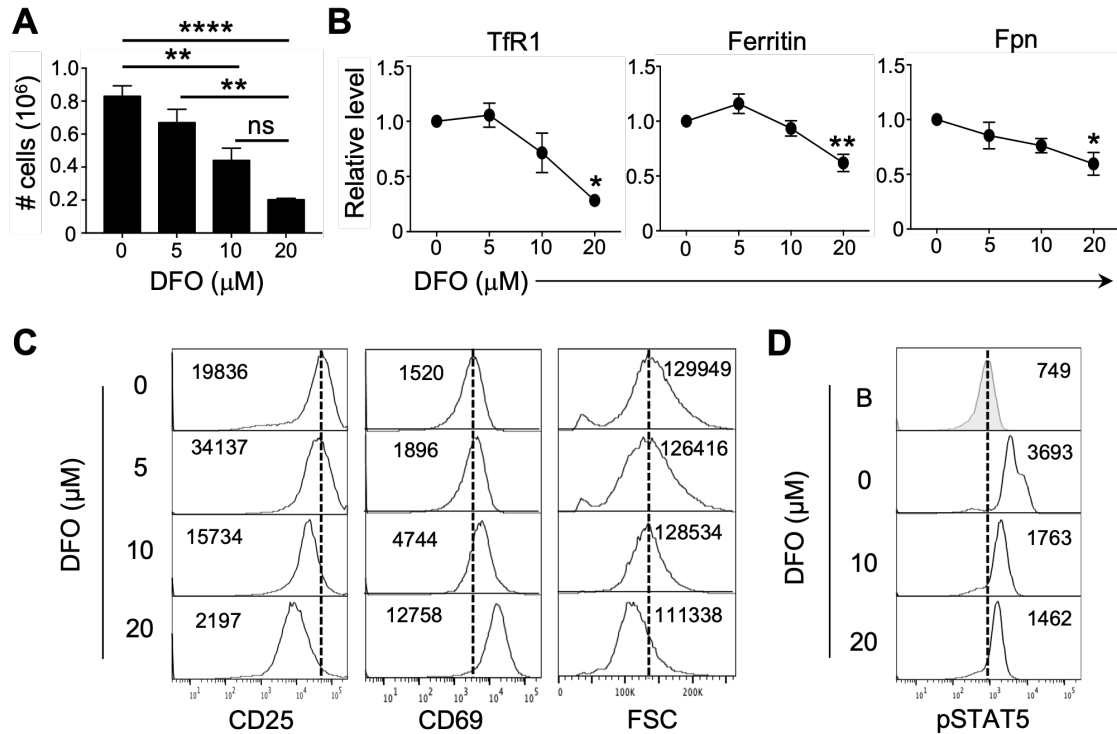
Figure 2.4 – T cell activation is blunted in the presence of iron chelators.
(A) Live CD4 T cells were counted via hemocytometer based on Trypan Blue exclusion. Bar graph represents the pooled cell count data from CD4 T cell cultures treated with the indicated concentrations of DFO. (n=4) (B) Splenic CD4 T cells were enriched and stimulated with αCD3/αCD28 antibodies for 2 days in either the presence (5 µM, 10 µM, and 20 µM) or absence (0 µM) of DFO. Cells were then stained for TfR1, ferritin, and Fpn as described in the Materials and Methods. Graphs are representative of 3 independent experiments. Statistics in (B) were performed by comparing each DFO concentration to the DFO-free condition (0 µM). (C) Representative histograms show the expression of CD25 (n=3) and CD69 (n=5) as well as cell size (FSC) (n=3) in enriched CD4 T cells at each of the indicated DFO concentrations relative to untreated cells. Numbers in each frame represent the mean fluorescent intensity (MFI) at the designated DFO treatment condition. (D) Splenic CD4 T cells were stimulated for 48 h with αCD3/αCD28 in the presence of 0 µM, 10 µM, or 20 µM DFO and analyzed for pSTAT5 expression. Representative histograms show the expression of pSTAT5 at each of the indicated DFO treatment conditions. The blank (B) panel represents stimulated CD4 T cells that were not stained with pSTAT5 antibody. The numbers in each frame represent the MFI of pSTAT5 at the indicated condition. (n=3). Error bars represent mean ± SEM. *$p<0.05$, **$p<0.005$, ****$p<0.0001$, ns: not significant.

Fig. 2.4C). Additionally, DFO treatment had only a marginal effect on T cell growth as measured by FSC (Fig. 2.4C, right panel).

It is known that CD25 expression is dependent on both TCR signaling and IL-2 sensing (80). Additionally, IL-2 is known to be a critical mediator of T cell survival and proliferation (81). Therefore, we next asked whether iron regulates IL-2 synthesis. We hypothesized that DFO

treatment would decrease IL-2 production by activated T cells; however, CD4 T cells cultured in iron-deficient conditions secreted copious amounts of IL-2 (Fig. 2.5B). This was further supported by the fact that DFO treatment led to increased frequencies of IL-2$^+$ CD4 T cells (Fig. 2.5C). The observed accumulation of IL-2 in the media after activation may be due to the continuous secretion of cytokine by cells that do not have the capability to use it. As such, we hypothesized that DFO-treated cells do not produce enough IL-2 during early TCR stimulation. However, the addition of exogenous IL-2 to the culture media was not sufficient to overcome the antiproliferative effect of DFO (Fig. 2.5D), as shown previously (72).

Collectively, our data indicated that insufficient iron levels during T cell activation leads to defective IL-2R signaling. To determine whether the IL-2R signaling pathway was impaired by iron chelation, we analyzed phosphorylated STAT5 (pSTAT5) levels in DFO-treated CD4 T cells, as CD25 expression is governed by STAT5 (82). The data showed that DFO reduced the amount of pSTAT5 in activated CD4 T cells (Fig. 2.5E and Fig. 2.4D), suggesting that iron is necessary for optimal IL-2R signaling following T cell stimulation. Together, our findings show that iron modulates T cell proliferation by controlling intracellular IL-2 signaling rather than IL-2 production.

Iron is essential for increased mitochondrial function following T cell activation

To further study the role of iron in T cell biology, we examined whether iron chelation negatively impacts cell cycle progression. DFO treatment significantly decreased the percentages of activated T cells in the S and G$_2$ phases of the cell cycle (Fig. 2.6A), corroborating previous findings that DFO is a potent S phase inhibitor in T lymphocytes (75). Iron is also known to play a role in the generation of mitochondrial ROS (mtROS), which have been shown to be important for T cell activation (83). Therefore, we hypothesized that iron availability during stimulation may impact mitochondrial dynamics. Indeed, iron chelation led to a sharp decrease in mitochondrial mass, mitochondrial potential, and mtROS levels over time after T cell activation (Fig. 2.6B and Fig. 2.7A).
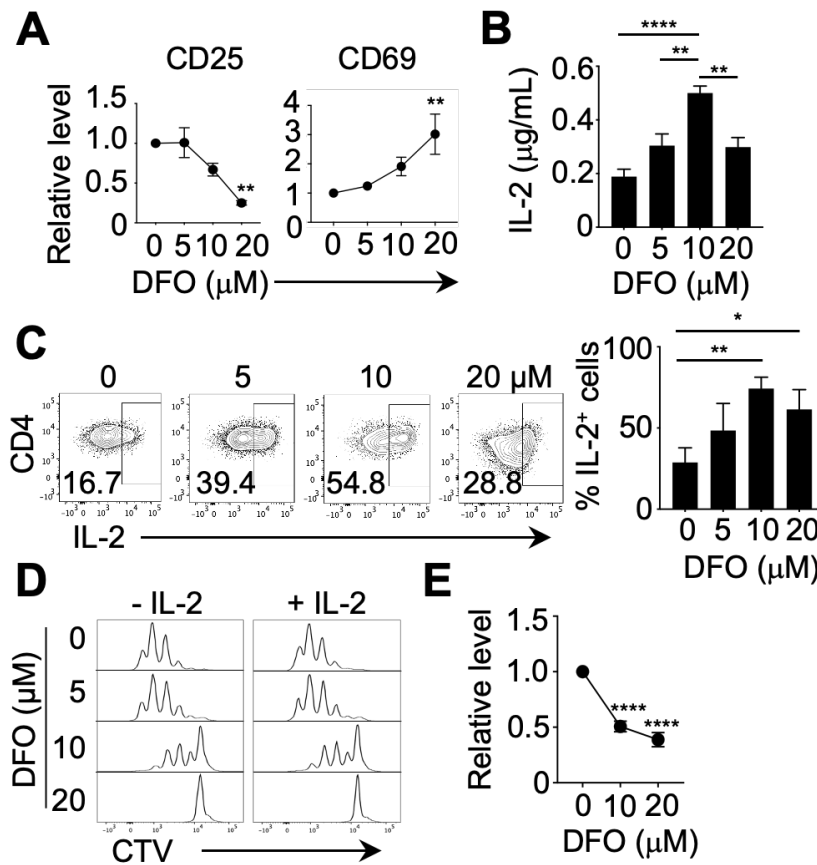
Figure 2.5 – Iron chelation does not affect IL-2 production by activated T cells.
(A-C) Enriched CD4 T cells were stimulated for 3 days in the presence (5, 10, 20 µM) or absence (0 µM) of DFO. (A) The graph represents the fold change in mean fluorescent intensity (MFI) of CD25 and CD69 at each of the indicated DFO concentrations relative to untreated cells. Statistics in (A) were performed by comparing each DFO concentration to untreated cells (0 µM). (n=3) (B) Graphs show IL-2 levels (µg/mL) in media collected from CD4 T cells as measured by ELISA. (n=3) (C) Representative dot plots show the % IL-2$^+$ CD4 T cells after 3 days of stimulation followed by re-stimulation with PMA and Ionomycin for 4 h. The bar graph shows the cumulative percentages of IL-2$^+$ cells from 3 independent experiments. (D) Enriched CD4 T cells were stained with CellTrace Violet (CTV) and stimulated in the absence (0 µM) or presence (5, 10, 20 µM) of DFO either with or without 50 units of recombinant IL-2. Representative histograms show cell proliferation at day 3 post-activation as measured by CTV dilutions. (n=3) (E) Enriched CD4 T cells were stimulated for 48 h in the presence (10 µM, 20 µM) or absence (0 µM) of DFO and stained for pSTAT5. The pooled graph shows pSTAT5 levels at each treatment condition. Statistics in (E) were performed by comparing DFO-treated conditions to the untreated (0 µM) condition. (n=3). Error bars represent mean ± SEM. *p<0.05, **p<0.005, ****p<0.0001.
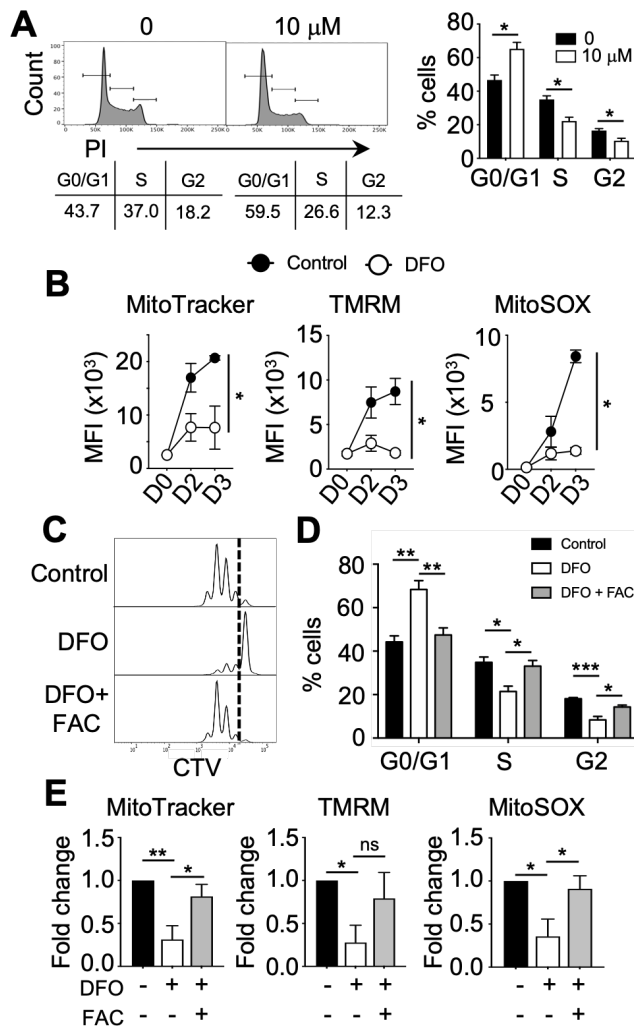
Figure 2.6 – Intracellular iron stores promote T cell proliferation by controlling mitochondrial function.
(A) Enriched CD4 T cells were stimulated in the presence or absence of 10 μM DFO for 48 h. Representative histograms show the percentage of cells in the G0/G1, S, and G2 phases of the cell cycle using PI. The bar graph shows the cumulative percentages of cells in each phase either with or without DFO treatment. (n=4) (B) Graphs show the pooled mean fluorescent intensities (MFI) of MitoTracker Green, TMRM, or MitoSOX in CD4 T cells stimulated for 3 days in the presence or absence of 10 μM DFO. (n=3) (C-E) CD4 T cells were stimulated either with or without 10 μM DFO. After 24 h of stimulation, 10 μM FAC was added to the DFO-treated cultures. (C) Representative histograms depict cell proliferation of CellTrace Violet (CTV)-stained CD4 T cells at day 3 post-activation. (n=3) (D) The bar graph depicts the cumulative percentages of CD4 T cells in the different phases of the cell cycle after 48 h of culture. (n=4) (E) Bar graphs show the fold change in MFI of MitoTracker, TMRM, and MitoSOX in CD4 T cells after 3 days of stimulation. Data are cumulative of 3 independent experiments. Error bars represent mean ± SEM. *$p<0.05$, **$p<0.005$, ***$p<0.0005$, ns: not significant.

Lastly, we investigated whether the adverse effects of DFO on mitochondrial function and proliferation could be reversed by the addition of exogenous iron. The results showed that iron supplementation via ferric ammonium citrate (FAC) treatment rescued cell proliferation in the presence of DFO (Fig. 2.6C). Furthermore, the negative effects of DFO on cell cycle progression were abrogated by the addition of iron to the culture media (Fig. 2.6D and Fig. 2.7B). FAC treatment also restored mitochondrial mass, mitochondrial potential, and mtROS production (Fig. 2.6E), further supporting a role for iron in maintaining mitochondrial biogenesis and function after stimulation.
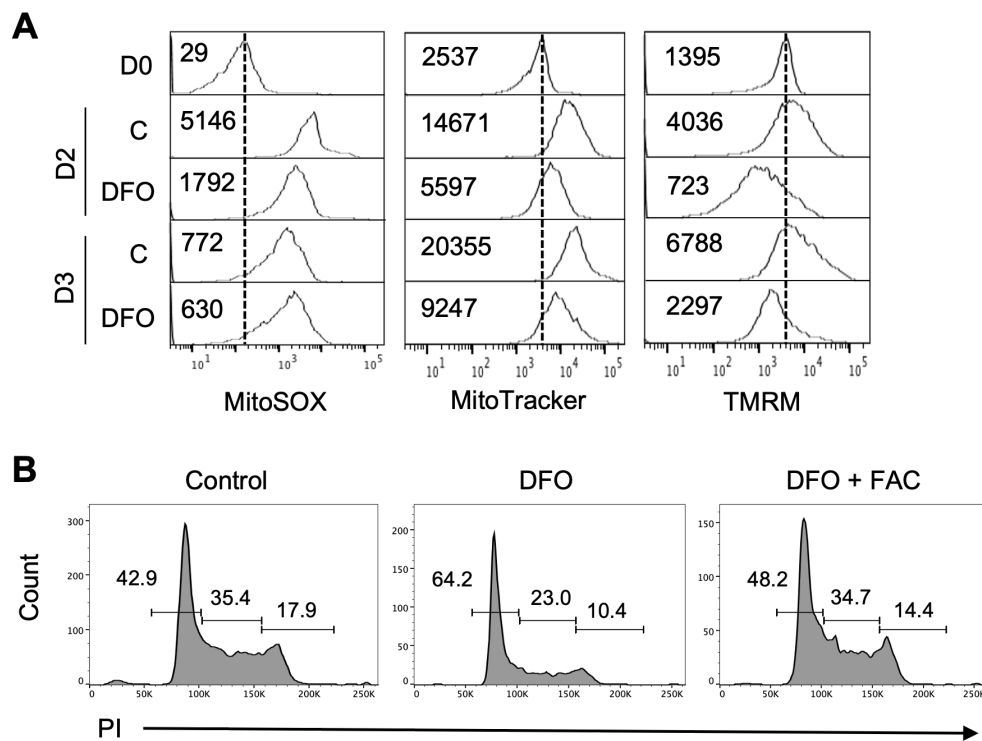
Figure 2.7 – Iron chelation negatively impacts mitochondrial function and cell cycle progression in activated T cells.
(A) Enriched CD4 T cells were stimulated in the presence (DFO) or absence (C) of 10 µM DFO for either 48 (D2) or 72 (D3) h. Representative histograms show the expression of MitoSOX, MitoTracker Green, and TMRM in CD4 T cells at each time point as a function of mean fluorescent intensity (MFI). The D0 panel denotes the staining pattern of each mitochondrial parameter in freshly isolated CD4 T cells. (n=3) (B) CD4 T cells were stimulated for 48 h either alone (control), in the presence of 10 µM DFO (DFO), or in the presence of 10 µM DFO and 10 µM FAC (DFO + FAC). Representative histograms show the percentage of cells in the G_0/G_1, S, and G_2 phases of the cell cycle by propidium iodide (PI) staining. (n=4).

Discussion

In summary, our findings indicate that intracellular iron levels impact T cell proliferation by promoting optimal IL-2R signal transduction and mitochondrial function. T cell activation leads to a drastic loss of intracellular iron, which ultimately results in accumulation of iron in the culture media. Together, these data suggest that T cells actively avoid iron overload during the response to TCR stimuli. Cells may try to prevent iron overload by exporting iron during activation; however, we showed that Fpn levels decrease dramatically after stimulation. Our findings suggest that T cells utilize a Fpn-independent mechanism of iron export. T cells are known to increase heme oxygenase 1 (HO-1) expression after activation, and overexpression of HO-1 has been shown to inhibit T cell proliferation (84). Therefore, it is possible that T cells try to prevent both iron overload and HO-1 overexpression during stimulation by exporting heme-bound iron. The heme-iron exporter feline leukemia virus subgroup C receptor 1 (FLVCR1) has been shown to be essential for T cell development and peripheral maintenance (85). Therefore, T cells may increase the export of heme-iron after activation via the action of FLVCR1; however, this possibility remains to be tested.

We also found that iron chelation suppresses TCR-induced expansion, and that this phenomenon was independent of the ability of the cell to produce IL-2. Instead, our results showed that IL-2R signaling in activated CD4 T cells depends on iron, as DFO treatment decreased pSTAT5 levels after stimulation. Interestingly, CD25 recycling after T cell activation occurs via the action of Tf^+ endosomes (80), indicating that CD25 expression after stimulation may be an iron-dependent process. Although the precise steps in the IL-2R signaling cascade that are affected by iron remain unknown, our data highlights a potential role for iron in regulating intracellular signaling in activated T cells.

The role of iron in immunity has been well established, particularly through the study of macrophage biology. It is well known that macrophages aid in the recycling of iron, and that this iron facilitates macrophage responses to intracellular and extracellular pathogens (86). Macrophage-mediated iron uptake has also been highlighted as a key mechanism of nutrient sequestration from tumor cells during the immune response to cancer (87). However, the role of T cell-derived iron metabolism in human disease states is relatively understudied. We found that CD4 and CD8 T cells maintain varying degrees of LIP during quiescence. Additionally, activation-induced reduction of LIP appears to be a lineage-wide phenomenon. Therefore, it is

possible that different T effector cell subsets require certain levels of iron for their function. Recent work has shown that iron overload can enhance T cell inflammatory cytokine production, leading to exacerbation of autoimmune diseases like EAE (88). Iron deficiency is also known to impair concanavalin A-induced T cell responses during acute liver inflammation (77). Therefore, the possibility that iron can modulate T helper cell differentiation in the context of human disease warrants further study and may open the door for the discovery of novel therapeutic strategies for patients.

Acknowledgements

Chapter 3 – Cullin 3 Promotes iNKT Cell Development and Survival by Maintaining Intracellular Iron Homeostasis

Abstract

The E3 ubiquitin ligase Cullin 3 (Cul3) has emerged as a critical regulator of invariant natural killer T (iNKT) cell development. iNKT cells lacking Cul3 have been shown to accumulate in the immature stages of development, and residual cells in both the thymus and the periphery fail to acquire an effector phenotype. However, the molecular mechanisms by which Cul3 mediates iNKT cell development are not fully understood. In this study, we sought to better characterize the role of Cul3 in iNKT cell development using NK1.1 expression to define immature and mature iNKT cell developmental stages. We found that NK1.1^{hi} iNKT cells lacking Cul3 proliferate and die more than wild type cells in the thymus. These cells also display aberrant metabolic phenotypes characterized by increased glucose metabolism and autophagy. Additionally, Cul3 deficient NK1.1^{hi} iNKT cells harbor higher levels of labile iron compared to wild type cells, which may contribute to cell death. In line with this idea, feeding a low iron diet to mice having a T cell-specific deletion of Cul3 partially restored both stage 3 iNKT cell frequencies and labile iron levels. Together, our data suggest that Cul3 promotes iNKT cell development and survival by regulating intracellular iron homeostasis.

Introduction

The E3 ubiquitin ligase Cullin 3 (Cul3) plays a key role in several processes in mammalian cells, including antioxidation, cell cycle progression, and differentiation. Cul3 interacts with BTB-domain containing adaptor proteins that allow Cul3 to specifically ubiquitinate and degrade target proteins (2). A classic example of how Cul3 modulates protein degradation is demonstrated by its role in the Cul3-Keap1-Nrf2 trimeric complex, which controls cellular redox states. Under normal conditions, Cul3 is connected to its target protein Nrf2 through the adaptor protein Keap1, allowing Cul3 to mediate the proteasomal degradation of

Nrf2 (18, 19). Under times of oxidative stress, this complex dissociates, allowing Nrf2 to evade ubiquitination and enter the nucleus. Once in the nucleus, Nrf2 activates a variety of antioxidation and detoxification genes. Similarly, Cul3 is known to work in concert with Cul1 to degrade cyclin E, modulating the transition from G_1 to S phase in proliferating cells (28, 29). Cul3 has also been shown to regulate neuronal development, adipogenesis, and myogenesis (89). However, the role of Cul3 in modulating the development and function of T cell-mediated immune responses is severely understudied.

Invariant natural killer T (iNKT) cells comprise an innate-like lineage of T cell that bridges both the innate and adaptive immune responses. iNKT cell development depends upon the expression of the lineage defining transcription factor promyelocytic leukemia zinc finger (PLZF) (38, 39). iNKT cells develop in the thymus, where they mature through 4 distinct stages: stage 0 ($CD24^+$ $CD44^-$ $NK1.1^-$), stage 1 ($CD24^-$ $CD44^-$ $NK1.1^-$), stage 2 ($CD24^-$ $CD44^+$ $NK1.1^-$), and stage 3 ($CD24^-$ $CD44^+$ $NK1.1^+$). Stage 0 and stage 1 iNKT cells are the most immature cells in the thymus, and these cells are characterized by having a high proliferative capacity, high glucose metabolism, and high mitochondrial activity (49). In contrast, stage 3 cells are the most mature cells, and these cells are quiescent (49). In contrast to conventional T cells, mature iNKT cells emerge from the thymus having an effector phenotype, allowing them to rapidly produce cytokines after encountering antigen (44). iNKT cells broadly recognize microbial glycolipid antigens in the context of the MHC class I-like molecule CD1d, allowing them to act as the first responders of the T cell-mediated immune response.

Cul3 has recently been shown to be a critical regulator of iNKT cell development. iNKT cells lacking Cul3 accumulate in the immature stages of development and fail to acquire the classical effector phenotype of iNKT cells (36). However, the mechanistic pathways by which Cul3 controls iNKT cell development remain unknown. Here, we show that Cul3 deficient $NK1.1^{hi}$ iNKT cells, which are analogous to stage 3 iNKT cells, proliferate and die more than wild type cells. Additionally, these cells display a metabolically active phenotype that is uncharacteristic of mature iNKT cells in the thymus. We also show that stage 3 iNKT cells lacking Cul3 exhibit an iron overloaded phenotype, suggesting that Cul3 plays a role in controlling iron homeostasis in developing iNKT cells. In line with this, a low iron diet partially reversed iron overload in Cul3 deficient $NK1.1^{hi}$ iNKT cells in the thymus. However, a low iron

diet did not completely restore iNKT cell development in Cul3 deficient mice, indicating that Cul3 regulates multiple pathways to ensure proper iNKT cell development.

Materials and Methods

Mice

       T cell-specific Cul3 deficient mice (Cul3$^{fl/fl}$ CD4-Cre, referred to as Cul3 KO) were generated by crossing Cul3$^{fl/fl}$ mice with CD4-Cre expressing mice maintained in our colony. PLZF$^{-/-}$ mice were generated by crossing PLZF$^{+/-}$ parents. In all experiments, either Cul3$^{fl/fl}$ or PLZF$^{+/+}$ littermates (referred to as WT) were used as controls. A mix of male and female mice ranging from 8-16 weeks of age were used in all experiments. All mice were bred in-house and kept in specific pathogen free conditions. All animal experiments were performed in accordance with the Institutional Animal Care and Use Committee of the University of Michigan.

Cell Isolation and Staining Conditions

       Thymi were mechanically disrupted and transferred onto a 100μm cell strainer to collect single cell suspensions. Homogenized thymocytes were treated with 1.66% NH_4Cl for 10 minutes to lyse RBCs, washed twice with 1X PBS, and resuspended in 1X PBS + 1% FBS (FACS buffer). iNKT cells were identified by flow cytometry by co-staining with TCR-β and PBS-57-loaded CD1d tetramers (NIH Tetramer Core). Complete media, defined as RPMI 1640 medium supplemented with 10% FBS, 2 mM glutamine, and penicillin/streptomycin, served as the staining medium for several of the assays used in this chapter.

Flow Cytometry Assays

       The fluorescently-conjugated antibodies used for surface and intracellular staining in the presence of anti-FcγR mAb (2.4G2) were: anti-mouse TCR-β (H57-597) APC/Pacific Blue, anti-mouse CD4 (GK1.5) PerCP-Cy5.5/APC-Cy7, anti-mouse CD8 (53-6.7) FITC/PE/PE-Cy7/Am Cyan, anti-mouse CD24 (M1/69) PE Texas Red, anti-mouse CD44 (IM7) FITC/PE/PerCP-Cy5.5, anti-mouse NK1.1 (PK136) PerCP-Cy5.5/PE-Cy7, anti-mouse CD127 (A7R34) PE-Cy7, anti-mouse CD122 (5H4) PE, anti-mouse CD5 (53-7.3) FITC/PE, anti-mouse CD71 (R17217) FITC/PerCP-Cy5.5, anti-mouse CD62L (MEL-14) BV605, anti-Ki-67 (SolA15) PerCP-Cy5.5, anti-mouse Nur77 (12.14) PE, anti-mouse PLZF (Mags.21F7) FITC/PE, anti-mouse RORγt

(AFKJS-9) Pacific Blue, and anti-mouse T-bet (eBio4B10) PerCP-Cy5.5. Antibodies were purchased from eBioscience, Biolegend, or BD Bioscience.

For Fpn, fixed cells were incubated with metal transporter protein antibody (rabbit anti-mouse MTP1/IREG1/Ferroprotein, Fpn) (Alpha Diagnostic) in FACS buffer. Ferritin, p62, and HK2 expression were measured by anti-mouse ferritin (EPR3004Y) (Abcam), anti-p62 (Sequestosome-1) (11C9.2) (Millipore Sigma), and anti-hexokinase II (EPR20839) (Abcam) staining, respectively, in cytoplasmic permeabilization buffer (BD Bioscience) after fixation. For ferritin and HK2, an AF488-conjugated anti-rabbit IgG secondary antibody (Invitrogen) was used. For p62, a PE-conjugated anti-mouse IgM secondary antibody (II/41) (Invitrogen) was used. Dead cells were excluded from the analysis based on propidium iodide (PI) (1 µg/mL), LIVE/DEAD ^{TM} Fixable Aqua Dead Cell Stain (Invitrogen), or LIVE/DEAD ^{TM} Fixable Yellow Dead Cell Stain (Invitrogen) signal. Cells were acquired on a FACS Canto II (BD Bioscience), and data was analyzed using FlowJo (TreeStar software ver. 10.8.1).

In Vivo BrdU Incorporation

Eight- to sixteen-week-old WT and Cul3 KO mice were injected twice intraperitoneally (6 h apart) with 0.5 mg of BrdU (Sigma-Aldrich) in 0.2 mL PBS. Approximately 18 h after the last injection, animals were euthanized, and single cell suspensions were prepared from thymi as described earlier. Following surface staining, 3×10^6 whole thymocytes were stained for BrdU incorporation using a BrdU flow kit (BD Bioscience) as per the manufacturer's protocol.

Annexin V Staining

To measure cell death via apoptosis, 3×10^6 whole thymocytes were stained for surface markers in the presence of anti-FcγR mAb (2.4G2). Cells were then washed with 1X Annexin V Binding Buffer (BD Bioscience) and stained with PE-conjugated Annexin V (Invitrogen) and PerCP-Cy5.5-conjugated 7-AAD (Invitrogen).

Metabolic Parameters

For each parameter, whole thymocytes (3×10^6) were incubated with each of the following reagents as indicated. Cells were analyzed by flow cytometry following all metabolic stainings.

Total cellular ROS was measured by staining for 2',7'-dichlorodihydrofluorescein diacetate (H_2DCFDA) (1 mM) (Invitrogen). Cells were treated with H_2DCFDA in complete media for 30 min at 37°C.

To measure glucose uptake, cells were incubated in 2-(N-(7-nitrobenz-2-oxa-1,3-diaxol-4-yl) amino)-2-deoxyglucose (2-NBDG) (Invitrogen) (20 µM) for 1 h at 37°C in glucose-free RPMI 1640 media containing 5% dialyzed FBS. HK2 expression was measured by incubating cells with HK2 antibody for 1 h at room temperature in the dark in cytoplasmic permeabilization buffer (BD Biosciences).

Mitochondrial potential, mitochondrial mass, and mitochondrial ROS (mtROS) were measured using tetramethylrhodamine methyl ester perchlorate (TMRM) (60 nM) (Invitrogen), MitoTracker™ Green (30 nM) (Invitrogen), and MitoSOX (2.5 µM) (Invitrogen), respectively. Cells were treated with MitoTracker™ Green and TMRM for 30 min and MitoSOX for 25 min at 37°C.

Lipid Peroxidation Assay

3 x 10^6 thymocytes were stained with 0.5X Lipid Peroxidation Sensor (Abcam) for 30 min at 37°C according to the manufacturer's instructions. Cells were then stained with surface markers in the presence of anti-FcγR mAb (2.4G2) and analyzed by flow cytometry.

Labile Iron Pool (LIP)

To measure LIP, 3 x 10^6 thymocytes were stained with calcein-acetomethoxy (Calcein-AM) dye (0.02 µM) (Thermofisher) for 10 min at 37°C and analyzed by flow cytometry. LIP was calculated based on the ratio of Calcein MFI of WT vs. Cul3 KO samples.

Low Iron Diet Studies

WT and Cul3 KO mice were placed on either AIN-93G Purified Rodent Diet (DYET #110700) (~35ppm iron) or Iron Deficient AIN-93G Purified Rodent Diet (DYET #115072) (3-5ppm iron) at weaning. Both chows were purchased from Dyets, Inc. Mice were kept on their assigned diets for 6 weeks, and all mice were weighed weekly. After 6 weeks of feeding, mice were sacrificed, and the indicated parameters were measured using 3 x 10^6 whole thymocytes.

Serum Iron Assay

Blood was collected from WT and Cul3 KO mice via cardiac puncture and rested in a standing position at room temperature for 30 min. Whole blood was then spun down at 1500g for 10 min at 4°C. After spin down, serum was collected. Serum iron levels were measured using the QuantiChrom™ Iron Assay Kit (BioAssay Systems) according to the manufacturer's protocol.

Statistical Analysis

All graphs were prepared using Graphpad Prism software (Prism version 9.2.0; Graphpad Software, San Diego, CA). For comparison among multiple groups, data was analyzed using one-way ANOVA with multi-comparison post-hoc test. For comparison between two groups, unpaired Student t-tests were used. $P < 0.05$ was considered statistically significant.

Results

Stage 3 iNKT cells exhibit a hyperproliferative phenotype in the absence of Cul3

Published work has shown that Cul3 deficiency leads to a dramatic reduction in thymic iNKT cell frequencies and numbers (36). These data suggest that Cul3 deficient thymic iNKT cells may proliferate less than wild type (WT) cells. Therefore, we examined spontaneous proliferation by staining for Ki-67, a marker of cells that have recently proliferated, in total thymic iNKT cells from either WT mice or mice having a T cell-specific deletion of Cul3 (Cul3$^{fl/fl}$ CD4-Cre, referred to as Cul3 KO). More Cul3 KO iNKT cells expressed Ki-67 than WT cells (Fig. 3.1A, left panels). We also investigated whether Cul3 deficient iNKT cells were actively undergoing proliferation in the thymus by staining for BrdU, a fluorescent nucleotide analog that incorporates into the DNA of proliferating cells. We found that thymic iNKT cells lacking Cul3 exhibited higher BrdU incorporation compared to WT cells (Fig. 3.1A, right panels). Together, these data indicate that Cul3 KO iNKT cells undergo uncontrolled proliferation in the thymus.

Previous work has shown that iNKT cells lacking Cul3 accumulate in the immature developmental stages (36). Thymic iNKT cells in stages 0 and 1, the most immature stages of iNKT cell development, are known to be highly proliferative (45, 49). Therefore, we next asked whether the observed increase in proliferation was due to the presence of more immature cells in the total iNKT cell population of Cul3 KO mice. To do this, we compared Ki-67 expression

between NK1.1 lowly expressing (NK1.1^{lo}) and NK1.1 highly expressing (NK1.1^{hi}) thymic iNKT cells after excluding CD24$^+$ cells from the analysis, as Cul3 deficiency does not affect stage 0 iNKT cell numbers (36). Therefore, NK1.1^{lo} cells represent both stage 1 and stage 2 iNKT cells, while NK1.1^{hi} cells represent stage 3 iNKT cells. Surprisingly, we found that the NK1.1^{hi} cell population is responsible for the increase in Ki-67 expression observed in total Cul3 KO iNKT cells (Fig. 3.1B, left panel). In fact, less Cul3 deficient NK1.1^{lo} iNKT cells in the thymus expressed Ki-67 compared to WT cells (Fig. 3.1B, right panel). These results suggest that Cul3 functions to restrain proliferation primarily in stage 3 iNKT cells in the thymus.
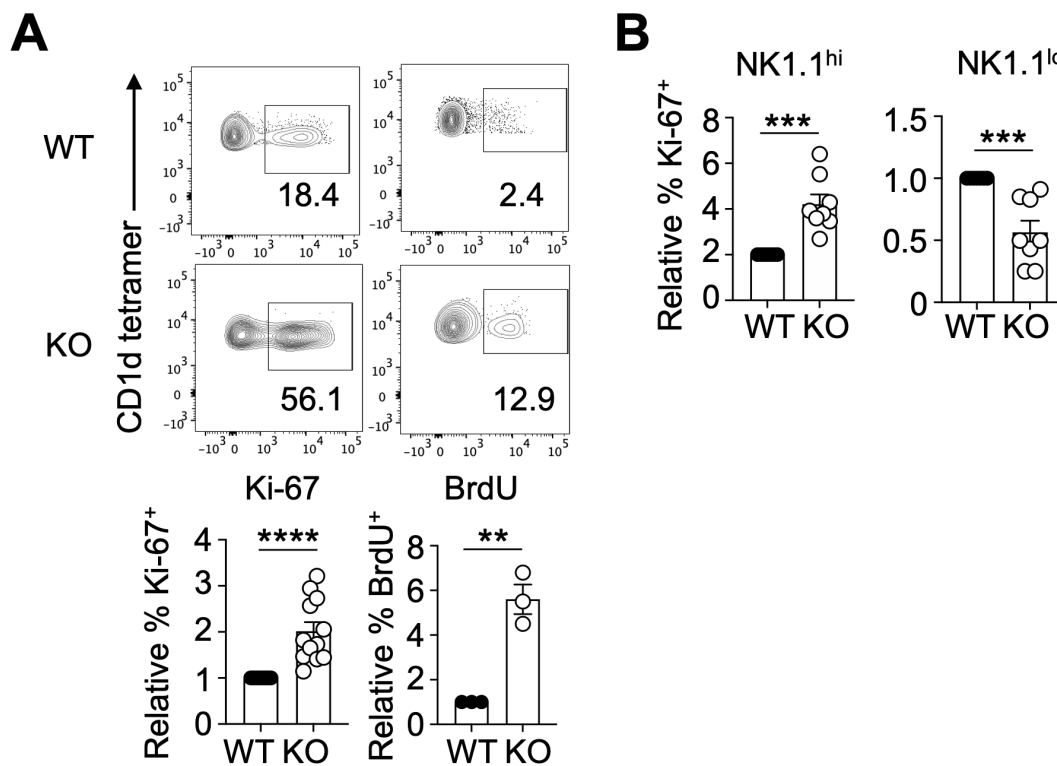
Figure 3.1 – Cul3 inhibits NKT cell proliferation during development.
(A) Representative dot plots show the % Ki-67$^+$ (left panels) and % BrdU$^+$ (right panels) iNKT cells present in whole thymocytes. Bar graphs show pooled data for Ki-67 (n=6) and BrdU (n=3). (B) Whole thymocytes from WT and Cul3 KO mice were stained for iNKT cell stagewise markers and Ki-67. Bar graphs illustrate the pooled data for % Ki-67$^+$ cells in either the NK1.1^{hi} or the NK1.1^{lo} iNKT cell populations. (n=3). Error bars represent mean ± SEM. **p<0.005, ***p<0.0005, ****p<0.0001.

Cul3 promotes thymic iNKT cell homeostasis through both TCR and cytokine receptor signaling

The observation that Cul3 deficient stage 3 iNKT cells proliferate more than WT cells prompted us to ask whether these cells were being activated by self-antigens in the thymus. We

began by measuring T cell receptor (TCR) expression on WT and Cul3 KO NK1.1^{hi} and NK1.1^{lo} iNKT cells. We found that Cul3 deficiency resulted in decreased TCR-β expression on both NK1.1^{hi} and NK1.1^{lo} cells (Fig. 3.2A). We wondered whether this decreased TCR-β expression impacted intracellular signaling downstream of the TCR. Therefore, we measured expression of CD5, a surface receptor that associates with the TCR and has been implicated as an indicator of proximal TCR signaling (90, 91). CD5 levels were not different between WT and Cul3 KO NK1.1^{hi} iNKT cells; however, NK1.1^{lo} iNKT cells lacking Cul3 displayed lower CD5 expression than WT cells (Fig. 3.2B). We also measured Nur77 expression by both NK1.1^{hi} and NK1.1^{lo}
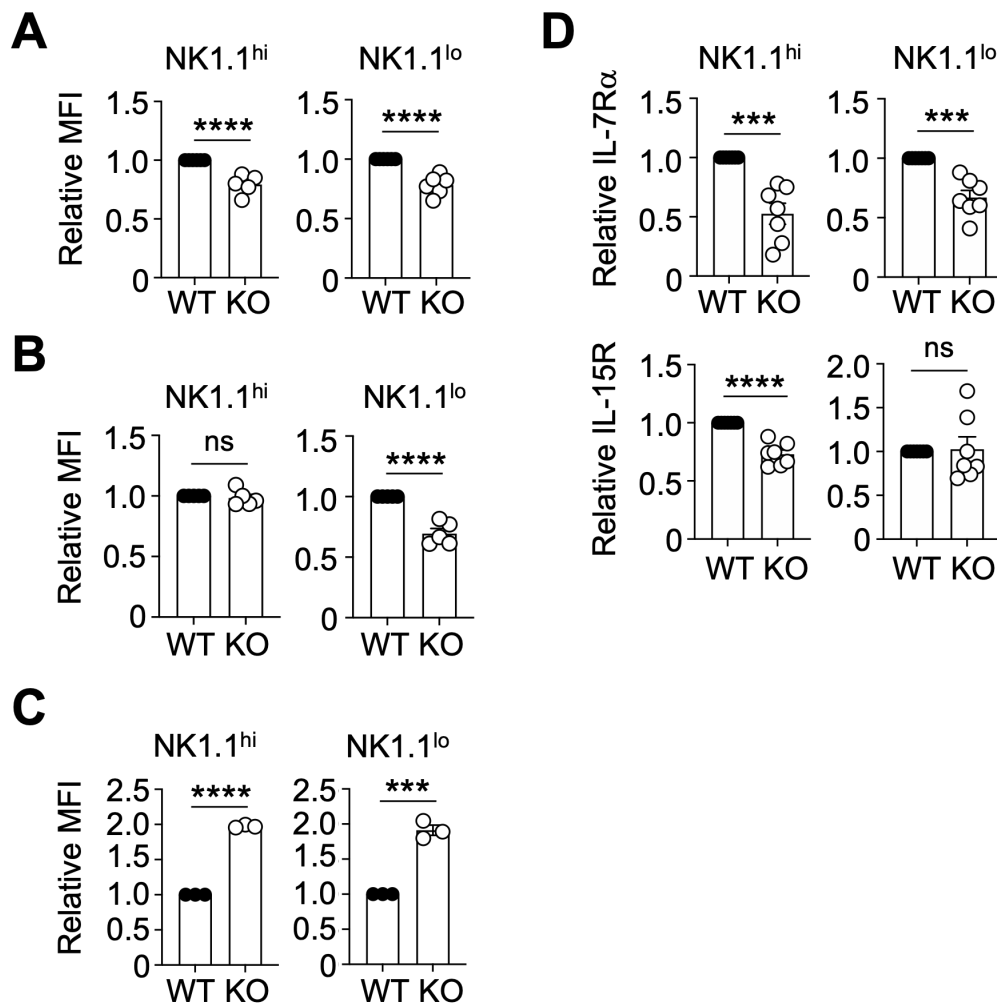
Figure 3.2 – Cul3 modulates TCR and cytokine receptor signaling in developing iNKT cells. Whole thymocytes from WT and Cul3 KO mice were stained for iNKT cell stagewise markers. Bar graphs show the fold change in mean fluorescent intensity (MFI) values of (A) TCR-β (n=4), (B) CD5 (n=3), (C) Nur77 (n=3), and (D) the cytokine receptors IL-7Rα and IL-15R (n=4) in either the NK1.1^{hi} or the NK1.1^{lo} iNKT cell populations. Error bars represent mean ± SEM. ***p<0.0005, ****p<0.0001, ns: not significant.

iNKT cells, as Nur77 is an indicator of TCR signaling strength downstream of the TCR (92). We found that Nur77 levels were higher in both groups of cells lacking Cul3 (Fig. 3.2C). These data indicate that Cul3 may play a larger role in restraining downstream TCR signaling than proximal TCR signaling in developing iNKT cells.

Increased proliferation in Cul3 deficient NK1.1^{hi} iNKT cells could also be explained by dysregulated cytokine receptor signaling during development. IL-7 receptor (IL-7Rα) signaling is crucial for the development of all T cell subsets, and IL-15 receptor (IL-15R) signaling has been highlighted as a key driver of iNKT cell development (93, 94). Therefore, we measured IL-7Rα and IL-15R expression on both NK1.1^{hi} and NK1.1^{lo} iNKT cells in the thymus. Although Cul3 deficiency decreased IL-7Rα expression on both NK1.1^{hi} and NK1.1^{lo} cells (Fig. 3.2D, top panels), IL-15R expression was specifically impaired on NK1.1^{hi} cells (Fig. 3.2D, bottom panels). Taken together, these data indicate that Cul3 may promote the maintenance of stage 3 iNKT cells through both TCR-mediated and cytokine receptor-mediated signaling pathways.

Cul3 deficiency impairs thymic iNKT subset distribution independently of PLZF expression

iNKT cells require expression of the transcription factor promyelocytic leukemia zinc finger (PLZF) to develop (38, 39). Cul3 and PLZF have been shown to interact in complex in the nuclei of iNKT cells, allowing Cul3 to ubiquitinate key epigenetic modifiers (36). However, PLZF has also been shown to be ubiquitinated, and this modification has important implications for its function (95). PLZF levels are known to be tightly regulated during iNKT cell development, with PLZF levels steadily decreasing as developing iNKT cells reach maturity (38). Therefore, degradation of PLZF during development appears to be crucial for iNKT cell survival and maturation. We hypothesized that Cul3 may ubiquitinate PLZF in iNKT cells, leading to proteasomal degradation of PLZF during iNKT cell development. To test this, we measured PLZF levels in WT and Cul3 KO thymic NK1.1^{hi} and NK1.1^{lo} iNKT cells, with the expectation that PLZF levels would be higher in Cul3 KO cells. However, we observed that PLZF levels were not affected by the loss of Cul3 (Fig. 3.3A), hinting that Cul3 may not regulate PLZF expression.

iNKT cells are known to differentiate into functional subsets during thymic development. Like conventional T helper cells, these subsets can be defined based on their expression of the transcription factors PLZF, T-bet, and RORγt. NKT17 cells, which express an intermediate level

of PLZF and high levels of RORγt, as well as NKT2 cells, which express the highest levels of PLZF, reach maturity at stage 2 of development (96). NKT1 cells, which express low levels of PLZF and high levels of T-bet, reach maturity at stage 3 of iNKT cell development (96). Therefore, most of the iNKT cells in a WT C57BL/6 mouse are iNKT1 cells (97). Because Cul3 deficiency leads to a block in iNKT cell development, we hypothesized that iNKT subset distribution would be skewed in the absence of Cul3. Indeed, NKT1 frequencies were decreased while NKT2 and NKT17 frequencies were increased in the absence of Cul3 (Fig. 3.3B), despite PLZF levels being unchanged (Fig. 3.3A). These data suggest that changes in iNKT cell subset distribution in Cul3 deficient mice is due to iNKT cell developmental arrest rather than the regulation of PLZF expression by Cul3.
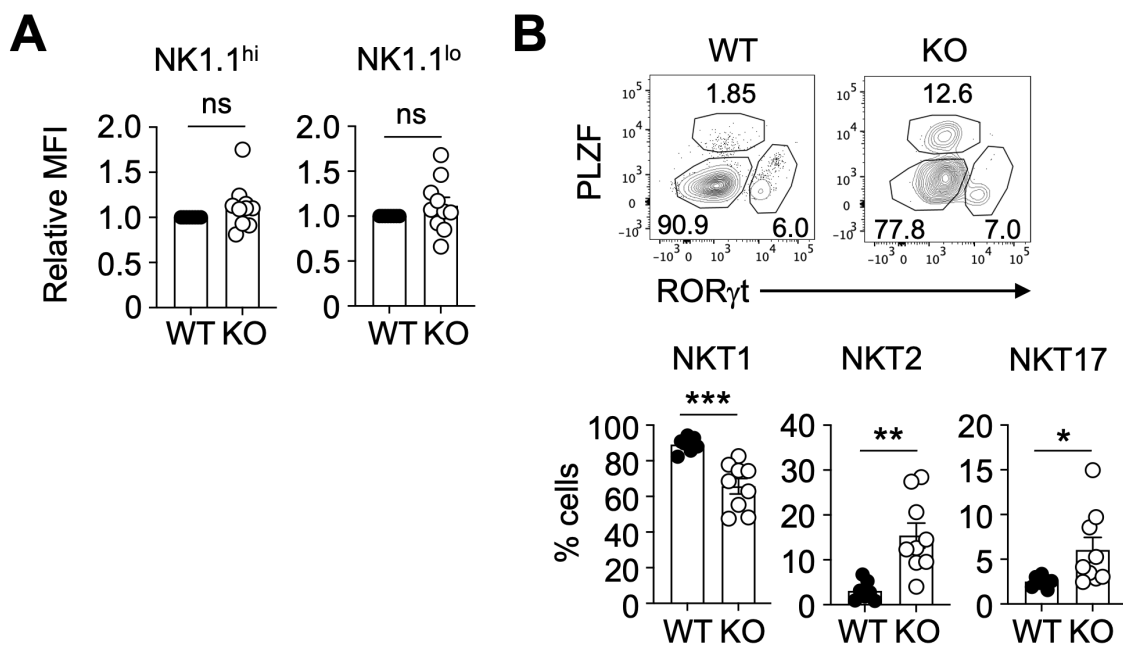
Figure 3.3 – Cul3 regulates iNKT cell subset differentiation independently of PLZF.
(A) Bar graphs show pooled data for the mean fluorescent intensity (MFI) values of PLZF in Cul3 KO NK1.1[hi] and NK1.1^{lo} iNKT cells relative to WT. (n=7). (B) Whole thymocytes from WT and Cul3 KO mice were stained for PLZF, T-bet, and RORγt. Representative dot plots show thymic iNKT cell subsets in WT and Cul3 KO mice. Bar graphs show the cumulative % of iNKT1, iNKT2, and iNKT17 cells in the thymi of mice from 4 independent experiments. Error bars represent mean ± SEM. *p<0.05, **p<0.005, ***p<0.0005, ns: not significant.

Cul3 regulates autophagy in developing iNKT cells

Although Cul3 KO NK1.1^{hi} iNKT cells in the thymus proliferate more than WT cells, their numbers are extremely low compared to those of WT (36). Together, these data indicate that Cul3 KO iNKT cells must also die more than WT cells do. We tested this hypothesis by staining for Annexin V, a marker of cells undergoing apoptotic cell death. Indeed, Cul3 deficient NK1.1^{hi} cells undergo more apoptotic cell death compared to WT cells in the thymus (Fig. 3.4A). Autophagy, a process by which cells recycle proteins and organelles during times of nutrient stress, can also lead to cell death when left unchecked. Autophagy is known to regulate the transition of developing iNKT cells from being highly metabolically active to becoming quiescent (49). Therefore, we asked whether the increase in apoptosis seen in thymic Cul3 KO iNKT cells is due to increased autophagy. To test this, we measured levels of p62, a protein that binds polyubiquitinated protein aggregates and delivers them to the autophagosome for degradation (98, 99). During this process, p62 itself is degraded (98). Therefore, high levels of p62 indicate low levels of autophagy, while low levels of p62 indicate high levels of autophagy. We found that both NK1.1^{hi} and NK1.1^{lo} Cul3 KO iNKT cells display significantly lower levels of p62 than WT cells do (Fig. 3.4B), indicating that autophagy is high in these cells.

Cul3 is also known to regulate cellular reactive oxygen species (ROS) levels through its involvement in the Cul3-Keap1-Nrf2 trimeric complex. Under normal conditions, Keap1 links Cul3 to Nrf2, allowing Cul3 to polyubiquitinate Nrf2 and mediate its degradation (15, 17, 18). However, in the absence of Cul3, Nrf2 levels would be unchecked, potentially causing an imbalance in intracellular redox dynamics. This could be particularly detrimental for iNKT cells, which acquire high levels of ROS as they egress to the periphery (100). Therefore, we wondered whether the increase in thymic iNKT cell death in the absence of Cul3 could be due to overactive ROS scavenging. We began by measuring total ROS levels in WT and Cul3 KO thymic iNKT cells using 2',7'-dichlorodihydrofluorescein diacetate (H$_2$DCFDA), a fluorescent dye that binds to ROS in the cytoplasm. Surprisingly, total ROS levels were not different between WT and Cul3 deficient iNKT cells in the thymus (Fig. 3.4C). In all, our data suggest that Cul3 controls iNKT cell death during thymic development by regulating autophagy rather than modulating cellular redox states.
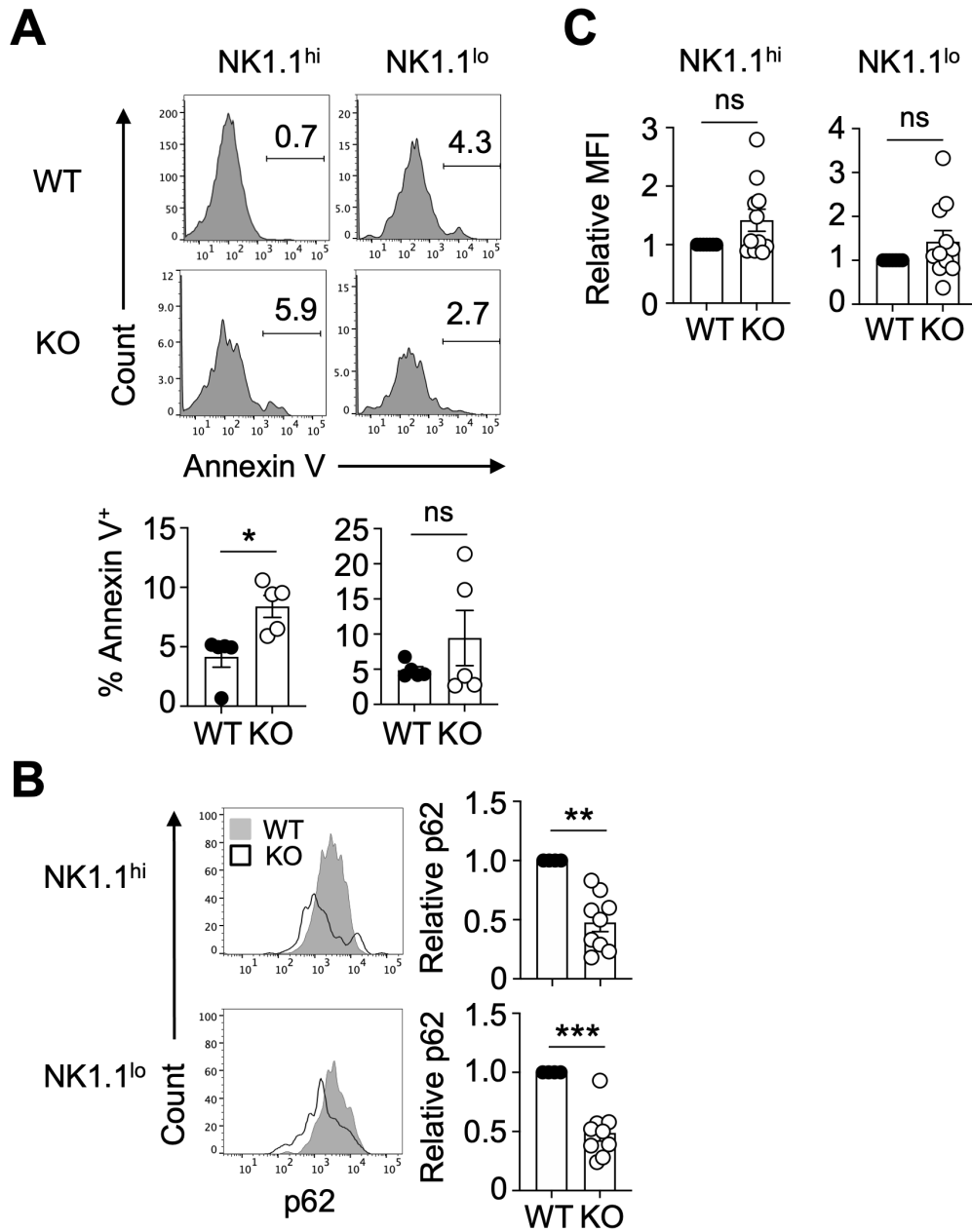
Figure 3.4 – Cul3 regulates cell death during iNKT cell development.
(A) Representative histograms show % Annexin V$^+$ thymic NK1.1^{hi} and NK1.1^{lo} cells from WT and Cul3 KO mice. Bar graphs show pooled % Annexin V$^+$ cells from 3 independent experiments. (B) Representative histograms show expression of p62 in WT (gray) and Cul3 KO (open) NK1.1^{hi} (top panels) and NK1.1^{lo} (bottom panels) cells. Bar graphs illustrate the mean fluorescent intensity (MFI) of p62 in Cul3 KO cells relative to WT cells from 3 independent experiments. (C) Bar graphs show the MFI of DCFDA in Cul3 KO NK1.1^{hi} and NK1.1^{lo} cells relative to WT. The data in (C) is representative of 5 independent experiments. Error bars represent mean ± SEM. *p<0.05, **p<0.005, ***p<0.0005, ns: not significant.

Cul3 restricts glucose metabolism but not mitochondrial function in developing iNKT cells

CD4 and CD8 T cells undergo metabolic rewiring after receiving an activation signal, during which they switch their metabolism from a more oxidative to a more glycolytic phenotype (101). This increase in glucose uptake and subsequent increase in glycolysis is crucial for conventional T cell proliferation. It is known that stage 0 and stage 1 iNKT cells require high levels of glucose to continue in the maturation process; however, the resolution of this high rate of glycolysis is crucial for the development of functional stage 3 iNKT cells (48). Therefore, we asked whether NK1.1^{hi} iNKT cells display increased glucose metabolism in the absence of Cul3. To begin, we analyzed glucose uptake in thymic iNKT cells by staining whole thymocytes with the fluorescent glucose analog 2-NBDG. We found that glucose uptake was higher in both NK1.1^{hi} and NK1.1^{lo} iNKT cells lacking Cul3 (Fig. 3.5A). To determine whether this increase in glucose uptake translates to an increase in glycolysis, we measured the expression of hexokinase II (HK2), the first enzyme in the glycolytic pathway, in WT and Cul3 KO iNKT cells. HK2 levels were also higher in Cul3 KO NK1.1^{hi} and NK1.1^{lo} iNKT cells compared to WT cells (Fig. 3.5B).

Peripheral iNKT cells have recently been shown to use glucose to fuel both the pentose phosphate pathway and mitochondrial metabolism rather than glycolysis (102). Although mitochondrial activity is high in the immature stages of iNKT cell development (48), it is unclear whether glucose is responsible for fueling this increased mitochondrial activity in the thymus. As such, we examined mitochondrial mass, mitochondrial potential, and mitochondrial ROS (mtROS) production in NK1.1^{hi} and NK1.1^{lo} iNKT cells using MitoTracker^{TM} Green, TMRM, and MitoSOX dyes, respectively. Cul3 deficient NK1.1^{hi} cells had lower mitochondrial mass and potential compared to WT cells despite producing similar levels of mtROS (Fig. 3.5C, top panels). In contrast, mitochondrial function was not affected by the loss of Cul3 in NK1.1^{lo} cells (Fig. 3.5C, bottom panels). Lipid peroxidation, a metabolic process by which cellular phospholipids are broken down by oxygen radicals, can also occur in the mitochondria (103). We measured lipid peroxidation in Cul3 KO iNKT cells using a fluorescent sensor that can be oxidized by cellular free radicals. As the sensor is oxidized, the fluorescent signal shifts from PE to FITC, allowing for detection via flow cytometry. The ratio of these two fluorescent signals can then tell us the rate of lipid peroxidation within the cell, as a high FITC/PE ratio indicates high levels of lipid peroxidation. We found that Cul3 deficiency did not affect lipid peroxidation

in thymic iNKT cells (Fig. 3.5D), consistent with both our total ROS (Fig. 3.4C) and mtROS (Fig. 3.5C) data. Together, Cul3 may restrain glycolysis in developing iNKT cells but does not appear to control mitochondrial dynamics during iNKT cell development.
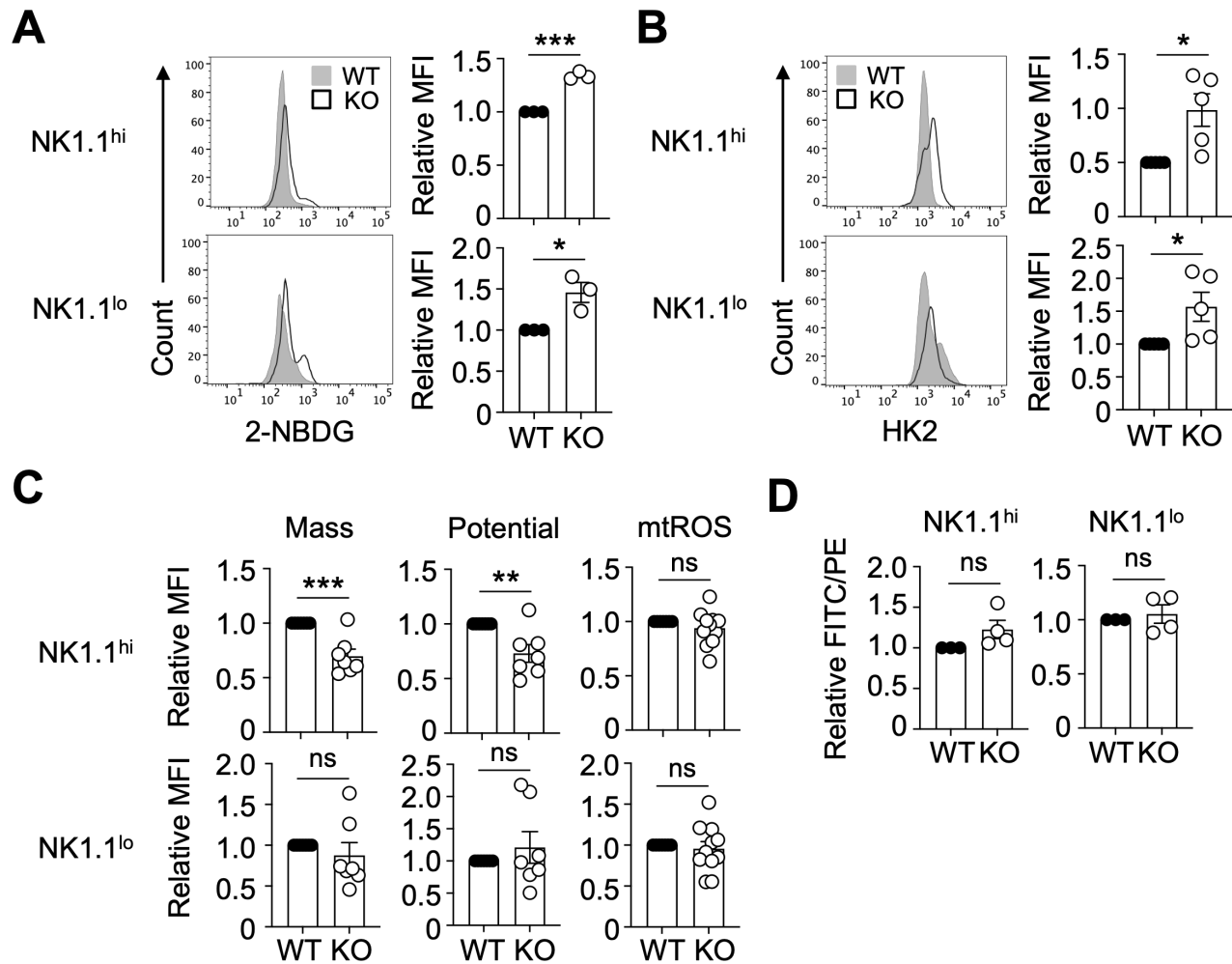

Figure 3.5 – Cul3 primarily influences glucose metabolism in developing iNKT cells.
(A-B) WT data is illustrated using a gray histogram while Cul3 KO data is displayed using an open histogram outlined in black. (A) Representative histograms show glucose uptake in thymic NK1.1^{hi} and NK1.1^{lo} cells. Bar graphs show mean fluorescent intensity (MFI) values of 2-NBDG from Cul3 KO cells relative to WT cells. (n=3). (B) Representative histograms show expression of HK2 in NK1.1^{hi} and NK1.1^{lo} iNKT cells. Bar graphs illustrate the MFI of HK2 in Cul3 KO cells relative to WT cells from 3 independent experiments. (C) Bar graphs show the MFI of MitoTracker^{TM} Green (n=3), TMRM (n=3), and MitoSOX (n=5) in Cul3 KO NK1.1^{hi} and NK1.1^{lo} cells relative to WT. (D) Bar graphs show pooled lipid peroxidation levels as a function of FITC fluorescence divided by PE fluorescence in thymic Cul3 KO iNKT cells relative to WT iNKT cells. Data in (D) is cumulative from 3 independent experiments. Error bars represent mean ± SEM. *p<0.05, **p<0.005, ***p<0.0005, ns: not significant.

Cul3 prevents iron overload in stage 3 iNKT cells in the thymus

We showed in Chapter 2 that the regulation of iron homeostasis is critical for CD4 T cell activation and proliferation (104). However, nothing is known about the role of iron in controlling iNKT cell development and function. We began by measuring the levels of iron import, storage, and export proteins during stagewise development in the thymus. Stage 1 iNKT cells, the most highly proliferative of all developing iNKT cells, showed the highest expression of the iron import protein transferrin receptor 1 (TfR1) as well as the iron storage protein ferritin (Fig. 3.6A). Together, these data imply that stage 1 iNKT cells need more iron to mediate their expansion. However, expression of the iron exporter ferroportin (Fpn) is also relatively high in stage 1 iNKT cells (Fig. 3.6A), indicating that iron flux is just as important for proliferating iNKT cells as it is for proliferating CD4 T cells (104). TfR1, ferritin, and Fpn levels decrease through stages 2 and 3 (Fig. 3.6A), in line with the fact that iNKT cells become quiescent as they mature. We also measured the labile iron pool (LIP) at each of the iNKT cell developmental stages. We found that LIP levels are lowest in stage 1 iNKT cells and steadily increase as iNKT cells mature, with stage 3 cells harboring the highest LIP levels in the thymus (Fig. 3.6B). These data indicate that iron is tightly regulated over iNKT cell development.

iNKT cells egress from the thymus as effector cells. Whether naive and effector T cells differ in their requirements for iron is currently unknown. We attempted to address this question by measuring LIP in naive CD4 T cells, effector CD4 T cells, and iNKT cells in the spleens of WT mice. As mentioned in Chapter 2, LIP can be measured using Calcein-AM dye. As Calcein binds iron, the fluorescent signal is quenched, leading to a concomitant decrease in mean fluorescent intensity (MFI). As such, high levels of Calcein correlate with low LIP levels. Interestingly, naive CD4 T cells displayed a sharp Calcein peak, whereas both effector CD4 T cells and iNKT cells display a much broader Calcein peak (Fig. 3.6C). The broadness of the peak also correlated with LIP level, as iNKT cells displayed the broadest Calcein peak and harbored the highest level of LIP of all 3 tested cell types (Fig. 3.6C). These data suggest that effector T cells maintain higher basal levels of LIP than naive T cells do, which may allow effector cells to rapidly respond to infection.

Naturally, we next asked whether Cul3 modulates iNKT cell development by controlling iron homeostasis. We found that LIP levels are higher in Cul3 deficient NK1.1^{hi} iNKT cells but not NK1.1^{lo} iNKT cells compared to WT cells (Fig. 3.6D). This was corroborated by stagewise
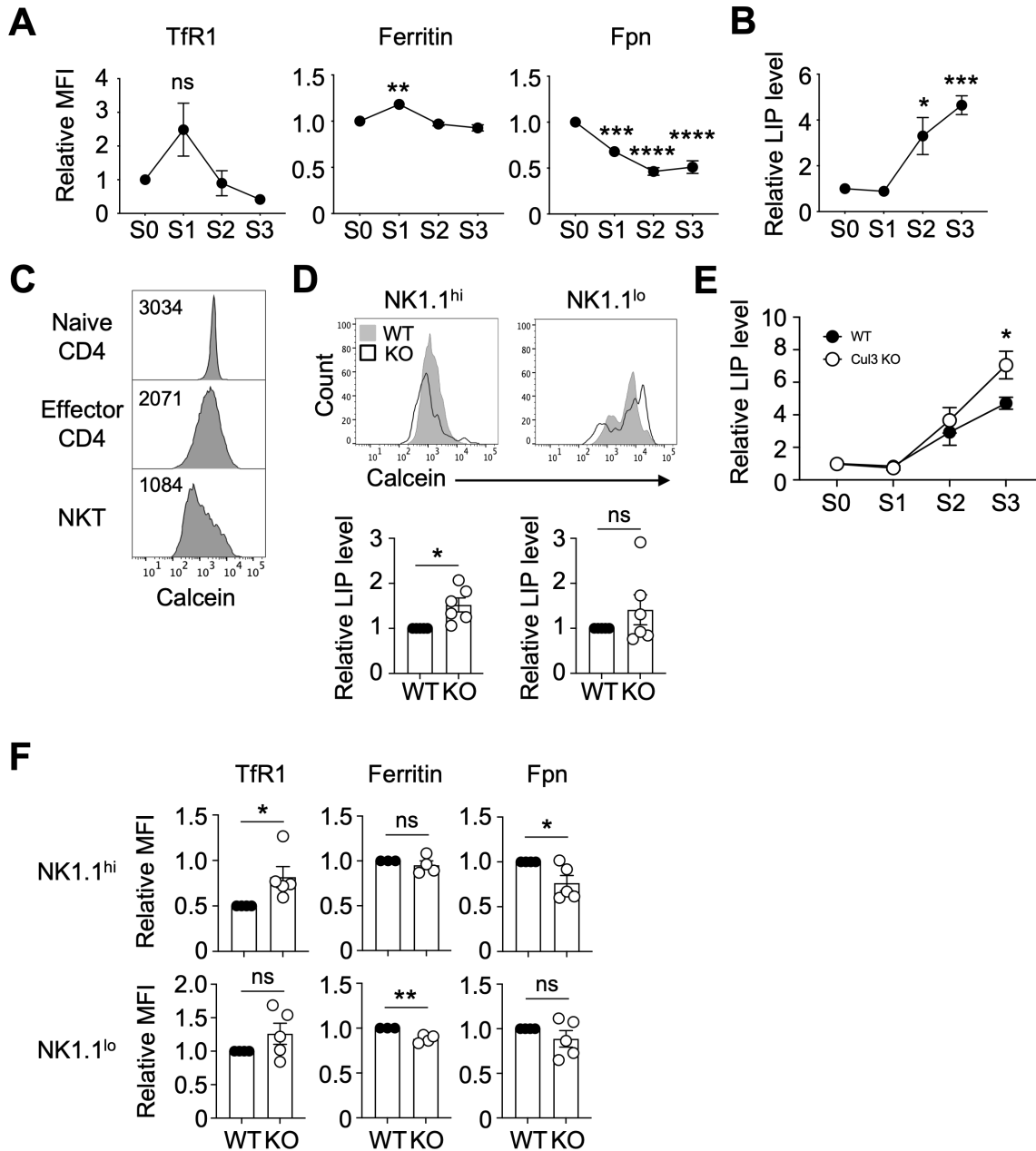
Figure 3.6 – Cul3 modulates iron homeostasis during iNKT cell development.
(A) Graphs show relative mean fluorescent intensity (MFI) values of TfR1, ferritin, and Fpn in WT iNKT cells in the thymus. All data is relative to stage 0 (S0) cells. (n=3). (B) Graph shows the LIP level at each stage of thymic development in WT iNKT cells relative to S0. (n=3). (C) Representative histograms show Calcein staining in splenic naive CD4 T cells, effector CD4 T cells, and iNKT cells. Numbers represent the MFI of Calcein for each cell type. Data is representative of 3 independent experiments. (D) Representative histograms illustrate Calcein staining in WT (gray) and Cul3 KO (open) NK1.1[hi] and NK1.1^{lo} cells. Bar graphs illustrate the LIP level in Cul3 KO cells relative to WT cells. (n=3). (E) Graph shows LIP levels in Cul3 KO iNKT cells at each stage of development relative to WT S0 cells. Data is cumulative of 4 independent experiments. (F) Graphs show MFI values of TfR1, ferritin, and Fpn in NK1.1[hi] and NK1.1^{lo} cells lacking Cul3 relative to WT cells. (n=3). Error bars represent mean ± SEM. *p<0.05, **p<0.005, ***p<0.0005, ****p<0.0001, ns: not significant.

44

analysis of LIP in WT and Cul3 KO thymocytes, which showed that LIP is higher in Cul3 deficient iNKT cells at stage 3 only (Fig. 3.6E). NK1.1^{hi} iNKT cells lacking Cul3 also displayed higher levels of TfR1, lower levels of Fpn, and similar levels of ferritin in comparison to WT cells (Fig. 3.6F, top panels). In contrast, iron homeostasis in NK1.1^{lo} iNKT cells was less affected by the loss of Cul3, as these cells showed no difference in either TfR1 or Fpn expression and only a minor decrease in ferritin expression compared to WT cells (Fig. 3.6F, bottom panels). Together, these data indicate that Cul3 limits iron accumulation during iNKT cell development, as iron overload can cause cell death.

Low iron diet partially rescues defective iron homeostasis in stage 3 iNKT cells lacking Cul3

Our data suggest that Cul3 is a critical regulator of iron homeostasis in developing iNKT cells, and that dysregulation of LIP is detrimental for stage 3 iNKT cells. As such, we asked whether a low iron diet could rescue iNKT cell development in the absence of Cul3. To test this, both WT and Cul3 KO mice were fed either a control diet containing approximately 35ppm of iron or an iron-deficient diet containing 3-5ppm of iron for 6 weeks post-weaning. Mice on all diets were weighed once weekly, and we found that both WT and Cul3 KO mice fed a low iron diet fail to gain weight at a normal pace (Fig. 3.7A). Notably, Cul3 KO mice from the low iron diet group were significantly smaller than WT mice from the normal diet group starting at 3 weeks post-weaning (Fig. 3.7A). To ensure that mice fed a low iron diet became anemic, we measured serum iron levels after 6 weeks of feeding. Indeed, both WT and Cul3 KO mice fed a low iron diet had lower serum iron levels than their normal diet counterparts (Fig. 3.7B). However, systemic iron deficiency did not rescue iNKT cell development, as total thymic iNKT cell frequencies were not different between Cul3 KO mice fed either diet (Fig. 3.7C). We hypothesized that 6 weeks may not have been enough time to see restoration of total iNKT cell frequencies. Therefore, we examined the frequencies and numbers of stage 3 iNKT cells from Cul3 KO mice fed a low iron diet. Although not statistically significant, stage 3 iNKT cell frequencies and numbers were slightly higher in Cul3 KO mice fed a low iron diet compared to Cul3 KO mice fed a normal diet (Fig. 3.7D). We also wondered if systemic iron deficiency influenced LIP in Cul3 deficient NK1.1^{hi} iNKT cells, which exhibit an iron overloaded phenotype. Our results showed that LIP levels trended downward in NK1.1^{hi} iNKT cells from Cul3 deficient mice that were fed a low iron diet (Fig. 3.7E), but this is also not statistically

significant. In contrast, a low iron diet exacerbates the hyperproliferative phenotype exhibited by Cul3 KO NK1.1^{hi} iNKT cells, as evidenced by Ki-67 expression (Fig. 3.7F). Therefore, Cul3 may control some aspects of iNKT cell development by regulating iron homeostasis. However, Cul3 appears to have iron independent effects on iNKT cell development as well.
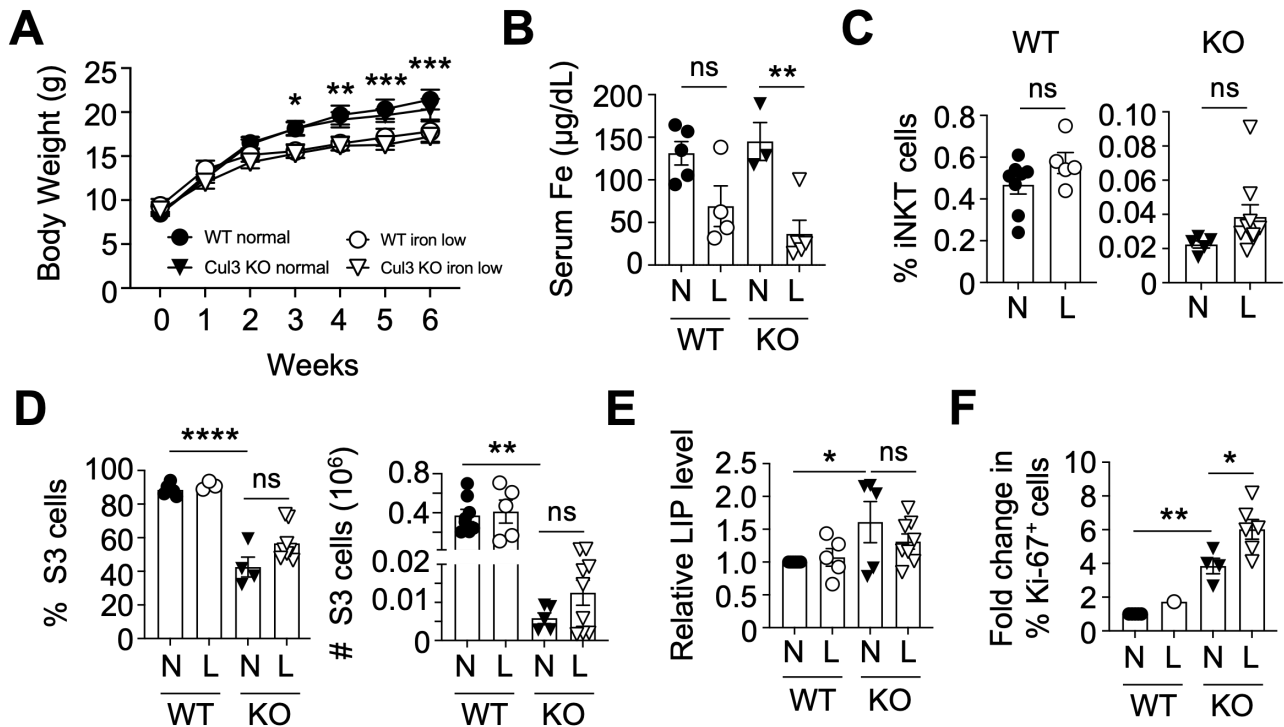

Figure 3.7 – Low iron diet partially restores NKT cell development in the absence of Cul3.
In all graphs, WT mice fed a normal iron diet (N) are represented by closed circles, while Cul3 KO mice fed a normal iron diet are represented by closed triangles. WT mice fed a low iron diet (L) are represented by open circles, while Cul3 KO mice fed a low iron diet are represented by open triangles. All data is cumulative of 3 independent experiments. (A) Graph shows pooled weights of mice from all 4 feeding groups. Stars represent time points at which Cul3 KO mice fed an iron deficient diet significantly differed from WT mice fed a normal diet. (B) Graph shows serum iron levels (µg/dL) in all 4 experimental groups. (C) Graphs show the frequencies of total thymic iNKT cells from WT mice (left panel) and Cul3 KO mice (right panel). (D) Bar graphs show the frequencies (left panel) and numbers (right panel) of stage 3 iNKT cells from all 4 experimental groups. (E) Graph shows LIP levels in NK1.1^{hi} iNKT cells relative to WT NK1.1^{hi} iNKT cells from mice fed a normal diet. (F) Bar graph shows the fold change in % Ki-67^{+} NK1.1^{hi} iNKT cells relative to NK1.1^{hi} iNKT cells from WT mice fed a normal diet. Error bars represent mean ± SEM. *p<0.05, **p<0.005, ***p<0.0005, ****p<0.0001, ns: not significant.

Cul3 and PLZF may control iNKT cell development independently of one another

Cul3 is known to interact with PLZF, the lineage defining transcription factor of iNKT cells, in the nuclei of thymic iNKT cells (36). However, it is unknown whether the interaction between Cul3 and PLZF is necessary for iNKT cell development. To begin testing this question, we examined NK1.1^{hi} and NK1.1^{lo} iNKT cells from PLZF$^{-/-}$ mice, which lack PLZF in all cells of the body. PLZF$^{-/-}$ mice display a severe block in iNKT cell development, resulting in extremely low iNKT cell frequencies and numbers in the thymus (Fig. 3.8A) (38, 39). Interestingly, PLZF$^{-/-}$ NK1.1^{hi} iNKT cells proliferate more than WT cells in the thymus (Fig. 3.8B), similar to Cul3 deficient NK1.1^{hi} iNKT cells (Fig. 3.1B). However, p62 levels trend upwards in PLZF$^{-/-}$ NK1.1^{hi} and NK1.1^{lo} iNKT cells (Fig. 3.8C), indicating that autophagy may be lower in PLZF$^{-/-}$ iNKT cells compared to WT cells. In contrast, Cul3 KO iNKT cells displayed lower levels of p62 than WT cells (Fig. 3.4B). Additionally, PLZF$^{-/-}$ NK1.1^{hi} and NK1.1^{lo} iNKT cells appear to have higher mitochondrial function than WT cells, as mitochondrial mass and mitochondrial potential were higher in PLZF$^{-/-}$ cells compared to WT cells (Fig. 3.8D and 3.8E). Therefore, PLZF may inhibit mitochondrial activity in developing iNKT cells, while Cul3 may dampen glucose metabolism in developing iNKT cells (Fig 3.5A and 3.5B). Lastly, PLZF$^{-/-}$ NK1.1^{hi} and NK1.1^{lo} iNKT cells harbor less LIP than WT cells (Fig. 3.8F); however, Cul3 deficient NK1.1^{hi} iNKT cells harbor more LIP than WT cells (Fig. 3.6D and 3.6E). In all, Cul3 and PLZF may cooperate to inhibit excessive proliferation in developing iNKT cells. However, Cul3 and PLZF appear to control iNKT cell development largely via independent mechanisms. More work is needed to verify this hypothesis and to fully dissect the mechanistic roles of Cul3 and PLZF in developing iNKT cells.
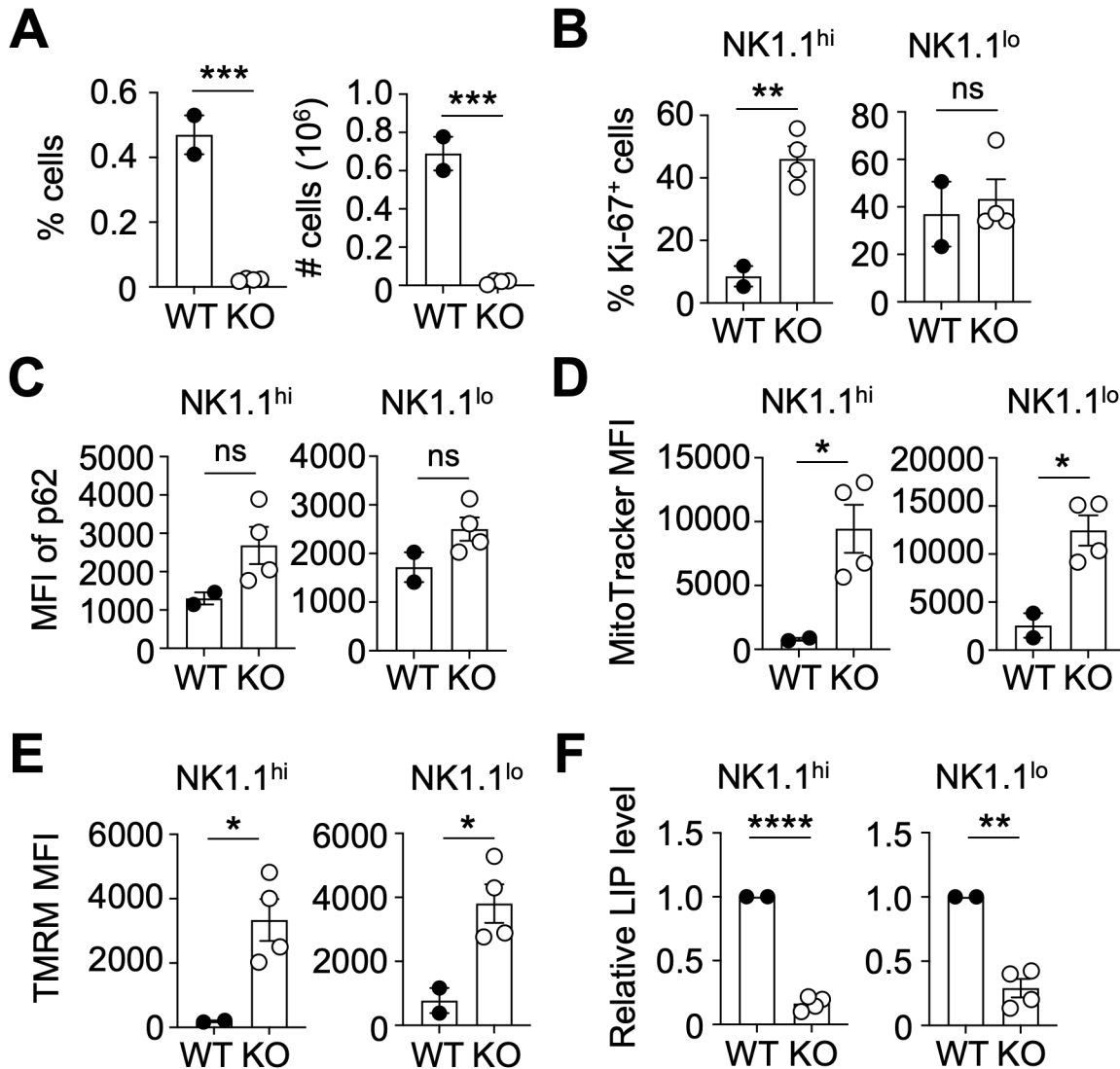
Figure 3.8 – Thymic PLZF deficient iNKT cells also exhibit a hyperproliferative phenotype.
Whole thymocytes from PLZF^{+/+} (WT) and PLZF^{-/-} (KO) mice were stained for iNKT cell stagewise markers. All data is cumulative of 2 independent experiments. (A) Bar graphs show the frequencies and numbers of thymic iNKT cells in WT and PLZF KO mice. (B) Bar graphs illustrate the % Ki-67^{+} cells in either the NK1.1[hi] or the NK1.1[lo] iNKT cell populations from WT and PLZF KO mice. (C-E) Graphs illustrate the mean fluorescent intensity (MFI) of p62 (C), MitoTracker[TM] Green (D), and TMRM (E) in NK1.1[hi] and NK1.1^{lo} cells. (F) Bar graphs show the relative LIP level in NK1.1[hi] and NK1.1^{lo} cells as a function of MFI of Calcein. Error bars represent mean ± SEM. *p<0.05, **p<0.005, ***p<0.0005, ****p<0.0001, ns: not significant.

Discussion

In summary, our data indicate that Cul3 controls iNKT cell development by regulating intracellular iron homeostasis and promoting the shift towards quiescence during terminal maturation. We found that Cul3 deficient NK1.1^{hi} iNKT cells exhibit a hyperproliferative phenotype, and that these cells also display enhanced glucose uptake and HK2 expression in comparison to WT cells. HK2 is a known target of Nrf2 (105), and Nrf2 has been shown to regulate a variety of genes involved in glycolysis and glutamine metabolism (106). Cul3 plays a major role in regulating Nrf2 expression and activity, as Cul3 interacts with Nrf2 in the Cul3-Keap1-Nrf2 trimeric complex. Under normal conditions, Cul3 ubiquitinates Nrf2, targeting Nrf2 for proteasomal degradation (18, 19). Therefore, in the absence of Cul3, it is possible that Nrf2 levels are high, leading to the uncontrolled activation of glucose metabolism-related genes. Interestingly, iNKT cells lacking Keap1 also display increased glucose metabolism and mitochondrial activity (107). Additionally, Keap1 deficiency leads to a block in iNKT cell development, which is rescued by T cell-specific deletion of Nrf2 (107). As such, high Nrf2 levels may be detrimental to iNKT cell development by preventing the transition from a metabolically active phenotype in stages 1-2 to a metabolically quiescent phenotype in stage 3. However, we have not measured Nrf2 levels in Cul3 KO iNKT cells. Generating mice with a T cell-specific deletion of both Cul3 and Nrf2 will be useful in determining whether Nrf2 is responsible for the block in iNKT cell development in the absence of Cul3.

Our study is also the first to show that iron homeostasis is dynamically regulated over the course of iNKT cell development. We found that both iron uptake and storage machinery peak during stage 1 of development. Additionally, levels of the iron export protein ferroportin (Fpn) are highest at stages 0 and 1 of iNKT cell development. Together, these data suggest that immature thymic iNKT cells require iron flux to fuel their increased proliferative rate, similar to what has been reported in CD4 T cells (104). Transferrin receptor, ferritin, and Fpn levels steadily decrease as iNKT cells mature beyond stage 1, in line with the establishment of a quiescent metabolic program in mature thymic iNKT cells. Additionally, iNKT cells harbor higher levels of LIP than CD4 and CD8 T cells in the thymus (data not shown) and the peripheral tissues. iNKT cells leave the thymus as effector cells whereas CD4 and CD8 T cells leave the thymus as naive cells. Therefore, high LIP levels may be a hallmark of effector T cells, as having high iron stores may allow for a faster response to foreign antigen encounter. We found that LIP

levels steadily increase during iNKT cell development, with stage 3 iNKT cells having the highest LIP levels in the thymus. In all, our data adds to existing knowledge by identifying iron homeostasis as a critical regulator of iNKT cell development (Fig. 3.9).

Furthermore, we hypothesize that the increased cell death seen in Cul3 deficient NK1.1^{hi} iNKT cells is due to dysregulated iron homeostasis. We showed that NK1.1^{hi} iNKT cells lacking Cul3 die more by apoptosis in comparison to WT cells. Additionally, Cul3 KO stage 3 iNKT cells retain higher levels of LIP than WT cells do, potentially leaving Cul3 deficient iNKT cells vulnerable to cell death via ferroptosis. CD71 has recently been reported to be a reliable marker of ferroptotic tumor cells (108), and Cul3 deficient NK1.1^{hi} iNKT cells display increased expression of CD71 compared to WT cells. Moreover, feeding a low iron diet to Cul3$^{fl/fl}$ CD4-Cre mice began to decrease LIP levels in NK1.1^{hi} iNKT cells and partially rescued stage 3 iNKT cell numbers.
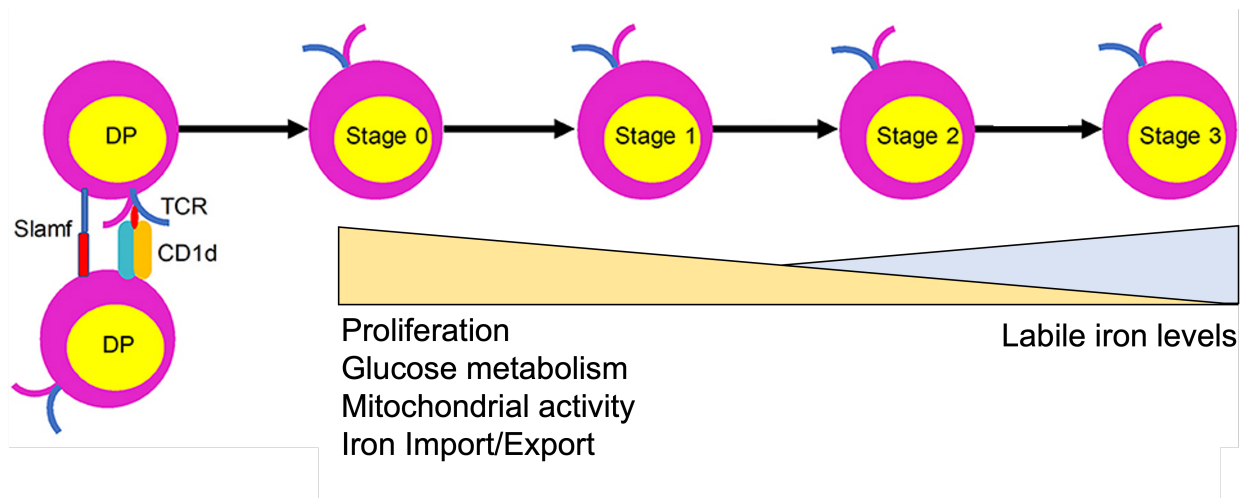

Figure 3.9 – Dynamic regulation of iron homeostasis during iNKT cell development.
Published studies have shown that immature thymic iNKT cells in stages 0 and 1 exhibit high rates of proliferation, glycolytic metabolism, and mitochondrial function that gradually resolve as they approach terminal differentiation. My thesis work builds on this knowledge by showing that the expression of iron import and export machinery is also high in immature thymic iNKT cells. In contrast, stage 3 iNKT cells have low expression of iron import and export proteins. However, cytoplasmic labile iron (LIP) levels steadily increase over the course of iNKT cell development, with immature cells having low LIP levels and mature cells having high LIP levels. Adapted from Yang, Driver, and Van Kaer 2018 (49).

More work is necessary to determine direct targets of Cul3 along the ferroptosis and iron homeostatic pathways; however, there are several possible mechanisms by which Cul3 may control iron metabolism in developing iNKT cells. For one, Cul3 may regulate iron homeostasis directly by mediating the proteasomal degradation of iron regulatory protein 2 (IRP2). IRP2 has been shown to be ubiquitinated by the SKP1-Cul1-FBXL5 ligase complex in HEK293 cells, leading to the degradation of IRP2 (109). Cul3 is known to work in concert with Cul1 to degrade targets in other cellular pathways (29); therefore, it is possible that Cul3 may also work with Cul1 to degrade IRP2. Therefore, in the absence of Cul3, both IRP2 and transferrin receptor (TfR1) levels are high, as TfR1 is a known target of IRP2 (110). IRP2 also inhibits Fpn expression (110), and our data showed that Fpn levels are low in thymic NK1.1^{hi} iNKT cells lacking Cul3. As such, IRP2 is a promising potential target for Cul3 in developing iNKT cells.

Alternatively, Cul3 may indirectly regulate iron homeostasis by controlling cellular epigenetic programs. Cul3 interacts in complex with PLZF and epigenetic modifiers like HDAC1 and DNMT1 in thymic iNKT cells (36). DNMT1 is a DNA methyltransferase that deposits methyl groups onto cytosine residues in gene promoter regions, preventing methylated genes from being transcribed (111). DNA methylation is beginning to be appreciated as a major regulator of iron homeostasis as well. In fact, dysregulation of the DNA methylation landscape has been shown to adversely impact cellular LIP levels, ferroptosis, and Fpn expression (112-114). Therefore, Cul3 may regulate iron homeostasis in thymic iNKT cells by modulating DNMT1 expression and subsequent DNA methylation levels. However, continued work is necessary to fully explore this possibility.

Our data also suggest that PLZF and Cul3 may control iNKT cell development through independent mechanisms. PLZF expression is known to be tightly regulated over the course of iNKT cell development (38, 39). However, whether Cul3 shows a similar expression pattern to PLZF during stagewise development remains unknown. We attempted to answer this question by measuring Cul3 levels at each stage of iNKT cell development by flow cytometry; however, lack of a specific Cul3 antibody prevented us from successfully doing so. Therefore, we sought to interrogate the importance of the Cul3-PLZF complex during iNKT cell development by comparing our Cul3 deficient iNKT cells to PLZF$^{-/-}$ iNKT cells. Both Cul3 KO and PLZF$^{-/-}$ NK1.1^{hi} iNKT cells proliferate more than WT cells in the thymus, suggesting that Cul3 and PLZF may work together to restrain proliferation in developing iNKT cells. However, all of the

51

other tested parameters showed different trends between Cul3 KO and PLZF$^{-/-}$ iNKT cells during development. Taken together, these data suggest that Cul3 and PLZF may not cooperate to control iNKT cell development. However, this idea does not disprove the hypothesis that the interaction between Cul3 and PLZF is important for developing iNKT cells. As mentioned previously, Cul3 and PLZF colocalize in the nuclei of thymic iNKT cells (36). This interaction was thought to be important for mediating the translocation of Cul3 from the cytoplasmic compartment to the nuclear compartment, where it has been shown to ubiquitinate several epigenetic modifiers (36). For example, Cul3 has been shown to ubiquitinate special AT-rich sequence-binding protein 1 (SATB1), a transcription factor known for regulating global chromatin structure (36). However, the implications of this ubiquitination for iNKT cell development and function are unknown. Performing an ATAC-seq assay between WT and Cul3 KO iNKT cells in the thymus may yield informative data about chromatin accessibility in the absence of Cul3, potentially uncovering novel targets for Cul3 in controlling iNKT cell development and lineage commitment. Therefore, a more focused genetic study is warranted to tease out the role of Cul3 in developing iNKT cells.

Finally, whether Cul3 is also important in peripheral iNKT cell homeostasis and function remains unknown. We sought to answer this question using a tamoxifen-inducible Cul3$^{fl/fl}$ CD4$^{ERT-Cre}$ murine model, which would allow us to delete Cul3 in peripheral iNKT cells without affecting thymic development. However, mature iNKT cells in the spleen were highly resistant to Cul3 knockdown (data not shown). Because of this tamoxifen resistance, we were unable to explore the roles of Cul3 in peripheral iNKT cell responses. However, the possibility that Cul3 may also regulate peripheral iNKT cell maintenance, proliferation, and effector function warrants further investigation.

Chapter 4 – Cullin 3 Mediates Peripheral T Cell Tolerance by Maintaining Naive CD4 T Cell Quiescence

Abstract

The E3 ubiquitin ligase Cullin 3 (Cul3) has been shown to modulate the differentiation of T regulatory cells and T follicular helper cells in the thymus and the periphery. However, whether Cul3 controls naive CD4 T cell maintenance has never been studied. Here, we show that Cul3 deficiency has minimal effects on single positive CD4 T cells in the thymus. In contrast, the absence of Cul3 leads to a dramatic loss of naive CD4 T cells in the spleen. Cul3 deficient naive CD4 T cells display a pre-activated phenotype characterized by increased proliferation, cell death, and expression of TCR signaling pathway components. Additionally, naive CD4 T cells lacking Cul3 proliferate better than wild type cells after activation, a phenotype that is accompanied by increased IFNγ production and glucose metabolism. Interestingly, the loss of naive T cells is abrogated in the antigen-specific OT-II system, indicating that the function of Cul3 is dependent on the existence of a polyclonal T cell pool. Future studies are necessary to elucidate the roles of Cul3 in monoclonal and polyclonal systems.

Introduction

Naive T cell maintenance in the periphery is a dynamic process that relies on a variety of intracellular and extracellular signals. For one, naive T cells continuously bind self-peptide/major histocompatibility complexes, which leads to weak signaling through the T cell receptor (TCR) (115). This process is known as tonic signaling. Tonic signaling is thought not only to promote naive T cell survival in the periphery but also to modulate TCR sensitivity to foreign antigens (115). IL-7 receptor (IL-7R) signaling also supports peripheral naive T cell survival by increasing the expression of anti-apoptotic genes (116, 117). Additionally, IL-7R signaling activates both phosphoinositide 3-kinase (PI3K) and mammalian target of rapamycin complex 1 (mTORC1), which regulate intracellular metabolic pathways critical for naive T cell

survival (118). In line with this, TSC1 has been shown to regulate naive T cell survival in the periphery by modulating mTORC1 activity (119). Additionally, PI3K activation downregulates the expression of FOXO1, which inhibits naive T cell proliferation by blocking cell cycle progression (118, 120). The GTPase-activating protein RASA1, which restrains TCR signaling in peripheral T cells, has also been shown to regulate naive CD4 T cell survival by modulating IL-7R signaling and apoptotic protein expression (121). In all, the interplay between intracellular signaling processes is crucial for ensuring naive T cell homeostasis.

However, the role of the E3 ubiquitin ligase Cullin 3 (Cul3) in controlling naive CD4 T cell maintenance is currently unknown. Cul3 deficiency leads to improper differentiation of both T regulatory and T follicular helper cell subsets (35, 36), yet the effects of Cul3 deficiency on naive T cell phenotype and function have never been studied. We show that Cul3 contributes to naive T cell maintenance by promoting naive CD4 T cell quiescence in the peripheral tissues.

Materials and Methods

Mice

T cell-specific Cul3 deficient mice (Cul3$^{fl/fl}$ CD4-Cre, referred to as Cul3 KO) were generated by crossing Cul3$^{fl/fl}$ mice with CD4-Cre expressing mice maintained in our colony. In all experiments with Cul3 KO mice, Cul3$^{fl/fl}$ littermates (referred to as WT) were used as controls. Cul3 deficient OT-II transgenic mice (Cul3$^{fl/fl}$ CD4-Cre OT-II$^+$; referred to as Cul3 KO OT-II) were generated by crossing Cul3$^{fl/fl}$ CD4-Cre mice with OT-II transgene expressing mice purchased from the Jackson Laboratories. In all experiments using Cul3 KO OT-II mice, Cul3$^{fl/fl}$ OT-II$^+$ littermates (referred to as OT-II) were used as controls. A mix of male and female mice ranging from 6-20 weeks of age were used in all experiments. All mice were bred in-house and kept in specific pathogen free conditions. All animal experiments were performed in accordance with the Institutional Animal Care and Use Committee of the University of Michigan.

Cell Isolation, Purification, and Culture

Thymi and spleens were mechanically disrupted and transferred onto a 100μm cell strainer to collect single cell suspensions. Homogenized cell suspensions were treated with 1.66% NH$_4$Cl for 10 minutes to lyse RBCs, washed twice with 1X PBS, and resuspended in 1X PBS + 1% FBS (FACS buffer).

Naive CD4 T cells were sorted from murine splenocytes using an MA900 Multi-Application Cell Sorter (Sony Biotechnology) based on CD62L and CD44 expression. Naive CD4 T cells T cells were activated with plate-bound αCD3 (5 μg/mL) and soluble αCD28 (1 μg/mL) antibodies (eBioscience) for an indicated time in RPMI 1640 medium supplemented with 10% FBS, 2 mM glutamine, and penicillin/streptomycin at 37°C. For cell proliferation, CD4 T cells were labeled with CellTrace™ Violet (CTV) (5 μM) (Invitrogen) in 1X PBS containing 0.1% BSA for 30 min at 37°C.

Flow Cytometry Assays

The fluorescently-conjugated antibodies used for surface and intracellular staining in the presence of anti-FcγR mAb (2.4G2) were: anti-mouse TCR-β (H57-597) PE-Cy7/APC/Pacific Blue, anti-mouse TCR-Vb5.1 (MR9-4) FITC/APC, anti-mouse TCR-Va2 (B20.1) PE/PE-Cy7, anti-mouse CD4 (GK1.5) PerCP-Cy5.5/APC-Cy7, anti-mouse CD8 (53-6.7) FITC/PE/PE-Cy7/Am Cyan, anti-mouse CD5 (53-7.3) FITC/PE, anti-mouse CD44 (IM7) FITC/PE/PerCP-Cy5.5, anti-mouse CD62L (MEL-14) PE/PE-Cy7/BV605, anti-mouse CD127 (A7R34) PE-Cy7, anti-mouse CD122 (5H4) PE, anti-mouse CD71 (R17217) FITC/PerCP-Cy5.5, anti-mouse CD25 (PC61.5) PerCP-Cy5.5/PE-Cy7, anti-mouse CD69 (H1.2F3) FITC/PE/PE-Cy7, anti-Ki-67 (SolA15) PerCP-Cy5.5, anti-active caspase-3 (C92-605) PE, anti-mouse Nur77 (12.14) PE, anti-IL-2 (JES6-5H4) PE, anti-IFNγ (XMG1.2) FITC/PE, phospho-p44/42 MAPK (ERK1/2) (Thr202/Tyr204) (197G2) AF488, phospho-S6 Ribosomal Protein (Ser235/236) (D57.2.2E) PE-Cy7, and phosphor-Stat5 (Tyr694) (C71E5) PE. Antibodies were purchased from eBioscience, Biolegend, or BD Bioscience.

For Fpn, fixed cells were incubated with metal transporter protein antibody (rabbit anti-mouse MTP1/IREG1/Ferroprotein, Fpn) (Alpha Diagnostic) in FACS buffer. Ferritin expression was measured by anti-mouse ferritin (EPR3004Y) (Abcam) staining in cytoplasmic permeabilization buffer (BD Bioscience) after fixation. For ferritin samples, AF488-conjugated anti-rabbit IgG secondary antibody (Invitrogen) was used. Active caspase-3 (C92-605) (BD Bioscience) staining was done in parallel with Ki-67 staining in nuclear permeabilization buffer. For intracellular cytokine expression, activated CD4 T cells were re-stimulated with 50 ng/mL of PMA (Sigma Aldrich) and 1.5 μM Ionomycin (Sigma Aldrich) in the presence of 3 μM Monensin for 4 h, followed by intracellular cytokine staining (BD Biosciences). Dead cells were excluded

from the analysis based on propidium iodide (PI) (1 µg/mL), LIVE/DEAD™ Fixable Aqua Dead Cell Stain (Invitrogen), or LIVE/DEAD™ Fixable Yellow Dead Cell Stain (Invitrogen) signal. Cells were acquired on a FACS Canto II (BD Bioscience), and data was analyzed using FlowJo (TreeStar software ver. 10.8.1).

In Vivo BrdU Incorporation

Seven- to sixteen-week-old WT and Cul3 KO mice were injected twice intraperitoneally (6 h apart) with 0.5 mg of BrdU (Sigma-Aldrich) in 0.2 mL PBS. Approximately 18 h after the last injection, animals were euthanized, and single cell suspensions were prepared from thymi as described earlier. Following surface staining, 3×10^6 whole thymocytes were stained for BrdU incorporation using a BrdU flow kit (BD Bioscience) as per the manufacturer's protocol.

Cell Signaling

To measure the expression of phospho-p44/42 MAPK (ERK1/2) (Thr202/Tyr204) (197G2) (Cell Signaling), phospho-S6 Ribosomal Protein (Ser235/236) (D57.2.2E) (Cell Signaling), and phosphor-Stat5 (Tyr694) (C71E5) (Cell Signaling), sorted naive CD4 T cells were permeabilized using 90% methanol. Cells were then stained with pERK, pS6, or pSTAT5 for 1 h at room temperature in the dark in cytoplasmic permeabilization buffer (BD Bioscience).

ELISA

Supernatants were collected from sorted WT and Cul3 KO naive CD4 T cells stimulated with plate-bound αCD3 (5 µg/mL) and soluble αCD28 (1 µg/mL) antibodies (eBioscience) for 3 days. ELISA assays were done in conjunction with the University of Michigan ELISA core.

Metabolic Parameters

For each parameter, either whole thymocytes (3×10^6) or sorted naive CD4 T cells were incubated with each of the following reagents as indicated. Cells were analyzed by flow cytometry following all metabolic stainings.

To measure glucose uptake**,** cells were incubated in 2-(N-(7-nitrobenz-2-oxa-1,3-diaxol-4-yl) amino)-2-deoxyglucose (2-NBDG) (Invitrogen) (20 µM) for 1 h at 37°C in glucose-free RPMI 1640 media containing 5% dialyzed FBS.

Mitochondrial potential, mitochondrial mass, and mitochondrial ROS (mtROS) were measured using tetramethylrhodamine methyl ester perchlorate (TMRM) (60 nM) (Invitrogen), MitoTracker™ Green (30 nM) (Invitrogen), and MitoSOX (2.5 µM) (Invitrogen), respectively. Cells were treated with MitoTracker™ Green and TMRM for 30 min and MitoSOX for 25 min at 37°C.

Seahorse Assay

Splenic naive CD4 T cells from WT and Cul3 KO mice were sorted and stimulated for 24 hours with plate-bound αCD3 (5 µg/mL) and soluble αCD28 (1 µg/mL) antibodies (eBioscience). In the XF96 well microplate coated with poly-L-lysine, 1.5×10^5 cells per well were plated in glucose-free Seahorse media (Sigma Aldrich) and the plate was briefly spun to affix the cells to the bottom of the wells. The plate was then incubated for 30 min in a non-CO_2 incubator to equilibrate. OCR was measured in stimulated naive CD4 T cells using oligomycin (2 mM, ATP coupler) (Sigma Aldrich), FCCP (1.5µM) (Sigma Aldrich), antimycin A (1 µM) (Sigma Aldrich), and rotenone (100 nM) (Sigma Aldrich) in Seahorse assay medium using Seahorse XFe96 bioanalyzer (Agilent Technologies).

Labile Iron Pool (LIP)

To measure LIP, cells were stained with calcein-acetomethoxy (Calcein-AM) dye (0.02 µM) (Thermofisher) for 10 min at 37°C and analyzed by flow cytometry. LIP was calculated based on the ratio of Calcein MFI of control vs. test samples.

Statistical Analysis

All graphs were prepared using Graphpad Prism software (Prism version 9.2.0; Graphpad Software, San Diego, CA). For comparison among multiple groups, data was analyzed using one-way ANOVA with multi-comparison post-hoc test. For comparison between two groups, unpaired Student t-tests were used. $P < 0.05$ was considered statistically significant.

Results

Cul3 does not control CD4 T cell development

As described in Chapter 3, Cul3 is a critical regulator of iNKT cell development in the thymus. Loss of Cul3 results in aberrant proliferation, death, and metabolic activity in developing iNKT cells. Therefore, we wondered whether Cul3 has similar effects on conventional CD4 T cell development in the thymus. We began by examining the effects of Cul3 on proliferation in thymic single positive (SP) CD4 T cells using both Ki-67 and BrdU staining. In contrast to iNKT cells, SP CD4 T cells do not spontaneously proliferate in the absence of Cul3 (Fig. 4.1A). Like iNKT cells, Cul3 deficient SP CD4 T cells showed lower TCR-β expression (Fig. 4.1B) that coincides with higher Nur77 expression (Fig. 4.1C), indicating that TCR signaling strength is higher in SP CD4 T cells lacking Cul3 (92, 122). Despite this increase in TCR signaling strength, thymic selection processes appear to be similar between WT and Cul3 KO SP CD4 T cells, as levels of the activation markers CD5 and CD69 are comparable in both cell types (Fig. 4.1D and 4.1E). We also investigated whether Cul3 controls cytokine receptor signaling in developing CD4 T cells by staining for the IL-7 receptor (IL-7Rα) and the IL-15 receptor (IL-15R). However, loss of Cul3 did not impact the expression of either receptor in SP CD4 T cells (Fig. 4.1F). Because Cul3 deficient thymic iNKT cells exhibit increased glucose metabolism, we measured glucose uptake in SP CD4 T cells using the fluorescent glucose analog 2-NBDG. Although statistically significant, glucose uptake was not hugely different between wild type (WT) and Cul3 deficient SP CD4 T cells (Fig. 4.1G). We also measured mitochondrial mass, mitochondrial potential, and mitochondrial ROS (mtROS) production using the fluorescent markers MitoTracker™ Green, TMRM, and MitoSOX, respectively. Loss of Cul3 slightly reduced mitochondrial potential in SP CD4 T cells (Fig. 4.1H, middle panel). However, mitochondrial mass (Fig. 4.1H, left panel) and mtROS production (Fig. 4.1H, right panel) were not affected by Cul3. Together, our data indicate that Cul3 is not important for CD4 T cell development in the thymus.

Cul3 is critical for naive CD4 T cell maintenance in the periphery

In addition to thymic SP CD4 T cells, we examined naive (CD4^{+} CD62L^{hi} CD44^{lo}) and effector (CD4^{+} CD62L^{lo} CD44^{hi}) CD4 T cells in the spleen. We found that Cul3 deficiency
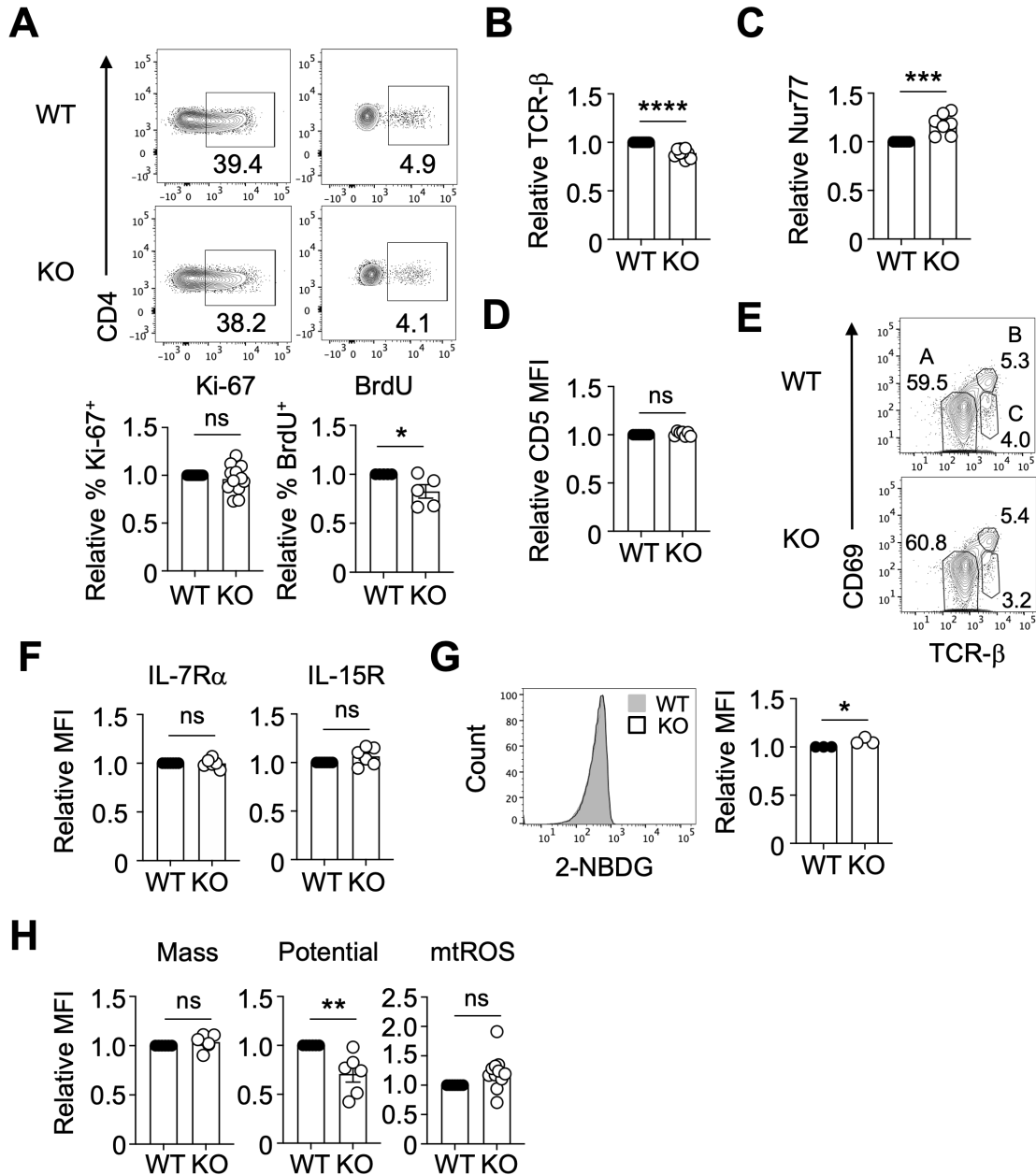
Figure 4.1 – Cul3 is not required for CD4 T cell thymic development.
(A) Representative dot plots show the relative % Ki-67^{+} (left panels) and % BrdU[+] (right panels) SP CD4 T cells present in whole thymocytes. Bar graphs show pooled data for Ki-67 (n=6) and BrdU (n=4). (B-D) Bar graphs illustrate the mean fluorescent intensity (MFI) of (B) TCR-β (n=7), (C) Nur77 (n=4), and (D) CD5 (n=4) in Cul3 KO SP CD4 T cells relative to WT cells. (E) Dot plots show positive selection as a function of CD69 expression in total thymocytes from WT and Cul3 KO mice. Group A shows cells prior to selection, group B shows cells after selection, and group C represents mature cells. Data are representative of 3 independent experiments. (F) Bar graphs illustrate the MFI of IL-7Rα and IL-15R in Cul3 KO SP CD4 T cells relative to WT cells. (n=5). (G) Overlaid histogram shows 2-NBDG staining pattern in WT and Cul3 KO SP CD4 T cells. Bar graph shows the pooled MFI values of 2-NBDG from Cul3 KO SP CD4 T cells relative to WT cells. (n=3). (H) Bar graphs show the MFI of MitoTracker[TM] Green (n=3), TMRM (n=3), and MitoSOX (n=5) in Cul3 KO SP CD4 T cells relative to WT. Error bars represent mean ± SEM. *p<0.05, **p<0.005, ***p<0.0005, ****p<0.0001, ns: not significant.

results in a severe loss of peripheral naive CD4 T cells that is accompanied by a gain in effector CD4 T cells (Fig. 4.2A and 4.2B). These data suggest that naive CD4 T cells lacking Cul3 spontaneously transition into effector cells *in vivo*. Signaling through the IL-7R is known to be important for naive CD4 T cell homeostasis in the periphery (116-118). Therefore, we measured the expression of IL-7Rα as well as the expression of IL-15R in splenic naive CD4 T cells. IL-7Rα expression was reduced on peripheral naive CD4 T cells lacking Cul3 (Fig. 4.2C, left panel). However, Cul3 did not affect IL-15R expression in splenic naive CD4 T cells (Fig. 4.2C, right panel). IL-7R signaling is known to promote naive CD4 T cell survival by modulating the expression of anti-apoptotic proteins (116, 117). Consistent with decreased IL-7Rα expression, Cul3 KO naive CD4 T cells died more than WT cells as measured by active caspase 3 staining (Fig. 4.2D). However, splenic naive CD4 T cells lacking Cul3 simultaneously underwent more spontaneous proliferation than WT cells as measured by Ki-67 expression (Fig. 4.2D). Additionally, Cul3 deficient naive CD4 T cells produced higher levels of the inflammatory cytokine IFNγ *ex vivo* compared to WT cells (Fig. 4.2E). Both proliferation and cytokine production occur downstream of T cell receptor signaling in naive T cells. Therefore, we examined the expression of TCR signaling proteins in the absence of Cul3. Cul3 deficient naive CD4 T cells had higher basal levels of phosphorylated ERK (pERK) and phosphorylated STAT5 (pSTAT5) than WT cells (Fig. 4.2F). Although IL-7R signaling modulates mTORC1 signaling in naive CD4 T cells, phosphorylated levels of the mTORC1 target protein S6 (pS6) were not affected by the loss of Cul3 (Fig. 4.2F). In all, these data indicate that peripheral naive CD4 T cells lacking Cul3 are pre-activated *in vivo*.

Cul3 restrains activation-induced proliferation and cytokine production in naive CD4 T cells

Because Cul3 deficient naive CD4 T cells appear to be pre-activated, we wondered whether Cul3 plays a role in modulating naive CD4 T cell responses after TCR ligation. To test this question, we sorted splenic naive CD4 T cells from either Cul3$^{fl/fl}$ (WT) or Cul3$^{fl/fl}$ CD4-Cre (Cul3 KO) mice based on CD62L and CD44 expression. Naive cells were then stimulated for up to 3 days *in vitro* with αCD3 and αCD28 antibodies. We found that Cul3 KO naive CD4 T cells proliferate better than WT cells at both day 2 and day 3 post-activation (Fig. 4.3A). The central dogma of T cell biology is that naive T cells require signals from the TCR, the co-stimulatory receptor CD28, and extracellular cytokines to proliferate and differentiate into effector cells
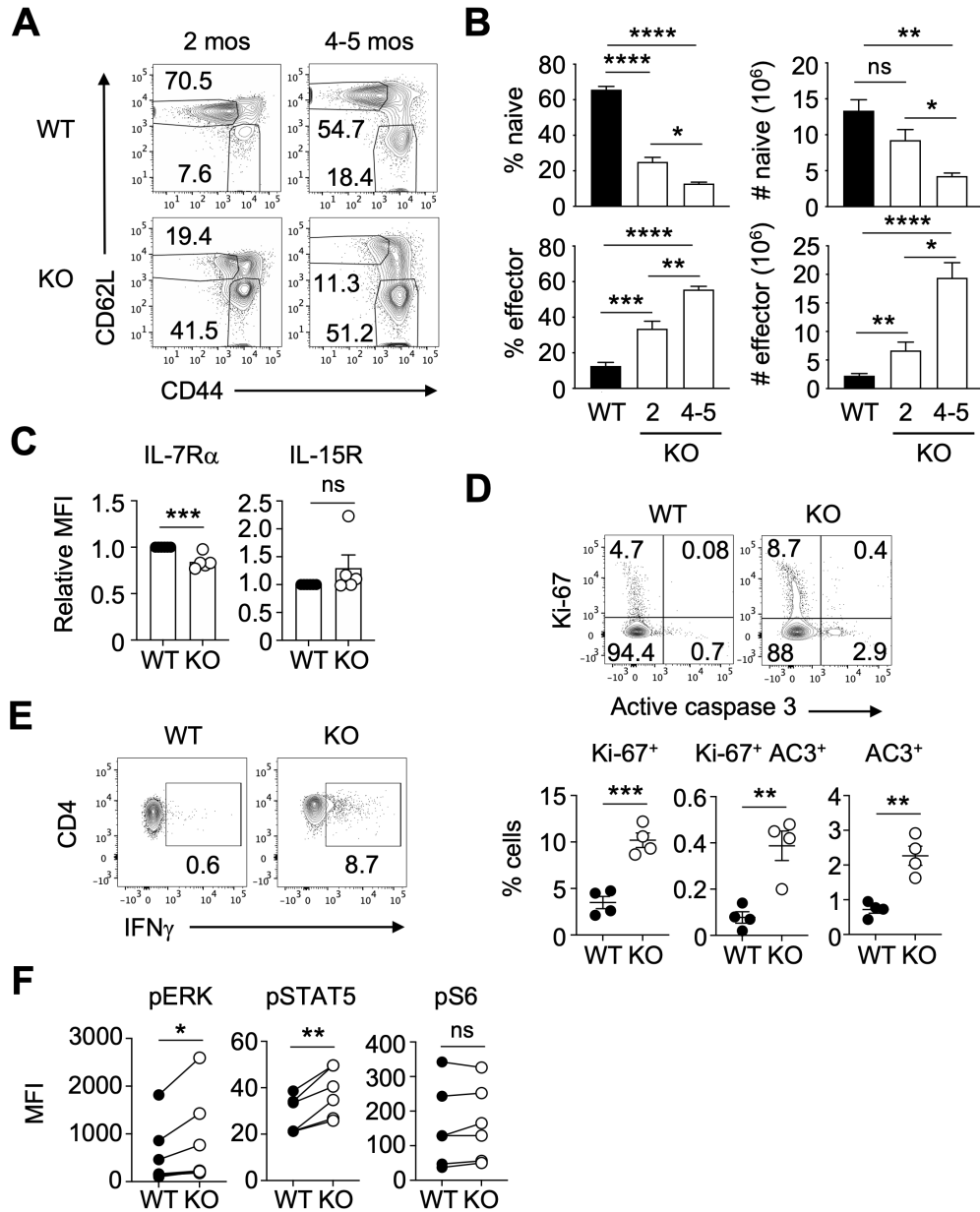
Figure 4.2 – Cul3 is critical for naive CD4 T cell homeostasis in the periphery.
(A) Representative dot plots show naive (CD62L^{hi} CD44^{lo}) and effector (CD44^{hi} CD62L^{lo}) CD4 T cell frequencies in the spleens of WT and either 2 month (mos) old or 4-5 month old Cul3 KO mice. (B) Pooled percentages and numbers of naive and effector CD4 T cells are illustrated by the bar graphs. n=3-6 mice per group. (C) Graphs show the mean fluorescent intensity (MFI) of IL-7Rα and IL-15R in Cul3 KO naive CD4 T cells relative to WT cells. (n=4). (D) Representative dot plots show the Ki-67 and active caspase 3 (AC3) staining pattern of sorted naive CD4 T cells collected from the spleens of WT and Cul3 KO mice. Graphs show the pooled frequencies of cells that are spontaneously proliferating (Ki-67$^+$), proliferating and dying (Ki-67$^+$ AC3$^+$), or undergoing cell death (AC3$^+$). (n=4). (E) Representative dot plots show IFNγ expression in freshly sorted WT and Cul3 KO naive CD4 T cells. (F) Graphs show the raw MFI values of pERK (n=7), pSTAT5 (n=6), and pS6 (n=6) in freshly sorted WT and Cul3 KO naive CD4 T cells. Error bars represent the mean ± SEM. *p<0.05, **p<0.005, ***p<0.0005, ****p<0.0001, ns: not significant.

(123). However, Cul3 deficient naive CD4 T cells appear to be more effector-like *in vivo* due to their increased expression of TCR signaling molecules and their capacity for cytokine production (Fig. 4.2E and 4.2F). Therefore, we tested the requirement for co-stimulatory signaling by activating WT and Cul3 KO naive CD4 T cells in the absence of αCD28. The results showed that naive CD4 T cells lacking Cul3 proliferate better than WT cells without co-stimulation (Fig. 4.3B). These data further support the hypothesis that Cul3 prevents spontaneous activation of naive CD4 T cells *in vivo*.

We also wondered whether the observed proliferative advantage of Cul3 KO naive CD4 T cells is due to increased production of IL-2, which is necessary for proper T cell proliferation and survival (81). As such, we measured intracellular IL-2 and IFNγ expression by activated naive CD4 T cells after PMA and ionomycin restimulation. Surprisingly, Cul3 deficient naive CD4 T cells expressed less IL-2 but more IFNγ than WT cells at both day 2 and day 3 post-activation (Fig. 4.3C and 4.3D). To determine whether naive CD4 T cells can efficiently secrete cytokine in the absence of Cul3, we measured IL-2 and IFNγ levels in the culture media at day 3 post-stimulation by ELISA. In contrast to the intracellular staining data, Cul3 deficient naive CD4 T cells secrete higher levels of IL-2 and IFNγ than WT cells at day 3 post-activation (Figure 4.3E). In line with this observation, Cul3 deficient naive CD4 T cells express higher levels of the mature IL-2 receptor CD25 at day 2 post-activation compared to WT cells (Fig. 4.3F). In all, Cul3 deficient naive CD4 T cells proliferate better than WT cells after activation, and this proliferative advantage may be due to increased responsiveness to IL-2.

Cul3 may control naive CD4 T cell proliferation by inhibiting glucose metabolism

Resting naive CD4 T cells in the periphery favor an oxidative metabolic phenotype (101). However, after activation, naive CD4 T cells undergo a metabolic switch from oxidative metabolism to glycolytic metabolism (101). This increased reliance on glycolysis is thought to fuel the rapid proliferation necessary for clonal expansion. Because Cul3 KO naive CD4 T cells proliferate better than WT cells after activation, we hypothesized that these cells would also rely more on glucose for their function. Indeed, Cul3 deficient naive CD4 T cells take up more glucose at day 2 post-activation compared to WT cells (Fig. 4.4A). Cul3 KO naive CD4 T cells appear to use this glucose to fuel glycolysis, as extracellular lactate levels were significantly higher in cultures containing Cul3 deficient naive CD4 T cells compared to those containing WT
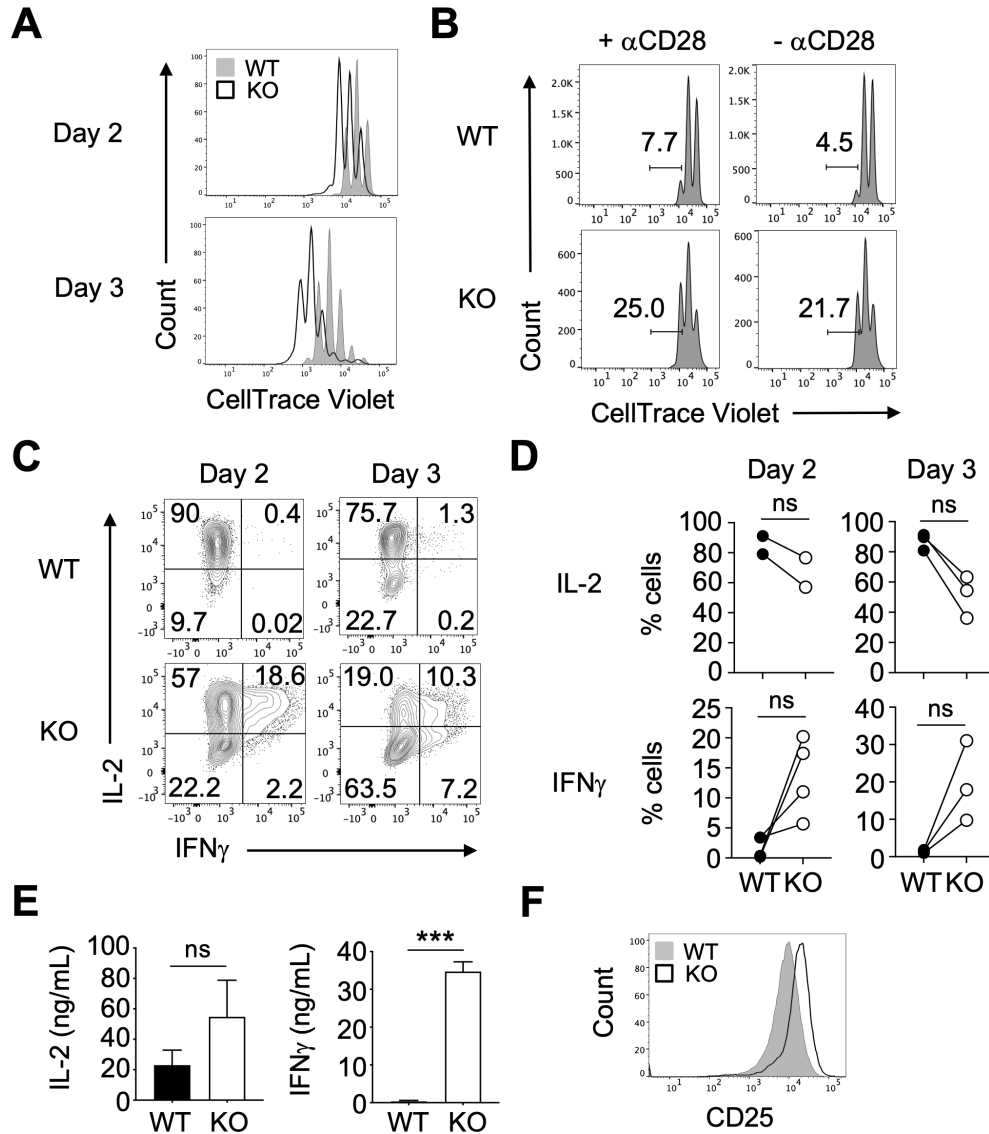
Figure 4.3 – Cul3 restrains proliferation and cytokine production in naive CD4 T cells after activation.

(A, C-F) WT and Cul3 KO naive CD4 T cells were sorted and stimulated in the presence of 5μg/mL αCD3 and 1μg/mL αCD28. (A) Histograms show the typical proliferation pattern of WT and Cul3 KO naive CD4 T cells at days 2 and 3 post-activation as measured by CellTrace Violet dilutions. (n=3). (B) WT and Cul3 KO naive CD4 T cells were sorted and stimulated with 5μg/mL αCD3 and either the presence or absence of 1ug/mL αCD28. Histograms show proliferation of WT and Cul3 KO naive CD4 T cells at day 2 post-activation as measured by CellTrace Violet dilutions. (n=2). (C) Dot plots show both IL-2 and IFNγ expression by WT and Cul3 KO naive CD4 T cells following either 2 or 3 days of *in vitro* activation and 4 hours of re-stimulation with 50ng/mL PMA and 1.5μM ionomycin. (D) Bar graphs show the pooled frequencies of IL-2$^+$ or IFNγ$^+$ naive T cells at each of the indicated time points. n=2-4 per group. (E) Graphs show IL-2 and IFNγ levels (ng/mL) in media collected from WT and Cul3 KO naive CD4 T cells at day 3 post-activation as measured by ELISA. (n=3). **(**F) Representative histograms show CD25 expression on WT and Cul3 KO naive CD4 T cells at day 2 post-activation. (n=3). Error bars represent the m in the presence of ean ± SEM. ***p<0.0005, ns: not significant.

naive CD4 T cells (Fig. 4.4B). Metabolites generated by glycolysis often go on to fuel the TCA cycle in the mitochondria. Therefore, we examined mitochondrial function in naive CD4 T cells after stimulation. Naive CD4 T cells lacking Cul3 appear to have higher mitochondrial mass than WT cells at day 3 post-activation (Fig. 4.4C, left panel); however, mitochondrial potential and mitochondrial reactive oxygen species (mtROS) production are not significantly affected by the loss of Cul3. These data seem to suggest that Cul3 KO naive CD4 T cells harbor high numbers of hypoactive mitochondria. To test this, we performed Seahorse analysis on WT and Cul3 KO naive CD4 T cells stimulated for 24 h with αCD3 and αCD28 antibodies. Seahorse is a powerful tool that can reveal a plethora of information regarding mitochondrial activity via the measurement of oxygen consumption rate (OCR). An OCR plot can be broken down into 4 discrete segments: basal respiration, ATP-coupled respiration, spare respiratory capacity, and non-mitochondrial oxygen consumption (124). Analysis of WT and Cul3 KO naive CD4 T cells revealed that both basal respiration (Fig. 4.4D, section A) and ATP-coupled mitochondrial respiration (Fig. 4.4D, section B) were similar between the two cell types at 24 h post-activation. Surprisingly, Cul3 deficient naive CD4 T cells have higher spare respiratory capacity compared to WT cells (Fig. 4.4D, section C). This finding indicates that naive CD4 T cells lacking Cul3 may respond better to cellular stress than WT cells, as their mitochondria are better able to produce ATP under oxidative stress. Additionally, non-mitochondrial oxygen consumption is virtually nonexistent in WT and Cul3 KO naive CD4 T cells after stimulation (Fig. 4.4D, section D). Together, these data indicate that mitochondria from Cul3 deficient naive CD4 T cells are indeed hyperactive rather than hypoactive. Therefore, Cul3 may restrain activation-induced naive CD4 T cell proliferation by dampening both glycolysis and mitochondrial activity.
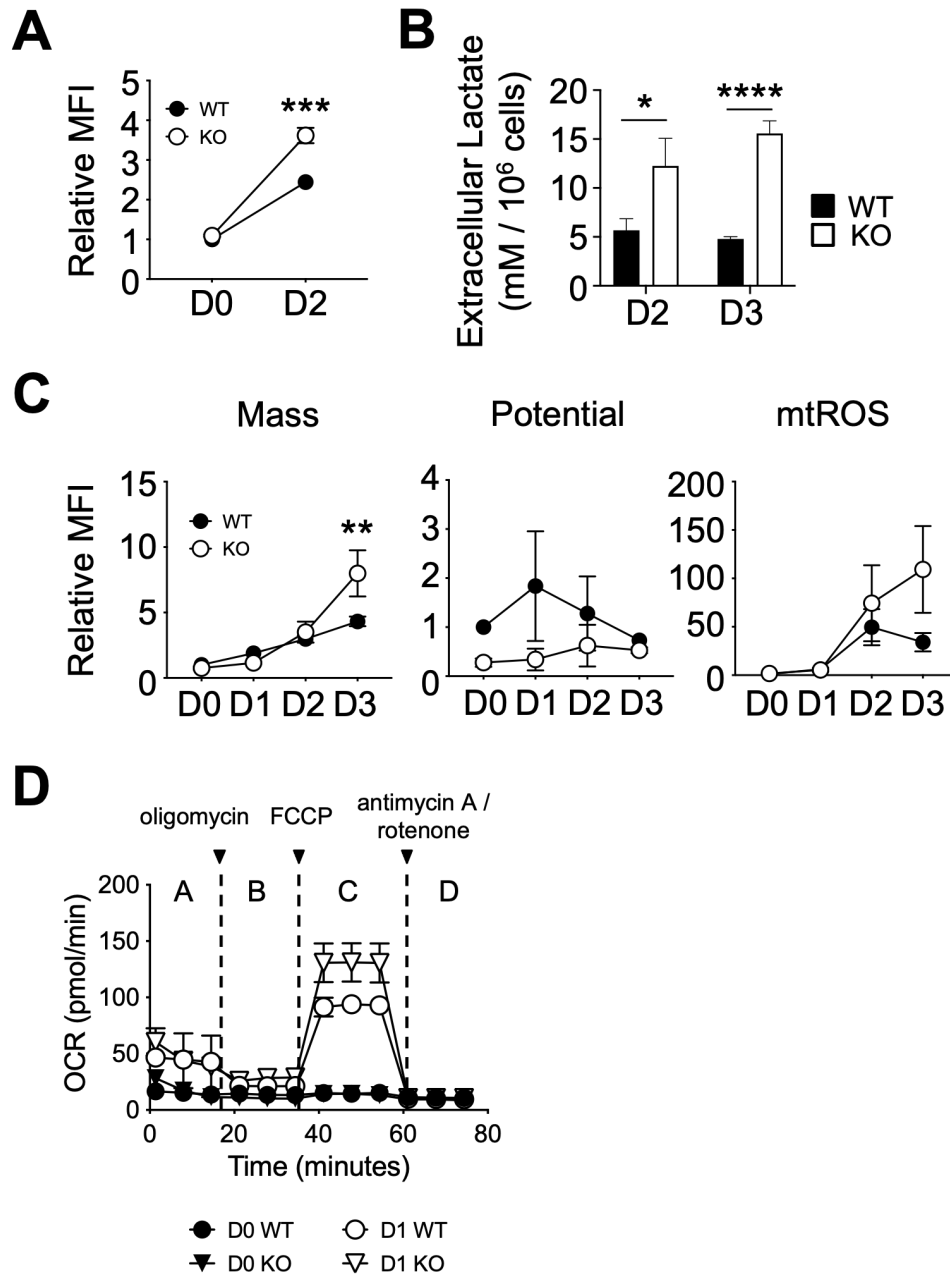
Figure 4.4 - Cul3 inhibits glycolytic metabolism and mitochondrial activity in activated naive CD4 T cells.

(A) Graph shows the pooled mean fluorescent intensity (MFI) values of 2-NBDG from sorted WT and Cul3 KO naive CD4 T cells at D0 and D2 post-activation. Relative MFI was calculated using WT D0 as a reference point. (n=3). (B) Bar graphs show the extracellular lactate levels (mM/10^6 cells) in media taken from WT and Cul3 KO naive CD4 T cell cultures at day 2 and day 3 post-activation. Data is cumulative of 3 independent experiments. (C) Pooled graphs show the MFI of MitoTracker Green, TMRM, and MitoSOX in stimulated WT and Cul3 KO naive CD4 T cells relative to WT day 0 (D0). (n=3). (D) Graph show the oxygen consumption rate (OCR) in sorted WT and Cul3 KO naive CD4 T cells either at baseline (D0) or after 24 hours of stimulation (D1) with 5µg/mL αCD3 and 1µg/mL αCD28. Data in graph is representative of 3 independent experiments. Error bars represent the mean ± SEM. *p<0.05, **p<0.005, ***p<0.0005, ****p<0.0001, ns: not significant.
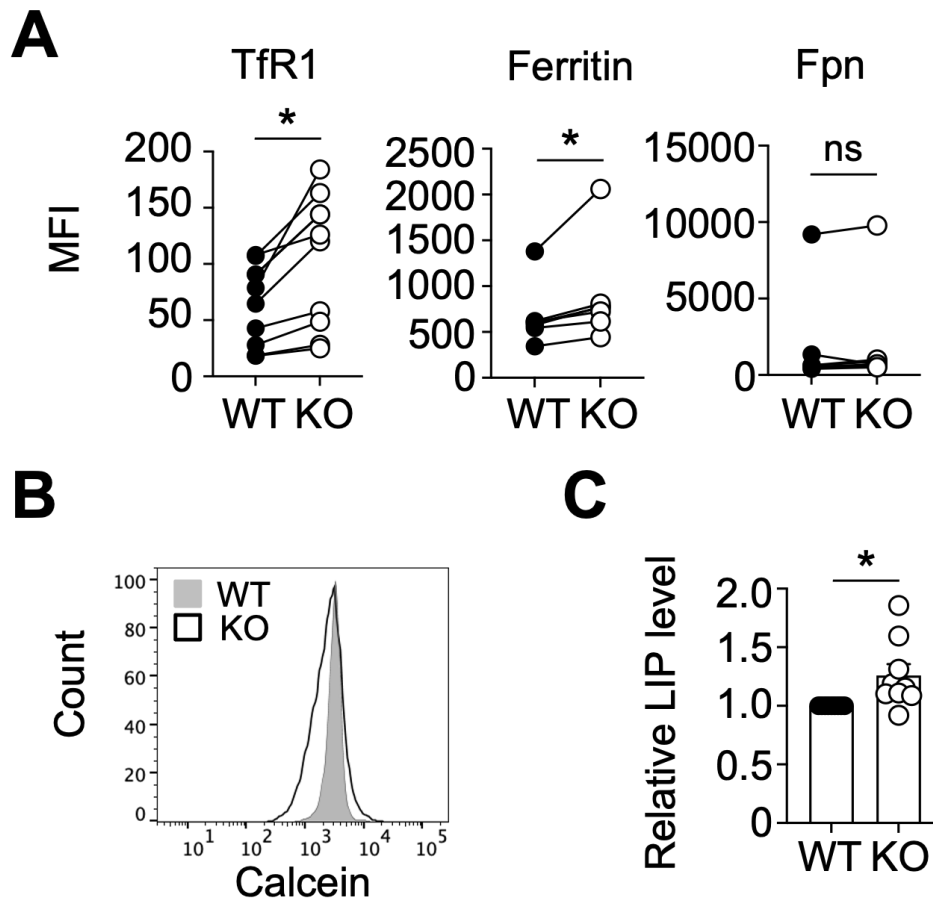
Figure 4.5 – Cul3 deficiency skews iron homeostasis in peripheral naive CD4 T cells.
(A) Graphs show the mean fluorescent intensity (MFI) values of TfR1 (n=10), ferritin (n=7), and Fpn (n=7) in freshly isolated WT and Cul3 KO naive CD4 T cells. (B) Overlaid histograms show the Calcein-AM staining pattern in WT (filled) and Cul3 KO (open) naive CD4 T cells isolated from whole splenocytes. Data are representative of 9 independent experiments. (C) Bar graph shows the LIP level in Cul3 KO naive CD4 T cells relative to WT cells as a function of Calcein MFI. (n=9). Error bars represent the mean ± SEM. *p<0.05, ns: not significant.

Intracellular iron homeostasis is disrupted in naive CD4 T cells lacking Cul3

We showed in Chapter 2 that intracellular iron flux is crucial for CD4 T cell proliferation after stimulation. We also found that Cul3 deficiency leads to iron overload in developing invariant natural killer T cells (iNKT) cells in Chapter 3. Therefore, we asked whether the loss of Cul3 affects iron homeostasis in peripheral naive CD4 T cells. We began by examining the expression of iron import, storage, and export proteins on WT and Cul3 deficient naive CD4 T cells. Naive CD4 T cells lacking Cul3 showed higher expression of the iron importer transferrin

receptor 1 (TfR1) as well as the iron storage protein ferritin (Fig. 4.5A). However, Cul3 did not affect the expression of the iron export protein ferroportin (Fpn) (Fig. 4.5A). Taken together, these data suggest that Cul3 deficient naive CD4 T cells have an increased need for iron compared to WT cells. Indeed, Cul3 KO naive CD4 T cells displayed a broader Calcein peak in comparison to that of WT naive CD4 T cells (Fig. 4.5B), indicating that Cul3 deficient naive CD4 T cells harbor higher labile iron levels (LIP) than WT cells (Fig. 4.5C). The broad Calcein staining pattern displayed by Cul3 KO naive CD4 T cells mirrors that of an effector CD4 T cell (Fig. 3.6C), again suggesting that Cul3 silences effector T cell programs in naive CD4 T cells.

OT-II transgene expression restores naive CD4 T cell maintenance in Cul3 deficient mice

Finally, we wanted to explore the role of Cul3 in regulating naive CD4 T cell responses in a more physiological system, as αCD3 and αCD28 antibody stimulation is highly artificial. Therefore, we crossed Cul3$^{fl/fl}$ CD4-Cre mice with OT-II transgene expressing mice, in which the majority of CD4 T cells express a TCR specific for ovalbumin. We planned to use these mice to examine the effects of Cul3 on antigen-specific CD4 T cell responses. However, initial characterization of these mice revealed that there was no difference in naive and effector cell frequencies in the spleens of OT-II and Cul3 KO OT-II mice (Fig. 4.6). This finding suggests that tonic signaling in the polyclonal Cul3 KO system leads to aberrant activation of naive CD4 T cells, leading to the loss of the naive CD4 T cell pool. However, future experiments examining the differences between Cul3 KO and Cul3 KO OT-II naive CD4 T cells are highly warranted to test this hypothesis.
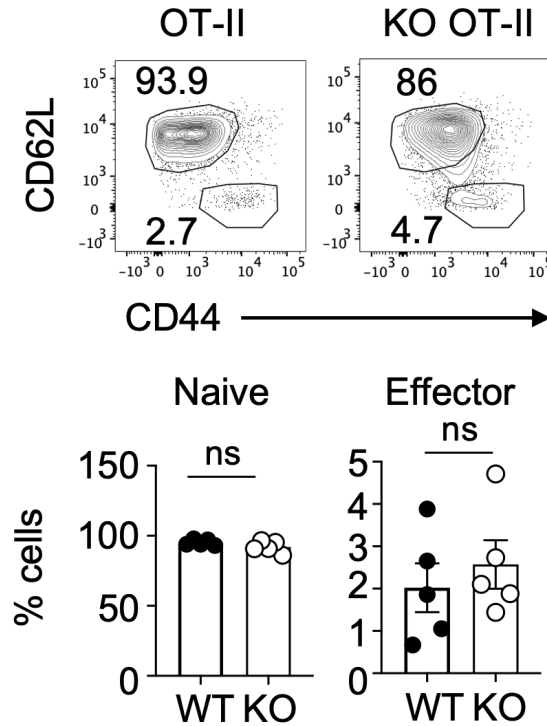
Figure 4.6 – Loss of naive CD4 T cells is abrogated in Cul3 KO OT-II mice.
Representative dot plots show naive (CD62L^{hi} CD44^{lo}) and effector (CD44^{hi} CD62L^{lo}) CD4 T cell frequencies in the spleens of OT-II and Cul3 KO OT-II mice. Bar graphs show the pooled percentages of naive and effector CD4 T cells from both types of mice. (n=5). Error bars represent the mean ± SEM. ns: not significant.

Discussion

Here, we show that Cul3 regulates naive CD4 T cell homeostasis by maintaining quiescence. Although dispensable for CD4 T cell thymic development, Cul3 is crucial for naive CD4 T cell maintenance in the periphery. Peripheral naive CD4 T cells lacking Cul3 displayed increased rates of spontaneous proliferation and cell death as well as increased basal levels of TCR signaling molecules. Similar phenotypes have recently been reported in Cul3 deficient B cells, which show increased spontaneous proliferation, cell death, and basal levels of BCR signaling molecules compared to WT B cells (34). Therefore, regulation of peripheral tolerance by Cul3 may be a lymphocyte lineage-wide phenomenon. More work is necessary to further investigate this possibility.

Our data also suggest that Cul3 prevents aberrant activation of quiescent naive CD4 T cells in the periphery. Freshly isolated Cul3 deficient naive CD4 T cells produce higher amounts

of the inflammatory cytokine IFNγ, which is uncharacteristic of a naive T cell. Additionally, naive CD4 T cells lacking Cul3 proliferate well in the absence of co-stimulatory signaling, which is required for conventional naive CD4 T cells. Lastly, we found that Cul3 KO naive CD4 T cells mirror effector CD4 T cells in terms of their Calcein staining pattern. Together, this data suggests that naive CD4 T cells lacking Cul3 may spontaneously acquire an effector phenotype, but future studies are needed to fully test this theory.

The effects of Cul3 on naive CD4 T cell peripheral maintenance appear to be dependent upon the presence of a polyclonal T cell pool, as expression of the OT-II transgene rescued naive CD4 T cell frequencies in the absence of Cul3. This observation suggests that Cul3 deficient naive CD4 T cells may be encountering activating stimuli *in vivo*. One possible endogenous source of antigen could be the microbiota. T cells in the periphery are constantly sampling antigens from symbiotic microbes, an interaction that is important for shaping peripheral tolerance in T cells (125). In the absence of Cul3, a weak microbial antigen may elicit a strong TCR signaling response, triggering T cell activation. Treating WT and Cul3 KO mice with antibiotics and examining the naive CD4 T cell pool in the periphery may give valuable insight into this possibility. Additionally, naive CD4 T cells require tonic signaling from self-peptide/MHC complexes to persist in the peripheral tissues (115). Normally, T cells that are strongly self-reactive will be deleted in the thymus by negative selection. However, loss of Cul3 in peripheral naive CD4 T cells may lower the threshold for an antigen to elicit a strong TCR response. The transfer of WT and Cul3 KO naive CD4 T cells to MHC class II deficient hosts, which cannot present self-peptides to T cells, would lend valuable insight into whether Cul3 regulates tonic signaling in naive CD4 T cells.

In summary, Cul3 may control naive CD4 T cell survival and homeostasis by regulating tonic signaling downstream of the TCR. Reduced surface BCR expression has been shown to decrease tonic signaling in circulating B cells, leading to death of these cells (126). Cul3 deficient naive CD4 T cells display decreased TCR-β expression compared to WT cells; however, these cells also have increased TCR signaling strength as measured by Nur77, suggesting that tonic signaling may also be higher in naive CD4 T cells lacking Cul3. Cul3 KO naive CD4 T cells also have increased basal pERK and pSTAT5 levels compared to WT cells, further supporting this hypothesis. Altered mitochondrial activity, glucose metabolism, and iron homeostasis in Cul3 deficient naive CD4 T cells are likely byproducts of this increased TCR

signaling. Ubiquitin ligases are known to regulate various steps in the TCR signaling cascade (127); however, future work is necessary to uncover the molecular targets for Cul3 in intracellular TCR signaling pathways in naive CD4 T cells.

Acknowledgements

Chapter 5 – Conclusions and Future Directions

Summary

My thesis work began with a single aim: to uncover a mechanistic role for the E3 ubiquitin ligase Cullin 3 (Cul3) in controlling invariant natural killer T (iNKT) cell development. This seemingly simple question would prove to be anything but simple. Over the course of my dissertation work, I have explored roles for Cul3 in both iNKT cells and naive CD4 T cells. Additionally, I have been able to link Cul3 to iron metabolism, an area of research that I pioneered as a side project. In this closing chapter, I will reiterate the key findings from each of the studies presented in this body of work and expand upon the importance of these findings for the field of T cell biology. I will also propose a working model for the role of Cul3 in developing iNKT cells.

Objectives, Major Findings, and Implications from Chapter 2

In Chapter 2, we sought to uncover mechanistic roles for iron in CD4 T cell activation and proliferation. We found that CD4 T cells rapidly export labile iron out of the cell after activation. Additionally, TCR stimulation prompts coordinated changes in the expression of iron import, storage, and export proteins in CD4 T cells. We also showed that intracellular iron flux influences CD4 T cell proliferation by regulating IL-2R signaling, as pSTAT5 levels were decreased in cells treated with the iron chelator DFO. Because DFO-treated CD4 T cells can produce high levels of IL-2, we hypothesized that iron controls IL-2R signaling by mediating recycling of the IL-2R. Lastly, we showed that iron is critical for maintaining proper mitochondrial function in activated CD4 T cells.

This study has important implications for the fields of T cell biology and iron homeostasis. For one, our data shows that CD4 T cells rapidly export iron upon receiving a stimulus. However, expression of the iron export protein Fpn decreases over the course of CD4 T cell activation. These findings suggest that T cells may utilize a Fpn-independent mechanism of

iron export, and one possibility is that T cells rely more heavily on heme-bound iron export than other cell types do. Published work has shown that deficiency in the heme-iron exporter feline leukemia virus subgroup C receptor 1 (FLVCR1) impairs T cell development and peripheral maintenance (85). Interestingly, B cell development is not affected by the loss of FLVCR1 (85), indicating that T cells have unique requirements for heme-bound iron. However, the mechanisms by which heme-bound iron controls T cell development, function, and peripheral maintenance remain unclear. Answering these questions will greatly enhance our knowledge of iron homeostasis in the context of T cell biology.

We also showed that intracellular iron dynamics are critical for proper T cell-mediated immune responses. Our findings are highly reproducible in both CD4 T and CD8 T cells. Dysregulation of iron homeostasis has also been shown to impact the differentiation of pathogenic T helper cell subsets (88), exacerbating T cell-mediated autoimmune diseases. The different T helper cell subsets are known to rely on different metabolic programs for the development of their effector functions (128). Additionally, we showed in Chapter 3 that effector CD4 T cells harbor higher levels of LIP than naive CD4 T cells, and this high level of LIP may help them quickly respond to invading pathogens. Therefore, it is interesting to speculate that the various T helper cell subsets may also have differential requirements for iron. However, this idea remains to be tested.

Objectives, Major Findings, and Implications from Chapter 3

In Chapter 3, we showed that Cul3 restrains cell proliferation and inhibits cell death in stage 3 iNKT cells in the thymus. Cul3 deficient NK1.1^{hi} iNKT cells fail to become quiescent as they reach terminal maturation, having a hyperproliferative phenotype that coincides with increased glucose metabolism and autophagy. Additionally, these cells exhibit iron overload in comparison to WT cells. Feeding mice a low iron diet partially reversed aberrant LIP accumulation in Cul3 deficient NK1.1^{hi} iNKT cells. However, an iron deficient diet did not fully rescue iNKT cell development in Cul3 KO mice. Therefore, we examined whether Cul3 modulates iNKT cell development through PLZF. Although both Cul3 deficient and PLZF deficient thymic iNKT cells proliferate more than WT cells, PLZF$^{-/-}$ iNKT cells differed from Cul3 KO NK1.1^{hi} iNKT cells in every other tested parameter, indicating that Cul3 and PLZF

may influence iNKT cell development largely independently of one another. However, future studies are warranted to fully test this hypothesis.

Based on the findings described in Chapter 3, I propose the following model (Fig. 5.1). I believe that Cul3 has three distinct functions in developing iNKT cells. First, Cul3 prevents iron overload in developing iNKT cells, protecting them from toxicity and subsequent cell death. However, the steps of the iron homeostatic pathway that are targeted by Cul3 are still unknown. Secondly, Cul3 appears to repress glycolytic metabolism in developing iNKT cells, allowing terminally differentiated iNKT cells to become quiescent. Cul3 may control this process by mediating the proteasomal degradation of Nrf2, preventing Nrf2 from entering the nucleus and activating a variety of metabolic genes. Lastly, my data suggests that Cul3 and PLZF work in concert to restrain iNKT cell proliferation during development, potentially targeting components of the TCR signaling cascade for degradation. Additionally, PLZF may transport Cul3 into the nucleus, where Cul3 can target genes involved in the cell cycle. Continued work is necessary to interrogate the exact targets of Cul3 in developing iNKT cells.
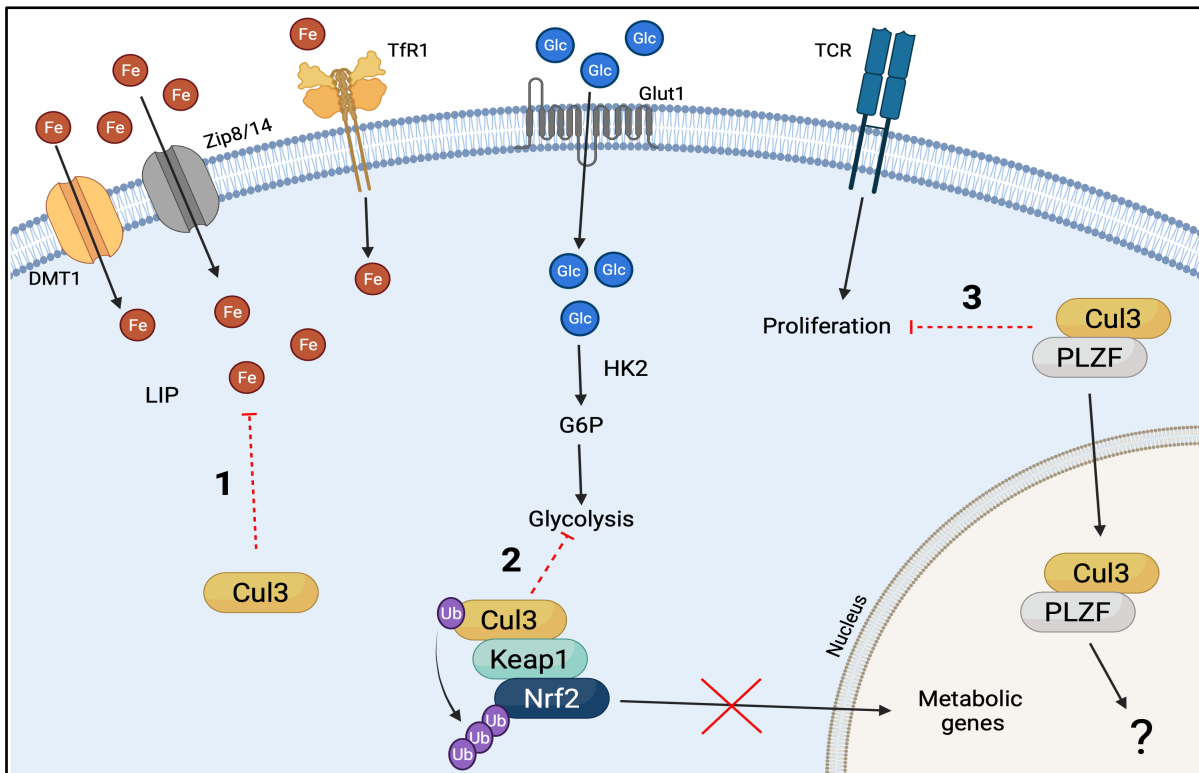

Figure 5.1 – Regulation of iNKT cell development by Cul3.
Ub = ubiquitin; Fe = iron; TFR1 = transferrin receptor 1; DMT1 = divalent metal transporter 1; ZIP8/14 = ZRT/IRT-like proteins 8/14; LIP = labile iron pool; Glc = glucose; Glut1 = glucose transporter 1; HK2 = hexokinase II; G6P = glucose 6 phosphate; TCR = T cell receptor. Created with BioRender.com.

Dysregulation of iron homeostasis leading to either iron overload or anemia has detrimental effects on T cell responses in human patients. Iron overload in patients with hereditary hemochromatosis (HH) and β-thalassemia leads to abnormal CD4 and CD8 T cell ratios in the peripheral tissues (76, 129-132). Frequencies and numbers of circulating iNKT cells are also reduced in HH patients (133), lending further support to the idea that balanced iron homeostasis is crucial for iNKT cell maintenance. Despite this, CD8 T cells from HH patients produce more inflammatory cytokines than CD8 T cells from healthy controls (134). Therefore, it is possible that increased susceptibility of HH and β-thalassemia patients to infection could be due to decreased peripheral T cell numbers. However, iron deficient patients also exhibit defects in T cell-mediated immune responses. Iron deficiency anemia leads to decreased T cell numbers and thymic atrophy in human patients (135). Patients with a missense mutation in the transferrin receptor gene also exhibit systemic iron deficiency, which results in decreased proliferative capacity of peripheral T cells (136). The negative impacts of both iron overload and deficiency on human T cell responses suggest that T cells exhibit a "Goldilocks effect" in terms of iron need. Systemic and cellular iron levels must be carefully balanced to ensure proper T cell function, as both too much and too little iron negatively impact T cell responses in a clinical setting. However, the effects of iron overload and anemia on iNKT cells in human patients is severely understudied. Addressing whether systemic iron levels impact iNKT cell trafficking and function *in vivo* could lead to a better understanding of the role of iNKT cells in iron overloaded and iron deficient patients.

Objectives, Major Findings, and Implications from Chapter 4

In Chapter 4, we showed that Cul3 is a critical regulator of peripheral naive CD4 T cell maintenance but not thymic CD4 T cell development. Additionally, naive CD4 T cells lacking Cul3 exhibit a pre-activated phenotype characterized by increased spontaneous proliferation and cytokine production as well as high levels of TCR signaling molecules at baseline. Cul3 also appears to restrain proliferation, cytokine production, and glycolytic metabolism in naive CD4 T cells after activation. We also showed that Cul3 deficient naive CD4 T cells become effector-like, losing the requirement for co-stimulation and harboring high levels of labile iron. Interestingly, generation of a monoclonal T cell pool by crossing Cul3$^{fl/fl}$ CD4-Cre mice with OT-II transgenic mice rescues peripheral naive CD4 T cell frequencies in the absence of Cul3, indicating that polyclonal naive CD4 T cells are becoming activated by tonic signaling in the
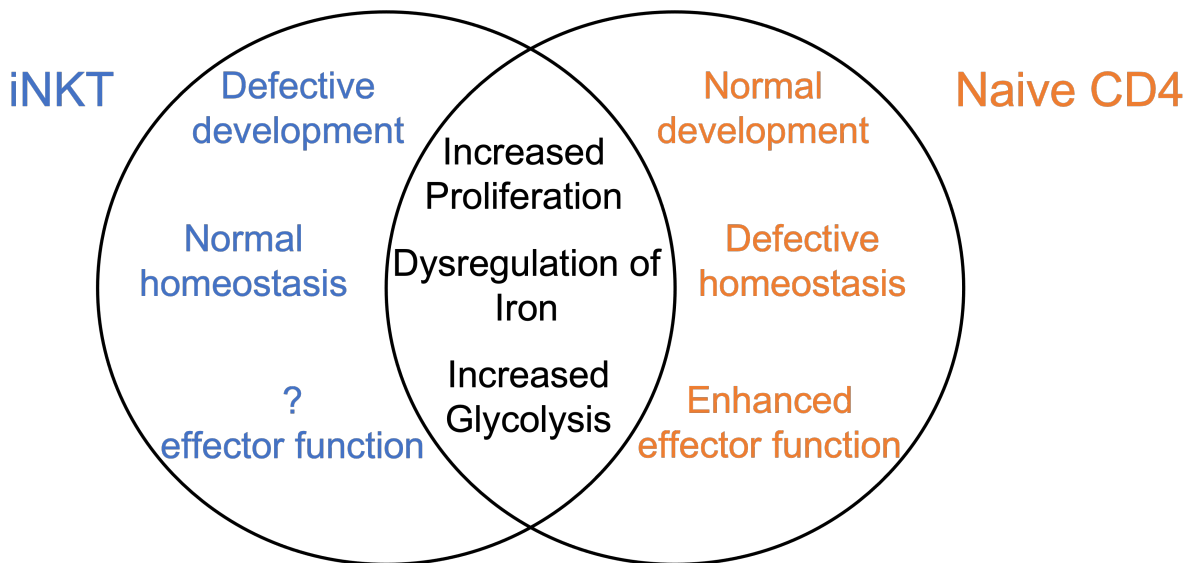
Figure 5.2 – Roles of Cul3 of iNKT cells and naive CD4 T cells.

absence of Cul3. However, mechanistic targets underlying the development of the observed phenotypes are still under investigation.

The cumulation of my data has highlighted roles for Cul3 that are common across several T cell types (Fig. 5.2). For example, Cul3 appears to inhibit proliferation and glycolytic metabolism in both thymic iNKT cells and splenic naive CD4 T cells. Additionally, Cul3 regulates iron homeostasis in both cell types. However, my data has also revealed that Cul3 controls T cell development and homeostasis in a cell type specific manner (Fig. 5.2). Moreover, Cul3 appears to inhibit cytokine production in naive CD4 T cells, but the effects of Cul3 on the development of effector functions in peripheral iNKT cells is still unknown (Fig. 5.2). These revelations have furthered our understanding of the role of Cul3 in T cell biology.

Final Thoughts

In all, my thesis has uncovered a novel role for Cul3 in modulating cellular iron homeostasis in both developing iNKT cells in the thymus and naive CD4 T cells in the periphery. However, Cul3 is critical for iNKT cell development but not for conventional T cell development. Single positive CD4 and CD8 T cell frequencies in the thymus are unchanged by the loss of Cul3, with phenotypic abnormalities arising only after these cells have migrated to the periphery. Why is Cul3 so crucial for developing iNKT cells but not CD4 and CD8 T cells? One possibility is that Cul3 could have different roles in naive and effector cells. iNKT cells egress

from the thymus as effector cells, while CD4 and CD8 T cells leave as quiescent naive cells. In Chapter 4, we showed that Cul3 helps maintain naive CD4 T cell populations in the periphery. However, we did not study the roles of Cul3 in effector CD4 T cell responses. Effector CD4 T cells in the periphery may show many of the same phenotypes as thymic iNKT cells lacking Cul3, but this possibility will need to be tested further.

Additionally, the Cul3-Keap1-Nrf2 trimeric complex may have differing levels of importance in innate-like T cells compared to conventional T cells. We know that resting peripheral iNKT cells harbor high levels of ROS, whereas resting peripheral CD4 T cells harbor low levels of ROS (100). Thymic iNKT cells contain considerably lower levels of ROS than peripheral iNKT cells (100), which may result from hyperactivity of the Cul3-Keap1-Nrf2 antioxidation system during iNKT cell development. Interestingly, Keap1 deficiency also results in a block in iNKT cell development, with cells in stages 2 and 3 proliferating and dying more than wild type cells (107). Additionally, thymic iNKT cells lacking Keap1 display increased glucose metabolism and mitochondrial activity but decreased ROS levels compared to wild type cells (107). All of these phenotypes were shown to be driven by increased Nrf2 levels in the absence of Keap1 (107). Therefore, developing iNKT cells may rely heavily on Cul3 and Keap1 to keep Nrf2 levels in check, as hypermetabolic activity mediated by Nrf2 target gene transcription appears to be detrimental for these cells. The metabolic quiescence displayed by mature thymic iNKT cells contrasts the metabolic phenotype of single-positive CD4 and CD8 T cells in the thymus, which have been shown to have higher rates of ECAR and OCR compared to double positive thymocytes (137). As such, a bump in glycolytic and oxidative activity induced by Nrf2 may not be as detrimental for conventional T cells in the thymus. Instead, aberrant metabolic activity may negatively influence CD4 and CD8 T cell quiescence in the periphery, leading to a break in peripheral tolerance as described in Chapter 4. Continued studies are warranted to fully explore this hypothesis.

My data therefore begs the question of whether Cul3 is important for the development and homeostasis of all innate-like T cells. To address this question, I examined γδ T cell frequencies in the thymi and spleens of wild type and Cul3$^{fl/fl}$ CD4-Cre mice. Cul3 deficiency did not affect γδ T cell percentages in the thymus (data not shown), suggesting that Cul3 does not regulate γδ T cell development. There are several possible explanations between the differing requirements of developing γδ T cells and iNKT cells for Cul3. For one, γδ T cells arise in the

prenatal thymus and serve one of the first lines of defense in the fetal immune system (138). In contrast, iNKT cells do not arise until after birth, accumulating as individuals age (138). Additionally, γδ T cells arise from the double negative stage of T cell development, whereas iNKT cells arise later in development from the double positive stage (138). Therefore, I hypothesize that Cul3 may be important for the development of innate-like T cells that arise during the double positive stage of thymic development, such as iNKT cells and MAIT cells. Future work is necessary to examine the role of Cul3 in MAIT cell development. Additionally, studying changes in Cul3 expression over the course of thymic development will help explain why Cul3 is important for the development of some T cell subsets but not others.

Finally, I would like to end on a personal anecdote dedicated to all of my fellow graduate students. When I started my PhD, I believed that I would easily solve my research questions. I would find the mechanism by which Cul3 controlled iNKT cell development, and I would publish in top tier journals. If you've read this far, you know that I did not achieve those goals. However, that does not diminish the immense value of my thesis work. It opened my eyes to new avenues of scientific investigation, allowed me to explore systems outside of immunology, and molded me into the scientist I am today. My thesis work has uncovered many more questions than answers, but these questions are the legacy I leave behind for the next generation of bright minds. One of my favorite quotes is from Walt Disney, and it reads:

"Around here, however, we don't look backwards for very long. We keep moving forward, opening up new doors and doing new things, because we're curious…and curiosity keeps leading us down new paths."

Stay curious, friends. You never know where that new path may take you, and it might just be the most exciting ride of your life.

Appendix

Author Contributions

<u>Chapter 1</u>

Portions of this chapter have been published.

Cul3 in Antioxidation section:

Emily L. Yarosz and Cheong-Hee Chang. The Role of Reactive Oxygen Species in Regulating T Cell-Mediated Immunity and Disease. *Immune Network*. 2018 Feb 22; 18 (1): e14. PMID: 29503744.

Introduction to Invariant Natural Killer T Cells section:

Emily L. Yarosz, Cheong-Hee Chang, and Ajay Kumar. Metabolism in Invariant Natural Killer T Cells: An Overview. *Immunometabolism*. 2021 Feb 10; 3(2); e210010. PMID: 33717605.

<u>Chapter 2</u>

This chapter has been published.

Emily L. Yarosz*, Chenxian Ye*, Ajay Kumar*, Chauna Black, Eun-Kyung Choi, Young-Ah Seo, and Cheong-Hee Chang. Activation-Induced Iron Flux Controls CD4 T Cell Proliferation by Promoting Proper IL-2R Signaling and Mitochondrial Function. *Journal of Immunology Cutting Edge*. 2020 Jan 30; 204(7);1708-1713. PMID: 32122995. *Authors contributed equally.

Chapter 3

This chapter is currently in preparation for submission.

Emily L. Yarosz, Ajay Kumar, and Cheong-Hee Chang. Cullin 3 Promotes iNKT Cell Development and Survival by Maintaining Intracellular Iron Homeostasis.

Chapter 4

The data described in this chapter is preliminary. Work to bring the project to a publishable point is ongoing.

Bibliography

1. Petroski, M. D., and R. J. Deshaies. 2005. Function and regulation of cullin-RING ubiquitin ligases. *Nat Rev Mol Cell Biol* 6: 9-20.
2. Sarikas, A., T. Hartmann, and Z. Q. Pan. 2011. The cullin protein family. *Genome Biol* 12: 220.
3. Fouad, S., O. S. Wells, M. A. Hill, and V. D'Angiolella. 2019. Cullin Ring Ubiquitin Ligases (CRLs) in Cancer: Responses to Ionizing Radiation (IR) Treatment. *Front Physiol* 10: 1144.
4. Enchev, R. I., B. A. Schulman, and M. Peter. 2015. Protein neddylation: beyond cullin-RING ligases. *Nat Rev Mol Cell Biol* 16: 30-44.
5. Kawakami, T., T. Chiba, T. Suzuki, K. Iwai, K. Yamanaka, N. Minato, H. Suzuki, N. Shimbara, Y. Hidaka, F. Osaka, M. Omata, and K. Tanaka. 2001. NEDD8 recruits E2-ubiquitin to SCF E3 ligase. *EMBO J* 20: 4003-4012.
6. Wu, J. T., H. C. Lin, Y. C. Hu, and C. T. Chien. 2005. Neddylation and deneddylation regulate Cul1 and Cul3 protein accumulation. *Nat Cell Biol* 7: 1014-1020.
7. Wu, K., A. Chen, and Z. Q. Pan. 2000. Conjugation of Nedd8 to CUL1 enhances the ability of the ROC1-CUL1 complex to promote ubiquitin polymerization. *J Biol Chem* 275: 32317-32324.
8. Boh, B. K., P. G. Smith, and T. Hagen. 2011. Neddylation-induced conformational control regulates cullin RING ligase activity in vivo. *J Mol Biol* 409: 136-145.
9. Stogios, P. J., G. S. Downs, J. J. Jauhal, S. K. Nandra, and G. G. Prive. 2005. Sequence and structural analysis of BTB domain proteins. *Genome Biol* 6: R82.
10. Genschik, P., I. Sumara, and E. Lechner. 2013. The emerging family of CULLIN3-RING ubiquitin ligases (CRL3s): cellular functions and disease implications. *EMBO J* 32: 2307-2320.
11. Emanuele, M. J., A. E. Elia, Q. Xu, C. R. Thoma, L. Izhar, Y. Leng, A. Guo, Y. N. Chen, J. Rush, P. W. Hsu, H. C. Yen, and S. J. Elledge. 2011. Global identification of modular cullin-RING ligase substrates. *Cell* 147: 459-474.
12. Itoh, K., T. Chiba, S. Takahashi, T. Ishii, K. Igarashi, Y. Katoh, T. Oyake, N. Hayashi, K. Satoh, I. Hatayama, M. Yamamoto, and Y. Nabeshima. 1997. An Nrf2/small Maf heterodimer mediates the induction of phase II detoxifying enzyme genes through antioxidant response elements. *Biochem Biophys Res Commun* 236: 313-322.
13. Liu, Y., J. T. Kern, J. R. Walker, J. A. Johnson, P. G. Schultz, and H. Luesch. 2007. A genomic screen for activators of the antioxidant response element. *Proc Natl Acad Sci U S A* 104: 5205-5210.
14. Moi, P., K. Chan, I. Asunis, A. Cao, and Y. W. Kan. 1994. Isolation of NF-E2-related factor 2 (Nrf2), a NF-E2-like basic leucine zipper transcriptional activator that binds to the tandem NF-E2/AP1 repeat of the beta-globin locus control region. *Proc Natl Acad Sci U S A* 91: 9926-9930.

15. Cullinan, S. B., J. D. Gordan, J. Jin, J. W. Harper, and J. A. Diehl. 2004. The Keap1-BTB protein is an adaptor that bridges Nrf2 to a Cul3-based E3 ligase: oxidative stress sensing by a Cul3-Keap1 ligase. *Mol Cell Biol* 24: 8477-8486.

16. Jaramillo, M. C., and D. D. Zhang. 2013. The emerging role of the Nrf2-Keap1 signaling pathway in cancer. *Genes Dev* 27: 2179-2191.

17. Itoh, K., N. Wakabayashi, Y. Katoh, T. Ishii, K. Igarashi, J. D. Engel, and M. Yamamoto. 1999. Keap1 represses nuclear activation of antioxidant responsive elements by Nrf2 through binding to the amino-terminal Neh2 domain. *Genes Dev* 13: 76-86.

18. Furukawa, M., and Y. Xiong. 2005. BTB protein Keap1 targets antioxidant transcription factor Nrf2 for ubiquitination by the Cullin 3-Roc1 ligase. *Mol Cell Biol* 25: 162-171.

19. Kobayashi, A., M. I. Kang, H. Okawa, M. Ohtsuji, Y. Zenke, T. Chiba, K. Igarashi, and M. Yamamoto. 2004. Oxidative stress sensor Keap1 functions as an adaptor for Cul3-based E3 ligase to regulate proteasomal degradation of Nrf2. *Mol Cell Biol* 24: 7130-7139.

20. Turley, A. E., J. W. Zagorski, and C. E. Rockwell. 2015. The Nrf2 activator tBHQ inhibits T cell activation of primary human CD4 T cells. *Cytokine* 71: 289-295.

21. Zagorski, J. W., A. E. Turley, H. E. Dover, K. R. VanDenBerg, J. R. Compton, and C. E. Rockwell. 2013. The Nrf2 activator, tBHQ, differentially affects early events following stimulation of Jurkat cells. *Toxicol Sci* 136: 63-71.

22. Suzuki, T., S. Murakami, S. S. Biswal, S. Sakaguchi, H. Harigae, M. Yamamoto, and H. Motohashi. 2017. Systemic Activation of NRF2 Alleviates Lethal Autoimmune Inflammation in Scurfy Mice. *Mol Cell Biol* 37.

23. Rockwell, C. E., M. Zhang, P. E. Fields, and C. D. Klaassen. 2012. Th2 skewing by activation of Nrf2 in CD4(+) T cells. *J Immunol* 188: 1630-1637.

24. Zhao, M., H. Chen, Q. Ding, X. Xu, B. Yu, and Z. Huang. 2016. Nuclear Factor Erythroid 2-related Factor 2 Deficiency Exacerbates Lupus Nephritis in B6/lpr mice by Regulating Th17 Cell Function. *Sci Rep* 6: 38619.

25. Noel, S., M. N. Martina, S. Bandapalle, L. C. Racusen, H. R. Potteti, A. R. Hamad, S. P. Reddy, and H. Rabb. 2015. T Lymphocyte-Specific Activation of Nrf2 Protects from AKI. *J Am Soc Nephrol* 26: 2989-3000.

26. Malumbres, M., and M. Barbacid. 2005. Mammalian cyclin-dependent kinases. *Trends Biochem Sci* 30: 630-641.

27. Dannenberg, J. H., A. van Rossum, L. Schuijff, and H. te Riele. 2000. Ablation of the retinoblastoma gene family deregulates G(1) control causing immortalization and increased cell turnover under growth-restricting conditions. *Genes Dev* 14: 3051-3064.

28. Singer, J. D., M. Gurian-West, B. Clurman, and J. M. Roberts. 1999. Cullin-3 targets cyclin E for ubiquitination and controls S phase in mammalian cells. *Genes Dev* 13: 2375-2387.

29. McEvoy, J. D., U. Kossatz, N. Malek, and J. D. Singer. 2007. Constitutive turnover of cyclin E by Cul3 maintains quiescence. *Mol Cell Biol* 27: 3651-3666.

30. Mulvaney, K. M., J. P. Matson, P. F. Siesser, T. Y. Tamir, D. Goldfarb, T. M. Jacobs, E. W. Cloer, J. S. Harrison, C. Vaziri, J. G. Cook, and M. B. Major. 2016. Identification and Characterization of MCM3 as a Kelch-like ECH-associated Protein 1 (KEAP1) Substrate. *J Biol Chem* 291: 23719-23733.

31. Sumara, I., M. Quadroni, C. Frei, M. H. Olma, G. Sumara, R. Ricci, and M. Peter. 2007. A Cul3-based E3 ligase removes Aurora B from mitotic chromosomes, regulating mitotic progression and completion of cytokinesis in human cells. *Dev Cell* 12: 887-900.

32. Moghe, S., F. Jiang, Y. Miura, R. L. Cerny, M. Y. Tsai, and M. Furukawa. 2012. The CUL3-KLHL18 ligase regulates mitotic entry and ubiquitylates Aurora-A. *Biol Open* 1: 82-91.

33. Li, X., Z. Zhang, L. Li, W. Gong, A. J. Lazenby, B. J. Swanson, L. E. Herring, J. M. Asara, J. D. Singer, and H. Wen. 2017. Myeloid-derived cullin 3 promotes STAT3 phosphorylation by inhibiting OGT expression and protects against intestinal inflammation. *J Exp Med* 214: 1093-1109.

34. Meyer, S. J., A. Boser, M. A. Korn, C. Koller, B. Bertocci, L. Reimann, B. Warscheid, and L. Nitschke. 2020. Cullin 3 Is Crucial for Pro-B Cell Proliferation, Interacts with CD22, and Controls CD22 Internalization on B Cells. *J Immunol* 204: 3360-3374.

35. Mathew, R., A. P. Mao, A. H. Chiang, C. Bertozzi-Villa, J. J. Bunker, S. T. Scanlon, B. D. McDonald, M. G. Constantinides, K. Hollister, J. D. Singer, A. L. Dent, A. R. Dinner, and A. Bendelac. 2014. A negative feedback loop mediated by the Bcl6-cullin 3 complex limits Tfh cell differentiation. *J Exp Med* 211: 1137-1151.

36. Mathew, R., M. P. Seiler, S. T. Scanlon, A. P. Mao, M. G. Constantinides, C. Bertozzi-Villa, J. D. Singer, and A. Bendelac. 2012. BTB-ZF factors recruit the E3 ligase cullin 3 to regulate lymphoid effector programs. *Nature* 491: 618-621.

37. Bendelac, A., O. Lantz, M. E. Quimby, J. W. Yewdell, J. R. Bennink, and R. R. Brutkiewicz. 1995. CD1 recognition by mouse NK1+ T lymphocytes. *Science* 268: 863-865.

38. Kovalovsky, D., O. U. Uche, S. Eladad, R. M. Hobbs, W. Yi, E. Alonzo, K. Chua, M. Eidson, H. J. Kim, J. S. Im, P. P. Pandolfi, and D. B. Sant'Angelo. 2008. The BTB-zinc finger transcriptional regulator PLZF controls the development of invariant natural killer T cell effector functions. *Nat Immunol* 9: 1055-1064.

39. Savage, A. K., M. G. Constantinides, J. Han, D. Picard, E. Martin, B. Li, O. Lantz, and A. Bendelac. 2008. The transcription factor PLZF directs the effector program of the NKT cell lineage. *Immunity* 29: 391-403.

40. Arrenberg, P., R. Halder, Y. Dai, I. Maricic, and V. Kumar. 2010. Oligoclonality and innate-like features in the TCR repertoire of type II NKT cells reactive to a beta-linked self-glycolipid. *Proc Natl Acad Sci U S A* 107: 10984-10989.

41. Behar, S. M., T. A. Podrebarac, C. J. Roy, C. R. Wang, and M. B. Brenner. 1999. Diverse TCRs recognize murine CD1. *J Immunol* 162: 161-167.

42. Lantz, O., and A. Bendelac. 1994. An invariant T cell receptor alpha chain is used by a unique subset of major histocompatibility complex class I-specific CD4+ and CD4-8- T cells in mice and humans. *J Exp Med* 180: 1097-1106.

43. Park, S. H., A. Weiss, K. Benlagha, T. Kyin, L. Teyton, and A. Bendelac. 2001. The mouse CD1d-restricted repertoire is dominated by a few autoreactive T cell receptor families. *J Exp Med* 193: 893-904.

44. Wang, H., and K. A. Hogquist. 2018. How Lipid-Specific T Cells Become Effectors: The Differentiation of iNKT Subsets. *Front Immunol* 9: 1450.

45. Godfrey, D. I., S. Stankovic, and A. G. Baxter. 2010. Raising the NKT cell family. *Nat Immunol* 11: 197-206.

46.	Benlagha, K., T. Kyin, A. Beavis, L. Teyton, and A. Bendelac. 2002. A thymic precursor to the NK T cell lineage. *Science* 296: 553-555.

47.	Benlagha, K., D. G. Wei, J. Veiga, L. Teyton, and A. Bendelac. 2005. Characterization of the early stages of thymic NKT cell development. *J Exp Med* 202: 485-492.

48.	Salio, M., D. J. Puleston, T. S. Mathan, D. Shepherd, A. J. Stranks, E. Adamopoulou, N. Veerapen, G. S. Besra, G. A. Hollander, A. K. Simon, and V. Cerundolo. 2014. Essential role for autophagy during invariant NKT cell development. *Proc Natl Acad Sci U S A* 111: E5678-5687.

49.	Yang, G., J. P. Driver, and L. Van Kaer. 2018. The Role of Autophagy in iNKT Cell Development. *Front Immunol* 9: 2653.

50.	Pei, B., M. Zhao, B. C. Miller, J. L. Vela, M. W. Bruinsma, H. W. Virgin, and M. Kronenberg. 2015. Invariant NKT cells require autophagy to coordinate proliferation and survival signals during differentiation. *J Immunol* 194: 5872-5884.

51.	Crosby, C. M., and M. Kronenberg. 2018. Tissue-specific functions of invariant natural killer T cells. *Nat Rev Immunol* 18: 559-574.

52.	Sag, D., P. Krause, C. C. Hedrick, M. Kronenberg, and G. Wingender. 2014. IL-10-producing NKT10 cells are a distinct regulatory invariant NKT cell subset. *J Clin Invest* 124: 3725-3740.

53.	LaMarche, N. M., H. Kane, A. C. Kohlgruber, H. Dong, L. Lynch, and M. B. Brenner. 2020. Distinct iNKT Cell Populations Use IFNgamma or ER Stress-Induced IL-10 to Control Adipose Tissue Homeostasis. *Cell Metab* 32: 243-258 e246.

54.	Lynch, L., X. Michelet, S. Zhang, P. J. Brennan, A. Moseman, C. Lester, G. Besra, E. E. Vomhof-Dekrey, M. Tighe, H. F. Koay, D. I. Godfrey, E. A. Leadbetter, D. B. Sant'Angelo, U. von Andrian, and M. B. Brenner. 2015. Regulatory iNKT cells lack expression of the transcription factor PLZF and control the homeostasis of T(reg) cells and macrophages in adipose tissue. *Nat Immunol* 16: 85-95.

55.	Park, J., J. Y. Huh, J. Oh, J. I. Kim, S. M. Han, K. C. Shin, Y. G. Jeon, S. S. Choe, J. Park, and J. B. Kim. 2019. Activation of invariant natural killer T cells stimulates adipose tissue remodeling via adipocyte death and birth in obesity. *Genes Dev* 33: 1657-1672.

56.	Harding, C., J. Heuser, and P. Stahl. 1983. Receptor-mediated endocytosis of transferrin and recycling of the transferrin receptor in rat reticulocytes. *J Cell Biol* 97: 329-339.

57.	Ohgami, R. S., D. R. Campagna, E. L. Greer, B. Antiochos, A. McDonald, J. Chen, J. J. Sharp, Y. Fujiwara, J. E. Barker, and M. D. Fleming. 2005. Identification of a ferrireductase required for efficient transferrin-dependent iron uptake in erythroid cells. *Nat Genet* 37: 1264-1269.

58.	Ohgami, R. S., D. R. Campagna, A. McDonald, and M. D. Fleming. 2006. The Steap proteins are metalloreductases. *Blood* 108: 1388-1394.

59.	Mims, M. P., and J. T. Prchal. 2005. Divalent metal transporter 1. *Hematology* 10: 339-345.

60.	Arezes, J., M. Costa, I. Vieira, V. Dias, X. L. Kong, R. Fernandes, M. Vos, A. Carlsson, Y. Rikers, G. Porto, M. Rangel, R. C. Hider, and J. P. Pinto. 2013. Non-transferrin-bound iron (NTBI) uptake by T lymphocytes: evidence for the selective acquisition of oligomeric ferric citrate species. *PLoS One* 8: e79870.

61.	Pinto, J. P., J. Arezes, V. Dias, S. Oliveira, I. Vieira, M. Costa, M. Vos, A. Carlsson, Y. Rikers, M. Rangel, and G. Porto. 2014. Physiological implications of NTBI uptake by T lymphocytes. *Front Pharmacol* 5: 24.

62.   McKie, A. T. 2008. The role of Dcytb in iron metabolism: an update. *Biochem Soc Trans* 36: 1239-1241.

63.   Liuzzi, J. P., F. Aydemir, H. Nam, M. D. Knutson, and R. J. Cousins. 2006. Zip14 (Slc39a14) mediates non-transferrin-bound iron uptake into cells. *Proc Natl Acad Sci U S A* 103: 13612-13617.

64.   Wang, C. Y., S. Jenkitkasemwong, S. Duarte, B. K. Sparkman, A. Shawki, B. Mackenzie, and M. D. Knutson. 2012. ZIP8 is an iron and zinc transporter whose cell-surface expression is up-regulated by cellular iron loading. *J Biol Chem* 287: 34032-34043.

65.   Zhou, L., B. Zhao, L. Zhang, S. Wang, D. Dong, H. Lv, and P. Shang. 2018. Alterations in Cellular Iron Metabolism Provide More Therapeutic Opportunities for Cancer. *Int J Mol Sci* 19.

66.   Dorner, M. H., A. Silverstone, K. Nishiya, A. de Sostoa, G. Munn, and M. de Sousa. 1980. Ferritin synthesis by human T lymphocytes. *Science* 209: 1019-1021.

67.   Donovan, A., A. Brownlie, Y. Zhou, J. Shepard, S. J. Pratt, J. Moynihan, B. H. Paw, A. Drejer, B. Barut, A. Zapata, T. C. Law, C. Brugnara, S. E. Lux, G. S. Pinkus, J. L. Pinkus, P. D. Kingsley, J. Palis, M. D. Fleming, N. C. Andrews, and L. I. Zon. 2000. Positional cloning of zebrafish ferroportin1 identifies a conserved vertebrate iron exporter. *Nature* 403: 776-781.

68.   Drakesmith, H., E. Nemeth, and T. Ganz. 2015. Ironing out Ferroportin. *Cell Metab* 22: 777-787.

69.   Macedo, M. F., M. de Sousa, R. M. Ned, C. Mascarenhas, N. C. Andrews, and M. Correia-Neves. 2004. Transferrin is required for early T-cell differentiation. *Immunology* 112: 543-549.

70.   Ned, R. M., W. Swat, and N. C. Andrews. 2003. Transferrin receptor 1 is differentially required in lymphocyte development. *Blood* 102: 3711-3718.

71.   Wang, S., X. He, Q. Wu, L. Jiang, L. Chen, Y. Yu, P. Zhang, X. Huang, J. Wang, Z. Ju, J. Min, and F. Wang. 2020. Transferrin receptor 1-mediated iron uptake plays an essential role in hematopoiesis. *Haematologica* 105: 2071-2082.

72.   Bierer, B. E., and D. G. Nathan. 1990. The effect of desferrithiocin, an oral iron chelator, on T-cell function. *Blood* 76: 2052-2059.

73.   Kuvibidila, S., B. S. Baliga, and K. K. Murthy. 1991. Impaired protein kinase C activation as one of the possible mechanisms of reduced lymphocyte proliferation in iron deficiency in mice. *Am J Clin Nutr* 54: 944-950.

74.   Kuvibidila, S. R., and C. Porretta. 2003. Iron deficiency and in vitro iron chelation reduce the expression of cluster of differentiation molecule (CD)28 but not CD3 receptors on murine thymocytes and spleen cells. *Br J Nutr* 90: 179-189.

75.   Lederman, H. M., A. Cohen, J. W. Lee, M. H. Freedman, and E. W. Gelfand. 1984. Deferoxamine: a reversible S-phase inhibitor of human lymphocyte proliferation. *Blood* 64: 748-753.

76.   Walker, E. M., Jr., and S. M. Walker. 2000. Effects of iron overload on the immune system. *Ann Clin Lab Sci* 30: 354-365.

77.   Bonaccorsi-Riani, E., R. Danger, J. J. Lozano, M. Martinez-Picola, E. Kodela, R. Mas-Malavila, M. Bruguera, H. L. Collins, R. C. Hider, M. Martinez-Llordella, and A. Sanchez-Fueyo. 2015. Iron Deficiency Impairs Intra-Hepatic Lymphocyte Mediated Immune Response. *PLoS One* 10: e0136106.

78. Motamedi, M., L. Xu, and S. Elahi. 2016. Correlation of transferrin receptor (CD71) with Ki67 expression on stimulated human and mouse T cells: The kinetics of expression of T cell activation markers. *J Immunol Methods* 437: 43-52.

79. Choi, E. K., T. T. Nguyen, N. Gupta, S. Iwase, and Y. A. Seo. 2018. Functional analysis of SLC39A8 mutations and their implications for manganese deficiency and mitochondrial disorders. *Sci Rep* 8: 3163.

80. Liao, W., J. X. Lin, and W. J. Leonard. 2013. Interleukin-2 at the crossroads of effector responses, tolerance, and immunotherapy. *Immunity* 38: 13-25.

81. Akbar, A. N., N. J. Borthwick, R. G. Wickremasinghe, P. Panayoitidis, D. Pilling, M. Bofill, S. Krajewski, J. C. Reed, and M. Salmon. 1996. Interleukin-2 receptor common gamma-chain signaling cytokines regulate activated T cell apoptosis in response to growth factor withdrawal: selective induction of anti-apoptotic (bcl-2, bcl-xL) but not pro-apoptotic (bax, bcl-xS) gene expression. *Eur J Immunol* 26: 294-299.

82. Nakajima, H., X. W. Liu, A. Wynshaw-Boris, L. A. Rosenthal, K. Imada, D. S. Finbloom, L. Hennighausen, and W. J. Leonard. 1997. An indirect effect of Stat5a in IL-2-induced proliferation: a critical role for Stat5a in IL-2-mediated IL-2 receptor alpha chain induction. *Immunity* 7: 691-701.

83. Sena, L. A., S. Li, A. Jairaman, M. Prakriya, T. Ezponda, D. A. Hildeman, C. R. Wang, P. T. Schumacker, J. D. Licht, H. Perlman, P. J. Bryce, and N. S. Chandel. 2013. Mitochondria are required for antigen-specific T cell activation through reactive oxygen species signaling. *Immunity* 38: 225-236.

84. Pae, H. O., G. S. Oh, B. M. Choi, S. C. Chae, Y. M. Kim, K. R. Chung, and H. T. Chung. 2004. Carbon monoxide produced by heme oxygenase-1 suppresses T cell proliferation via inhibition of IL-2 production. *J Immunol* 172: 4744-4751.

85. Philip, M., S. A. Funkhouser, E. Y. Chiu, S. R. Phelps, J. J. Delrow, J. Cox, P. J. Fink, and J. L. Abkowitz. 2015. Heme exporter FLVCR is required for T cell development and peripheral survival. *J Immunol* 194: 1677-1685.

86. Soares, M. P., and I. Hamza. 2016. Macrophages and Iron Metabolism. *Immunity* 44: 492-504.

87. Jung, M., C. Mertens, E. Tomat, and B. Brune. 2019. Iron as a Central Player and Promising Target in Cancer Progression. *Int J Mol Sci* 20.

88. Wang, Z., W. Yin, L. Zhu, J. Li, Y. Yao, F. Chen, M. Sun, J. Zhang, N. Shen, Y. Song, and X. Chang. 2018. Iron Drives T Helper Cell Pathogenicity by Promoting RNA-Binding Protein PCBP1-Mediated Proinflammatory Cytokine Production. *Immunity* 49: 80-92 e87.

89. Dubiel, W., D. Dubiel, D. A. Wolf, and M. Naumann. 2018. Cullin 3-Based Ubiquitin Ligases as Master Regulators of Mammalian Cell Differentiation. *Trends Biochem Sci* 43: 95-107.

90. Ashouri, J. F., L. Y. Hsu, S. Yu, D. Rychkov, Y. Chen, D. A. Cheng, M. Sirota, E. Hansen, L. Lattanza, J. Zikherman, and A. Weiss. 2019. Reporters of TCR signaling identify arthritogenic T cells in murine and human autoimmune arthritis. *Proc Natl Acad Sci U S A* 116: 18517-18527.

91. Tabbekh, M., M. Mokrani-Hammani, G. Bismuth, and F. Mami-Chouaib. 2013. T-cell modulatory properties of CD5 and its role in antitumor immune responses. *Oncoimmunology* 2: e22841.

92.   Ashouri, J. F., and A. Weiss. 2017. Endogenous Nur77 Is a Specific Indicator of Antigen Receptor Signaling in Human T and B Cells. *J Immunol* 198: 657-668.

93.   Hong, C., M. A. Luckey, and J. H. Park. 2012. Intrathymic IL-7: the where, when, and why of IL-7 signaling during T cell development. *Semin Immunol* 24: 151-158.

94.   Park, J. Y., Y. Jo, E. Ko, M. A. Luckey, Y. K. Park, S. H. Park, J. H. Park, and C. Hong. 2016. Soluble gammac cytokine receptor suppresses IL-15 signaling and impairs iNKT cell development in the thymus. *Sci Rep* 6: 36962.

95.   Kang, S. I., H. W. Choi, and I. Y. Kim. 2008. Redox-mediated modification of PLZF by SUMO-1 and ubiquitin. *Biochem Biophys Res Commun* 369: 1209-1214.

96.   Hogquist, K., and H. Georgiev. 2020. Recent advances in iNKT cell development. *F1000Res* 9.

97.   Lee, Y. J., K. L. Holzapfel, J. Zhu, S. C. Jameson, and K. A. Hogquist. 2013. Steady-state production of IL-4 modulates immunity in mouse strains and is determined by lineage diversity of iNKT cells. *Nat Immunol* 14: 1146-1154.

98.   Bjorkoy, G., T. Lamark, S. Pankiv, A. Overvatn, A. Brech, and T. Johansen. 2009. Monitoring autophagic degradation of p62/SQSTM1. *Methods Enzymol* 452: 181-197.

99.   Pankiv, S., T. H. Clausen, T. Lamark, A. Brech, J. A. Bruun, H. Outzen, A. Overvatn, G. Bjorkoy, and T. Johansen. 2007. p62/SQSTM1 binds directly to Atg8/LC3 to facilitate degradation of ubiquitinated protein aggregates by autophagy. *J Biol Chem* 282: 24131-24145.

100.   Kim, Y. H., A. Kumar, C. H. Chang, and K. Pyaram. 2017. Reactive Oxygen Species Regulate the Inflammatory Function of NKT Cells through Promyelocytic Leukemia Zinc Finger. *J Immunol* 199: 3478-3487.

101.   Pearce, E. L., M. C. Poffenberger, C. H. Chang, and R. G. Jones. 2013. Fueling immunity: insights into metabolism and lymphocyte function. *Science* 342: 1242454.

102.   Kumar, A., K. Pyaram, E. L. Yarosz, H. Hong, C. A. Lyssiotis, S. Giri, and C. H. Chang. 2019. Enhanced oxidative phosphorylation in NKT cells is essential for their survival and function. *Proc Natl Acad Sci U S A* 116: 7439-7448.

103.   Ayala, A., M. F. Munoz, and S. Arguelles. 2014. Lipid peroxidation: production, metabolism, and signaling mechanisms of malondialdehyde and 4-hydroxy-2-nonenal. *Oxid Med Cell Longev* 2014: 360438.

104.   Yarosz, E. L., C. Ye, A. Kumar, C. Black, E. K. Choi, Y. A. Seo, and C. H. Chang. 2020. Cutting Edge: Activation-Induced Iron Flux Controls CD4 T Cell Proliferation by Promoting Proper IL-2R Signaling and Mitochondrial Function. *J Immunol* 204: 1708-1713.

105.   He, F., L. Antonucci, and M. Karin. 2020. NRF2 as a regulator of cell metabolism and inflammation in cancer. *Carcinogenesis* 41: 405-416.

106.   Mitsuishi, Y., K. Taguchi, Y. Kawatani, T. Shibata, T. Nukiwa, H. Aburatani, M. Yamamoto, and H. Motohashi. 2012. Nrf2 redirects glucose and glutamine into anabolic pathways in metabolic reprogramming. *Cancer Cell* 22: 66-79.

107.   Pyaram, K., A. Kumar, Y. H. Kim, S. Noel, S. P. Reddy, H. Rabb, and C. H. Chang. 2019. Keap1-Nrf2 System Plays an Important Role in Invariant Natural Killer T Cell Development and Homeostasis. *Cell Rep* 27: 699-707 e694.

108.   Feng, H., K. Schorpp, J. Jin, C. E. Yozwiak, B. G. Hoffstrom, A. M. Decker, P. Rajbhandari, M. E. Stokes, H. G. Bender, J. M. Csuka, P. S. Upadhyayula, P. Canoll, K.

Uchida, R. K. Soni, K. Hadian, and B. R. Stockwell. 2020. Transferrin Receptor Is a Specific Ferroptosis Marker. *Cell Rep* 30: 3411-3423 e3417.

109. Vashisht, A. A., K. B. Zumbrennen, X. Huang, D. N. Powers, A. Durazo, D. Sun, N. Bhaskaran, A. Persson, M. Uhlen, O. Sangfelt, C. Spruck, E. A. Leibold, and J. A. Wohlschlegel. 2009. Control of iron homeostasis by an iron-regulated ubiquitin ligase. *Science* 326: 718-721.

110. Zhang, D. L., M. C. Ghosh, and T. A. Rouault. 2014. The physiological functions of iron regulatory proteins in iron homeostasis - an update. *Front Pharmacol* 5: 124.

111. Moore, L. D., T. Le, and G. Fan. 2013. DNA methylation and its basic function. *Neuropsychopharmacology* 38: 23-38.

112. Heinsberg, L. W., D. E. Weeks, S. A. Alexander, R. L. Minster, P. R. Sherwood, S. M. Poloyac, S. Deslouches, E. A. Crago, and Y. P. Conley. 2021. Iron homeostasis pathway DNA methylation trajectories reveal a role for STEAP3 metalloreductase in patient outcomes after aneurysmal subarachnoid hemorrhage. *Epigenetics Commun* 1.

113. Horniblow, R. D., P. Pathak, D. L. Balacco, A. Acharjee, E. Lles, G. Gkoutos, A. D. Beggs, and C. Tselepis. 2022. Iron-mediated epigenetic activation of NRF2 targets. *J Nutr Biochem* 101: 108929.

114. Jiang, L., J. Wang, K. Wang, H. Wang, Q. Wu, C. Yang, Y. Yu, P. Ni, Y. Zhong, Z. Song, E. Xie, R. Hu, J. Min, and F. Wang. 2021. RNF217 regulates iron homeostasis through its E3 ubiquitin ligase activity by modulating ferroportin degradation. *Blood* 138: 689-705.

115. Myers, D. R., J. Zikherman, and J. P. Roose. 2017. Tonic Signals: Why Do Lymphocytes Bother? *Trends Immunol* 38: 844-857.

116. Chetoui, N., M. Boisvert, S. Gendron, and F. Aoudjit. 2010. Interleukin-7 promotes the survival of human CD4+ effector/memory T cells by up-regulating Bcl-2 proteins and activating the JAK/STAT signalling pathway. *Immunology* 130: 418-426.

117. Vivien, L., C. Benoist, and D. Mathis. 2001. T lymphocytes need IL-7 but not IL-4 or IL-6 to survive in vivo. *Int Immunol* 13: 763-768.

118. Jiang, Q., W. Q. Li, F. B. Aiello, R. Mazzucchelli, B. Asefa, A. R. Khaled, and S. K. Durum. 2005. Cell biology of IL-7, a key lymphotrophin. *Cytokine Growth Factor Rev* 16: 513-533.

119. Yang, K., G. Neale, D. R. Green, W. He, and H. Chi. 2011. The tumor suppressor Tsc1 enforces quiescence of naive T cells to promote immune homeostasis and function. *Nat Immunol* 12: 888-897.

120. Barata, J. T., A. Silva, J. G. Brandao, L. M. Nadler, A. A. Cardoso, and V. A. Boussiotis. 2004. Activation of PI3K is indispensable for interleukin 7-mediated viability, proliferation, glucose use, and growth of T cell acute lymphoblastic leukemia cells. *J Exp Med* 200: 659-669.

121. Lapinski, P. E., Y. Qiao, C. H. Chang, and P. D. King. 2011. A role for p120 RasGAP in thymocyte positive selection and survival of naive T cells. *J Immunol* 187: 151-163.

122. Cheng, L. E., F. K. Chan, D. Cado, and A. Winoto. 1997. Functional redundancy of the Nur77 and Nor-1 orphan steroid receptors in T-cell apoptosis. *EMBO J* 16: 1865-1875.

123. Sckisel, G. D., M. N. Bouchlaka, A. M. Monjazeb, M. Crittenden, B. D. Curti, D. E. Wilkins, K. A. Alderson, C. M. Sungur, E. Ames, A. Mirsoian, A. Reddy, W. Alexander, A. Soulika, B. R. Blazar, D. L. Longo, R. H. Wiltrout, and W. J. Murphy. 2015. Out-of-

Sequence Signal 3 Paralyzes Primary CD4(+) T-Cell-Dependent Immunity. *Immunity* 43: 240-250.

124. Muller, B., N. Lewis, T. Adeniyi, H. J. Leese, D. R. Brison, and R. G. Sturmey. 2019. Application of extracellular flux analysis for determining mitochondrial function in mammalian oocytes and early embryos. *Sci Rep* 9: 16778.

125. Di Gangi, A., M. E. Di Cicco, P. Comberiati, and D. G. Peroni. 2020. Go With Your Gut: The Shaping of T-Cell Response by Gut Microbiota in Allergic Asthma. *Front Immunol* 11: 1485.

126. Rowland, S. L., C. L. DePersis, R. M. Torres, and R. Pelanda. 2010. Ras activation of Erk restores impaired tonic BCR signaling and rescues immature B cell differentiation. *J Exp Med* 207: 607-621.

127. Friend, S. F., F. Deason-Towne, L. K. Peterson, A. J. Berger, and L. L. Dragone. 2014. Regulation of T cell receptor complex-mediated signaling by ubiquitin and ubiquitin-like modifications. *Am J Clin Exp Immunol* 3: 107-123.

128. Kouidhi, S., M. Z. Noman, C. Kieda, A. B. Elgaaied, and S. Chouaib. 2016. Intrinsic and Tumor Microenvironment-Induced Metabolism Adaptations of T Cells and Impact on Their Differentiation and Function. *Front Immunol* 7: 114.

129. Grady, R. W., A. N. Akbar, P. J. Giardina, M. W. Hilgartner, and M. de Sousa. 1985. Disproportionate lymphoid cell subsets in thalassaemia major: the relative contributions of transfusion and splenectomy. *Br J Haematol* 59: 713-724.

130. Reimao, R., G. Porto, and M. de Sousa. 1991. Stability of CD4/CD8 ratios in man: new correlation between CD4/CD8 profiles and iron overload in idiopathic haemochromatosis patients. *C R Acad Sci III* 313: 481-487.

131. Khalifa, A. S., Z. Maged, R. Khalil, F. Sabri, O. Hassan, and M. el-Alfy. 1988. T cell functions in infants and children with beta-thalassemia. *Acta Haematol* 79: 153-156.

132. Pourgheysari, B., L. Karimi, and P. Beshkar. 2016. Alteration of T Cell Subtypes in Beta-Thalassaemia Major: Impact of Ferritin Level. *J Clin Diagn Res* 10: DC14-18.

133. Maia, M. L., C. S. Pereira, G. Melo, I. Pinheiro, M. A. Exley, G. Porto, and M. F. Macedo. 2015. Invariant Natural Killer T Cells are Reduced in Hereditary Hemochromatosis Patients. *J Clin Immunol* 35: 68-74.

134. Costa, M., E. Cruz, S. Oliveira, V. Benes, T. Ivacevic, M. J. Silva, I. Vieira, F. Dias, S. Fonseca, M. Goncalves, M. Lima, C. Leitao, M. U. Muckenthaler, J. Pinto, and G. Porto. 2015. Lymphocyte gene expression signatures from patients and mouse models of hereditary hemochromatosis reveal a function of HFE as a negative regulator of CD8+ T-lymphocyte activation and differentiation in vivo. *PLoS One* 10: e0124246.

135. Kuvibidila, S., M. Dardenne, W. Savino, and F. Lepault. 1990. Influence of iron-deficiency anemia on selected thymus functions in mice: thymulin biological activity, T-cell subsets, and thymocyte proliferation. *Am J Clin Nutr* 51: 228-232.

136. Jabara, H. H., S. E. Boyden, J. Chou, N. Ramesh, M. J. Massaad, H. Benson, W. Bainter, D. Fraulino, F. Rahimov, C. Sieff, Z. J. Liu, S. H. Alshemmari, B. K. Al-Ramadi, H. Al-Dhekri, R. Arnaout, M. Abu-Shukair, A. Vatsayan, E. Silver, S. Ahuja, E. G. Davies, M. Sola-Visner, T. K. Ohsumi, N. C. Andrews, L. D. Notarangelo, M. D. Fleming, W. Al-Herz, L. M. Kunkel, and R. S. Geha. 2016. A missense mutation in TFRC, encoding transferrin receptor 1, causes combined immunodeficiency. *Nat Genet* 48: 74-78.

137. Sun, V., M. Sharpley, K. E. Kaczor-Urbanowicz, P. Chang, A. Montel-Hagen, S. Lopez, A. Zampieri, Y. Zhu, S. C. de Barros, C. Parekh, D. Casero, U. Banerjee, and G. M.

Crooks. 2021. The Metabolic Landscape of Thymic T Cell Development In Vivo and In Vitro. *Front Immunol* 12: 716661.

138.   Pellicci, D. G., H. F. Koay, and S. P. Berzins. 2020. Thymic development of unconventional T cells: how NKT cells, MAIT cells and gammadelta T cells emerge. *Nat Rev Immunol* 20: 756-770.